Aspects of Gravity and Conformal Field Theories in Large Dimensions

Master's thesis

Written by

Frederik Holdt-Sørensen

Supervised by

David McGady & Niels Anne Jacob Obers

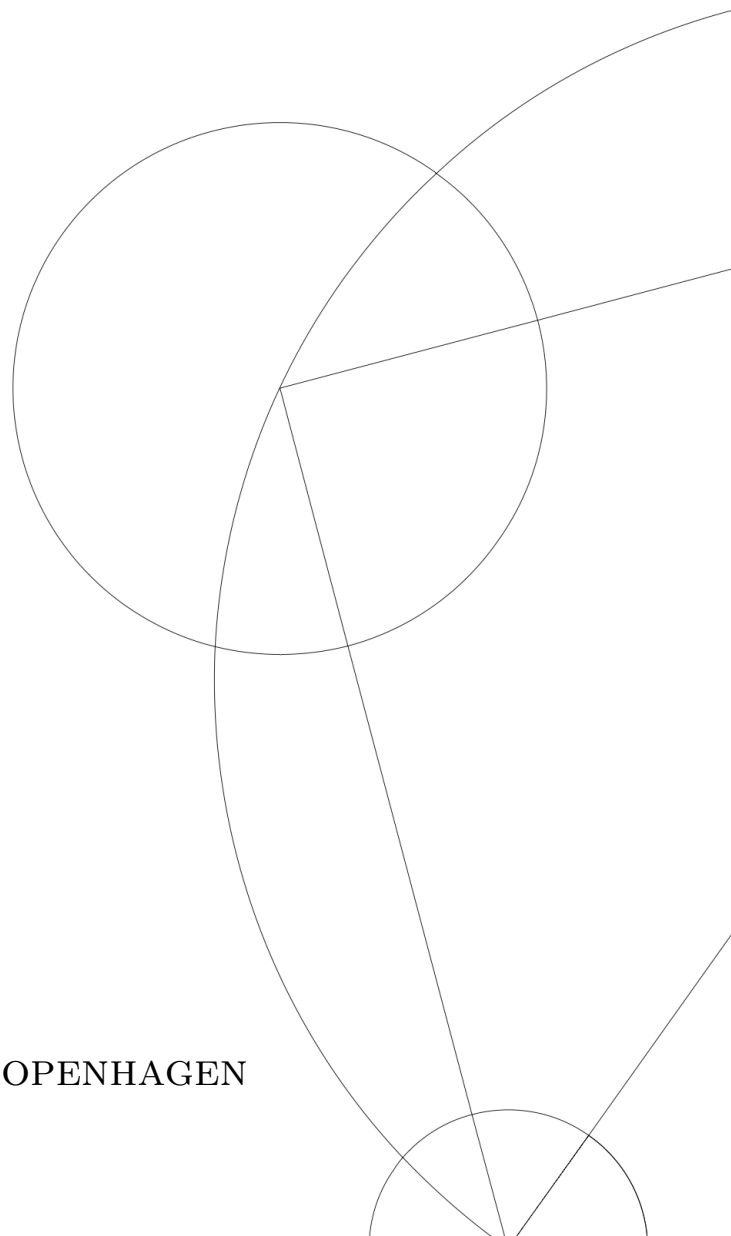

University of Copenhagen

UNIVERSITY OF COPENHAGEN

Faculty:	Science	
Institute:	Niels Bohr Institute	
Author:	Frederik Holdt-Sørensen	KU-ID: NDX115
Title:	Aspects of Gravity and Conformal Field Theories in Large Dimensions	
Supervisor:	David McGady	david.mcgady@su.se, dmcgady@alumni.princeton.edu
Supervisor:	Niels Anne Jacob Obers	obers@nbi.ku.dk
Handed in:	20^{th} of May 2021	
Defended:	31^{st} of May 2021	

Abstract

Four-point correlation functions in a general D-dimensional conformal field theory are described by conformal blocks which are evaluated in a radial/angular decomposition, a scalar block suggested large D composition, and a further simplified large D configuration. In this thesis, we outline the basics of Anti-de Sitter and conformal field theories and motivate the correspondence between the two theories. We introduce a Gegenbauer decomposition of the conformal block in the radial quantization, with a symmetric operator location configuration, and by recursion methods, we derive the first levels in the block's decomposition. Further, we point out that the transformation of the unit box in cross-ratio coordinates does not cover the unit circle in the radial/angular configuration, and relate this to crossing symmetry. For large D conformal theories another coordinate set related to the conformal invariant cross-ratios is applied to the Casimir equation and then solved for a negligible mixed term, leaving a simple conformal block expression that is symmetric in Δ and $1-l$. We compare this expression with the exact conformal block and the radial/angular conformal block for the case of $D = 4$ which resembles the structure remarkably. The conformal large D block can further be simplified by assuming a linear scaling of Δ and l with a saddle-point integral and a new coordinate set is applied which using the crossing relation can restrict the external scaling dimension to $\Delta_\phi / D > 1$. This type of block has another behavior compared to the previous three versions and therefore the validity of the linear scaling and the saddle-point integration is questioned. We show that the coordinate systems of the large D block and the radial/angular block are essentially the same and comment on the different large D limits that are implied for the Casimir equation. We further make suggestional derivations of the conformal blocks, in some of these large D limits.

Contents

Chapter 1

Introduction

The study of Anti-de Sitter (AdS) space/ Conformal Field Theory (CFT) duality, also known as the gauge/-gravity duality, is a powerful, surprising, deep, and qualitatively new synthesis of naively disparate physical forces. AdS space is a theory written in the language of General Relativity (GR), and using String Theory (ST) one can quantize the gravitational theory. CFT is a Yang-Mills (YM) theory in which the standard model of particle physics is written. We have seen syntheses between physical forces before in the history of physics. These syntheses sometimes lead to unification between forces of nature, even though it is not guaranteed. In this section, we will go through the history of unification between forces of nature in physics and fit in the AdS/CFT correspondence. Then we will further motivate why this correspondence, and especially CFTs are important and fascinating to study.

An example of unification between physical forces is from the 19th century between electricity and magnetism. Based on experiments, Maxwell was able in 1865 to formulate the equations of motion of electromagnetism, and thus combining the two forces. One of the solutions to the equations of motion is an electromagnetic wave moving at the speed of light. In other words, we obtained an even deeper understanding of how nature is connected. This allowed new technology to be developed in such a manner, that today it is hard to imagine an average weekday without all the possibilities unlocked by that unification. Therefore the potential and importance of a new unification between physical forces is huge.

After the unification of electricity and magnetism, it was believed that there was only a few subtle problems in physics, and beside those, the theory of physics was complete. The first of the two problems was that the planet of Mercury deviated slightly from its predicted trajectory. The second problem was that a blackbody in equilibrium should, according to classical physics, emit energy in all frequencies leading to instantaneous radiation of all energy, which of course is unphysical. The solution to these subtle problems turned into the theory of relativity and quantum mechanics (QM). Besides these two major naively disparate bodies of physical principles and laws, we have the classical version of gravity formulated by Newton in 1687. A simplified representation of the relationships of the theories is given in Figure 1.1. To explain Figure 1.1 in words, we first consider the orbits of planets around the sun. One needs a gravitational constant G in the theory, hence we must use classical mechanics. If one considers what happens at velocities approaching the speed of light c we use special relativity (SR) formulated by Einstein. If one considers how subatomic particles behave, then there is an uncertainty on e.g. the position or velocity when measuring both, which for the smallest possible value is of order $\hbar$, and one needs a theory of QM.

But what happens if you are in situations where you cannot neglect the two other theories? High velocities correspond to large energies, which is equivalent to large masses. So if you have an extremely massive object such as a star, you cannot neglect either the gravitational energy or SR. One needs another theory. Once again Einstein turned up with the theory of GR in 1916, which could explain such cases, with corrections to orbits of planets such as Mercury, that are close to a star, while the theory reduces to classical mechanics in the limit of large c, and SR in the limit of small G. Likewise for QM, if we are in the limit of

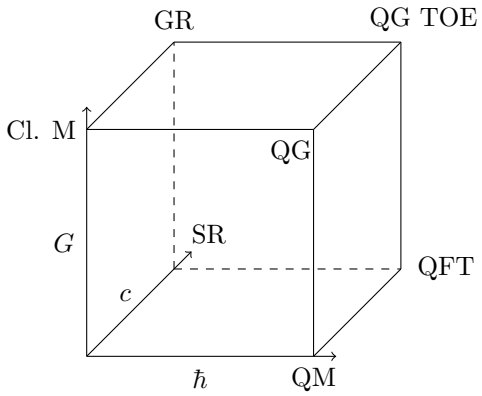

Figure 1.1: *A box representation of the relationship between the theories of physics and their dependency on fundamental physical constants.*

small $\hbar$ the energy spectrum of states would vanish and we would be left with a classical theory.

Another possible situation is when looking at subatomic particles i.e. quantum particles moving at great speeds approaching the speed of light. Then one should combine Schrödinger's equation from QM and Einstein's energy/mass/momentum relation from SR. This is what Dirac famously did in 1928, and it sparked the development of Quantum Field Theory (QFT). Looking at Figure 1.1 it seems as if we have yet to describe two corners to be able to describe all phenomena and processes in physics. These corners are relativistic and non-relativistic Quantum Gravity (QG). The non-relativistic version is where we need both the classical description of gravity and QM. To obtain the relativistic version, also called the theory of everything (TOE) we need a unification between GR and QFT. This has notoriously been a struggle to develop, since GR is a non-renormalizable theory in QFT, giving us mathematical infinities.

One place where we cannot neglect any of these aspects of physics is when considering a Black Hole (BH). The first non-trivial solution of Einstein's field equations came in 1916 by Schwarzschild. It became clear that there was a singularity in the metric at radius $r = 0$, and further at the Schwarzschild radius $r = r_s$ even light could not escape the massive object. This physical object is interpreted as a BH and has in recent years been observed directly [1]. In 1974 Hawking imagined that at the boundary of this BH, particles could pop in and out of existence due to quantum fluctuations in spacetime [2]. A particle pair was created at the boundary, where one particle would fall into the BH and the other particle would fly out into space. As a result, an observer far away would see this as radiation coming from the BH. Bekenstein and Hawking [3] could assign a temperature, T to the radiation and derive the entropy, S of the quantum information stored in the BH. This is referred to as a semi-classical description of gravity. The BH entropy law was of special interest since the scaling is proportional to the surface area A of the BH i.e. $S \sim A$. In comparison, the entropy scaling of an ideal gas goes with the volume, V i.e. $S \sim V$. Given that the entropy is an expression for the quantum information, this suggests that the information within the BH is stored on the boundary of the BH [4, 5]. Holograms use an effect of displaying a 3D image, even though the information is stored elsewhere in lower dimensions, therefore the entropy dependency gave rise to what came to be known as the holographic principle. In 1982 Hawking and Page [6] found that the same entropy scaling of BHs also applies in a negatively curved space, called AdS space.

Meanwhile, QFT had great success in quantizing the electromagnetic field, the weak force, and the strong force, using a YM theory. Electromagnetism was based on a unitary group $U(1)$, while the weak force was based on a special unitary group $SU(2)$ with the Lie algebra of 3 Pauli matrices, while the strong force was a special unitary group $SU(3)$ based on the Lie algebra of 8 Gell-Mann matrices. [1] These matrices satisfy an algebra which obey commutation relations that give structure constants. [2] A key feature of a YM

[1]The specific gauge group of the standard model is a combination of all these groups specifically $U(1) \times SU(2) \times SU(3)$

[2]Specifically we have generators T^a that carry an index and obey the commutation relation $[T^a, T^b] = if^{abc}T^c$ where f^{abc} is the structure constants.

theory is that the Lagrangian is invariant under gauge transformations and is written in the particular form with contracted field strength tensors [3], and if the theory is non-abelian, they are traced over.

The Feynman path integral method lets us quantize such a theory. A key part of this method is the partition function, which integrates over all possible paths that particles can travel from one location to another. It integrates over quantum fields while the information from the Lagrangian is needed as an input, through the action. The partition function can give us the correlation functions between operators, and one can derive the Feynman rules from the partition function. The Feynman rules are used when computing the cross-section and decay rate in scattering processes. Together with the correlation functions, these are some observables of any QFT. Using methods from QFT the g-factor of the magnetic dipole moment of the electron has been derived. The value was matched with the measured one and gave the best agreement between experiment and theory in all of science. [7]

It was then possible to unify the electromagnetic force and the weak force. Both forces are YM theories with the combined symmetry group [4], which gives rise to weak isospin fields W_1, W_2, W_3 and the weak hypercharge field B. When the energy exceeds the unification energy the forces merge into one. The photon γ and Z^0 boson can be seen as a rotation by the Weinberg angle from the W_3 and B bosons while the $W^{\pm}$ bosons are linear combinations of W^1 and W^2. Likewise, it is believed that at large energy scales, corresponding to small distances we should see a similar unification between all 3 forces of the standard model, including that of strong interaction.

Gravity does not fit into that puzzle. Gravity is not a YM theory but a theory of geometry and curved spacetime, so the mathematical languages are not directly related. GR can be understood as a theory of a massless spin 2 particle, the graviton, that couples to all matter via energy and momentum. This is different from a YM theory of several spin 1 particles. The Einstein-Hilbert action is non-renormalizable giving divergences in the path integral, even though the result is expected to be finite. QFT can make useful predictions when the strength of the interaction, i.e. coupling constant is small and close to a free field theory because QFT is based on a perturbative method. Gravity is a highly interacting theory, so applying the QFT techniques on gravity does often not work.

ST came up with a new approach to gravity. It replaced the picture of a particle with that of a string [8]. It went from the GR picture of a worldline to the ST picture of a world sheet embedded in the target space. The world sheet is a $D = 2$ CFT, and the target space is our real space. For bosonic ST the target space lives in $D = 26$. These extra dimensions should be thought of as compactified dimensions, which reduce to our everyday world in $D = 4$. The immediate problem for bosonic ST was that it produced a Tachyon [8], a particle that has negative mass squared and must be seen as unstable. To make a more consistent theory it was needed to impose supersymmetry (SUSY). Therefore a fermionic field on the worldsheet was introduced so that the fermionic and bosonic fields could transform into each other while leaving the action invariant. This reduced the number of dimensions to $D = 10$. Superstring theory's greatest success was its ability to reproduce gravity while quantizing it to the particle, namely the graviton, while it also gave rise to spacetime fermions. But the graviton is yet to be adapted into a single framework for the standard model.

In 1998 Maldacena [9] published a paper, followed by Polyakov et. al. [10] and Witten [11], with a conjecture of a duality between an AdS space and a CFT. The AdS/CFT correspondence says that we should have a duality between the bulk theory of gravity in AdS and a boundary YM theory of CFT as depicted in Figure 1.2. Thereby the theories themselves are holographic like the entropies were for the BH. In each slice of the AdS cylinder, one has a hyperbolic space. The hyperbolic space implies that the boundary, where the CFT lives is infinitely far away from any point in AdS space. The representation of the cylinder space can be generalized so that the AdS space lives in $D + 1$ dimensions and the CFT lives in D. The conjecture claims that any observable in one theory should have a counterpart in the other theory. Specifically, we have that the partition functions from each theory should agree $Z_{CFT} = Z_{AdS}$, where the AdS partition function is that of a ST. It is in the large N limit, where N refers to the gauge group rank, that certain

[3] The Lagrangian $\mathcal{L}$ is specifically $\mathcal{L} = -\frac{1}{4}F_{\mu\nu}F^{\mu\nu}$ where $F^{\mu\nu}$ is the field strength tensor related to the vector fields A_μ by $F_{\mu\nu} = \partial_\mu A_\nu - \partial_\nu A_\mu$

[4] This symmetry group is given by $U(1) \times SU(2)$

CFTs are equivalent to the superstring theory description. One of the early and explicit realizations of the correspondence has been with Type IIB ST, i.e. a specific type of superstring theory, on an $AdS_5 \times S^5$ manifold, where S^5 encodes some compact dimensions, that is dual to an $\mathcal{N} = 4$ SUSY YM in $D = 4$, where $\mathcal{N}$ refers to the amount of SUSY in the theory. One of the advantages of AdS/CFT is that the language of a CFT is more comparable to the standard model of elementary particles, and therefore we might fit gravity into the puzzle through this correspondence. The AdS/CFT correspondence should not be seen as a solution to how the real physics of gravity plays out. The spatial curvature of the universe has not yet been settled, but it seems to be consistent with a flat space [12]. To model the universe and other real-world physical systems the gauge/gravity duality should be developed in a flat space as well. The amount of supersymmetry that has been assumed in the realizations of the correspondence hasn't yet been detected in particle accelerators such as CERN. One should rather think of the AdS/CFT correspondence as a toy model for unifying QG with QFT for now, which we can develop to represent the actual physical world.

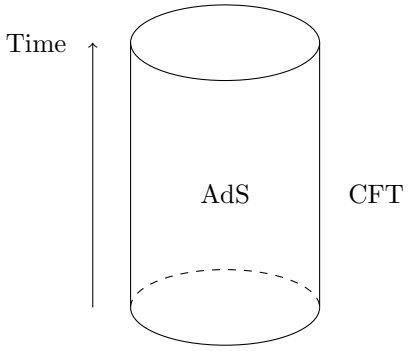

Figure 1.2: *A cylinder representation of the relationship between the bulk theory of an AdS space and boundary theory of a CFT.*

The fact that one can investigate aspects of gravity by a CFT on the boundary, and give qualitative descriptions of the dynamics and observables in purely gravitational physics in the bulk without using the principles of ST, is an interesting and fascinating new approach in physics. Similarly, aspects of gauge theory can further be developed, by the information from ST. Applying the correspondence to specific situations is complicated, so only a few cases of specific manifolds, dimensions, and symmetries have been explored. The potential of exploring the AdS/CFT correspondence is huge. Some examples of unsolved problems in physics that further development of the gauge/gravity duality has the potential to solve are listed:

- The AdS/CFT correspondence can be the stepping stone to a full theory of QG. QG may answer some of the most fundamental questions in physics such as what happens at the beginning of the universe and what the gravitational dynamics are inside a BH. These physical situations can only be described by a full theory of QG, since we cannot neglect the influence of quantum mechanical behavior nor gravity, in these extremely dense stages of the universe.
- The correspondence seems to give new insight into the framework of BH evaporation processes. It has long been an open question as to what happens to the quantum information that falls into a BH, then getting scrambled, and Hawking radiated. It violates unitarity and the fundamentals of information conservation in QM. There has been some progress in recent years, by applying the AdS/CFT correspondence on Islands inside BHs. [13, 14]
- The Hierarchy problem asks the question of why gravity is so much weaker than the other forces of nature. The problem occurs in QFT when quantizing gravity. Here the coupling constant and mass have a huge discrepancy from its effective value, measured by experiment. Typically these values are related by the renormalization procedure, which works fine when the discrepancy between the values is small. This is not the case for gravity. This problem can only be fixed by a non-perturbative theory because gravity is a highly interacting theory.

- The cosmological constant problem, which concerns the huge discrepancy of 120 orders of magnitude between the measured vacuum energy density in the entire universe and the zero-point energy predicted by QFT [15].
- The theory of QG may give information about gauge groups through the AdS/CFT correspondence. This might give new insight into the open questions in Quantum ChromoDynamics (QCD), such as the YM existence and mass gap question [16].
- Another open question in physics is concerning phase transitions at critical points. These critical points do not have a favored length scale, giving the scaling invariance, which a CFT includes. There are still unanswered questions of the physical behavior at critical points and on the bounds of critical exponents in the theory, [17].
- CFTs are also of great interest when talking about condensed matter systems [18]. The Ising model, which is a theory of ferromagnetic interactions, is a great example of a scale-invariant system where one divides the configuration of the magnets into ising spin blocks so that the behavior is equivalent when comparing small or large ising spin blocks.
- Large D aspects of CFTs. CFTs have been well established in $D = 2$ by ST and it has been constructed in up to 6 dimensions, but not in larger dimensions. We do not know whether non-trivial CFTs exist in $D > 6$. This is the main, central focus of this thesis, and we hope to shed some light on the behavior and bounds of CFTs in large D.

In this thesis, we will develop the language to understand the AdS/CFT correspondence, both from the many faces of the AdS metric, to the holographic principle and the CFT algebra and correlation functions. After establishing this language we will dive into the aspects of conformal theories in general dimensions D and uncover the different expressions of the conformal blocks. One of the long-term hopes is that our large D limit may simplify the equations to such an extent that we could explore the duality in $AdS_{D\gg1} \rightleftarrows CFT_{D\gg1}$. Large D CFTs may also simplify to an effective description which may reveal new physical insight which could not be found in low dimensions or even in general dimensions. These simple large D CFTs may also be put into concrete tests. This thesis is a tiny step in this direction. The main finding is a coordinate relation between a type of large D coordinates and a radial/angular coordinate configuration, which could help to better understand certain large D CFT observables.

The thesis is structured in the following way: In chapter 2 we look into metrics of AdS space and consider some thermodynamic properties such as the entropy of an AdS Schwarzschild BH. In chapter 3 we develop the language of CFTs, introducing the algebra, the structure of the correlation functions, and the CFT data with constraints. Further, we focus on the conformal blocks and how they satisfy the Casimir equation. In chapter 4 we investigate the decomposition of conformal blocks in Gegenbauer polynomials under the radial quantization. The levels are then computed using a recursion relation for the blocks. In chapter 5 we consider one of the only two papers concerning conformal blocks in large D. A nice set of variables are derived, that separates the solution of the conformal Casimir equation and is used to write up a simple version of the conformal block that is a great approximation to the exact conformal blocks at $D = 4$. In chapter 6 we consider the other paper that deals with large D conformal blocks and we derive a bound on the external scaling dimension for large D CFTs to exist from the bootstrap method. In chapter 7 we apply the knowledge of the previous chapters to explore a connection between the radial/angular coordinates of chapter 4 and the conformal block of chapter 5. It turns out that these blocks are described by essentially the same coordinates, which opens up a path of aspects for the conformal block to explore in chapter 8. In chapter 9 we comment on the possible future directions of the thesis and make a conclusion on our findings.

We will use natural units throughout the thesis $c = \hbar = G_N = k_B = 1$, and reinstate the constants if necessary. We will also use the Einstein convention for repeated spacetime indices.

Chapter 2

Gravity in Anti-de Sitter Space

In this chapter, we will introduce the mathematical language of an AdS space and couple it to the holographic principle which motivated the AdS/CFT correspondence. The theory of gravity is the theory of Einstein's general relativity, which has the Einstein field equations as the Equation Of Motion (EOM):

$$R_{\mu\nu} - \frac{1}{2}Rg_{\mu\nu} = 8\pi T_{\mu\nu}, \tag{2.0.1}$$

here $R_{\mu\nu}$ is the Ricci tensor, R is the Ricci scalar, $g_{\mu\nu}$ is the metric and $T_{\mu\nu}$ is the Energy-Momentum (EM) tensor/stress tensor. Each index encodes the specific coordinates and thereby counts the number of dimensions. The natural generalization to higher dimensions is by letting the index run $\mu = 0, 1, 2, ..., D-1$, i.e a total of D dimensions. This information of the EOM can be embedded in the Einstein-Hilbert action:

$$I_{EH} = \frac{1}{16\pi}\int_M d^D x\sqrt{-g}R, \tag{2.0.2}$$

with integration over the manifold M, and g is the determinant of the metric. If one applies the variational principle to this action, the Einstein field equations are obtained. Typically there will be a vanishing boundary on that derivation, but if we are in the case where the boundary on the manifold cannot be neglected, one should add the Gibbons-Hawking term to the Einstein-Hilbert action:

$$I_{GH} = \frac{1}{8\pi}\int_{\partial M} d^{D-1} y\varepsilon\sqrt{h}K, \tag{2.0.3}$$

with ∂M being the boundary of the Manifold, y is the coordinates on the boundary, h is the determinant of the induced metric, K is the trace of the second fundamental form i.e. the divergence of the normal vector to ∂M, called n^μ so $K = \nabla_\mu n^\mu$. And ε is a constant that is either $+1$ or -1 depending on whether the normal vector is spacelike or timelike. There exist several solutions to the Einstein field equations. Many of them may schematically be written on the spherically symmetric form:

$$ds^2 = -f(r)dt^2 + \frac{dr^2}{f(r)} + r^2 d\Omega^2_{D-2}, \tag{2.0.4}$$

where $d\Omega_{D-2}$ encodes the angular dependency of the metric. For the flat space solution, hence Minkowski space $f(r) = 1$, and for the Schwarzschild solution $f(r) = 1 - (r_0/r)^{D-3}$ with r_0 being the Schwarzschild radius. In both of these cases we assumed a vanshing EM tensor $T_{\mu\nu} = 0$.
We will now descrie the AdS space by embedding it in a larger space. One can write up a general metric with spacetime coordinates $(x_1, ...x_p, t_1, ...t_q)$ in the $\mathbb{R}^{p,q}$ space, where x_i is a spacelike direction and t_j is timelike:

$$ds^2 = -\sum_{j=1}^{q}(dt_j)^2 + \sum_{i=1}^{p}(dx_i)^2, \tag{2.0.5}$$

which is constrained to be on the quasi-sphere:

$$-\sum_{j=1}^{q} t_j^2 + \sum_{i=1}^{p} {x_i}^2 = ka^2, \tag{2.0.6}$$

where a is a spacial distance, which in cosmology is interpreted as the scale factor $a(t)$ that is time dependent, while in AdS space it is a constant called the AdS length scale. BHs in AdS space are classified as either small BH where $r_0 < a$ or big BHs where $r > a$. k determines the curvature of space. For $k = 1$ we have de Sitter (dS) space, which is positively curved, for $k = 0$ we have a flat space, and $k = -1$ we have the negatively curved Anti-de Sitter (AdS) space. These coordinates live in an embedding spacetime with one higher dimension than our target space i.e. $D + 1$ dimensional space. We get an Euclidean signature in our target space if we have one timelike coordinate and a Lorentzian signature if we have two timelike coordinates. We will now find the coordinates in our target space. One can use a parametrization of AdS space, from the embedding $\mathbb{R}^{D-1,2}$ space, using the global coordinates of $\{\tau, \rho, \theta_1, ...\theta_{D-2}\}$ by the transformation:

$$t_1 = a\cosh\rho\cos\tau, \quad t_2 = a\cosh\rho\sin\tau, \quad x_i = a\Omega_i\sinh\rho, \tag{2.0.7}$$

where $\sum_{i=1}\Omega_i^2 = 1$. The infinitesimal changes may be found using the chain rule:

$$dt_1 = \frac{dt_1}{d\tau}d\tau + \frac{dt_1}{d\rho}d\rho + \frac{dt_1}{d\Omega_i}d\Omega_i = -a\cosh\rho\sin\tau d\tau + a\sinh\rho\cos\tau d\rho, \tag{2.0.8}$$

similarly for dt_2 and dx_i. The metric is then:

$$ds^2 = -dt_1^2 - dt_2^2 + dx_i^2 = a^2(-\cosh^2\rho d\tau^2 + d\rho^2 + \sinh^2\rho d\Omega_{D-2}^2). \tag{2.0.9}$$

Apply yet another transformation $r = a\sinh\rho$, $t = a\tau$, so that ρ and its infinitesimal change is:

$$\rho = \sinh^{-1}\left(\frac{r}{a}\right), \qquad d\rho = \frac{dr}{\sqrt{a^2 + r^2}}, \tag{2.0.10}$$

which implies the following metric:

$$ds^2 = -f(r)dt^2 + \frac{dr^2}{f(r)} + r^2 d\Omega_{D-2}^2, \qquad f(r) = 1 + \frac{r^2}{a^2}. \tag{2.0.11}$$

In cosmology the convention of $a(t_0) = 1$ is often used for the scale factor, at time t_0 i.e. the age of the universe. In the case of a dS space, one would change to $k = +1$ and this would imply that $f(r) = 1 - r^2/a^2$. A negatively curved space also shows up as a solution for the geometry of the universe. Here one insists on a homogenous and isotropic universe and therefore a stress tensor is needed. The choice is the one from a perfect fluid:

$$T_{\mu\nu} = diag(-\rho, p, p, ..., p). \tag{2.0.12}$$

The solution to the Einstein field equations is given by the Friedmann-Lemaître-Robertson-Walker (FLRW) metric:

$$ds^2 = -dt^2 + \frac{a^2 dr^2}{1 - kr^2} + r^2 d\Omega_{D-2}^2. \tag{2.0.13}$$

In Appendix A.1 we investigate the FLRW metric further and derive the Friedmann equation.

2.1 Holography

The holographic principle was historically introduced when looking at BH information. We will therefore look into some thermodynamic properties, which are key when addressing BH information problems, of BHs in an asymptotically AdS space in this section. The static AdS space of Eq. (2.0.11) will have a locally

measured temperature when changing the space to Euclidean signature and periodically identifying the time coordinate as $t_E = -it$. This implies a period of an inverse temperature β. For radiation processes, there will be conformally invariant particles. This imposes a constraint on the EM tensor that it should be traceless $T^\mu_\mu = g^{\mu\nu}T_{\mu\nu} = 0$. Using the EM tensor for a perfect fluid in a flat background Eq. (2.0.12) the vanishing trace yields the constraint:

$$\rho = (D-1)p. \tag{2.1.1}$$

The energy-density ρ in D-dimensions is associated with the total radiated power from a blackbody source [19]:

$$\rho = P_{bb}(T) = \frac{N_{D,G}A_D}{(2\pi)^{D-1}}\int_0^\infty \frac{\omega^{D-1}d\omega}{e^{\beta\omega}-1} = \frac{N_{D,G}A_D}{(2\pi)^{D-1}}\zeta(D)\Gamma(D)T^D, \tag{2.1.2}$$

where $N_{D,G} = D(D-3)/2$ is the amount of Degrees Of Freedom (DOF) for the graviton, ω is the angular frequency, A_D is the surface area of an S^D unit sphere, $\zeta(D)$ is the Riemann ζ-function, $\Gamma(D)$ is the Γ-function, and T is the temperature. This enables us to write the EM tensor as:

$$T_{\mu\nu} = -(D-1)P_{bb}(T)\delta^0_\mu\delta^0_\nu + P_{bb}(T)\delta^i_\mu\delta^i_\nu, \tag{2.1.3}$$

with $i = 1, 2, 3, ..., D$. Redefine $N_{D,G}$ so that it absorbs a factor of $(D-1)(D-2)$, implying $N_{D,G} = D(D-1)(D-2)(D-3)/2$. The EM tensor is affected when changing the background from flat to AdS. The flat space has the metric: $ds^2 = -dt^2 + dr^2 + r^2 d\Omega^2_{D-2}$. Locally we can transform from the flat space to AdS by $t \to \sqrt{f(r)}t$. To have a smooth manifold the Euclidean time is periodic in $t \to t + \beta\sqrt{f(r)}$. This implies the local temperature $T_{loc} = \beta^{-1}f(r)^{-1/2}$. The temperature is given in our function $P_{bb}(T)$ so that we now have $T^4_{loc} = T^4 f(r)^{-2}$. Pulling out the $f(r)^{-2}$ so that the $P_{bb}(T)$ function is invariant, we obtain the EM tensor in an AdS background

$$\tilde{T}_{\mu\nu} = -(D-1)P_{bb}(T)f(r)^{-2}\delta^0_\mu\delta^0_\nu + P_{bb}(T)f(r)^{-2}\delta^i_\mu\delta^i_\nu. \tag{2.1.4}$$

Considering the Einstein field equations with a cosmological constant:

$$G_{\mu\nu} = 8\pi\left(T_{\mu\nu} - \frac{\Lambda}{8\pi}g_{\mu\nu}\right). \tag{2.1.5}$$

We can then absorb the cosmological constant into the EM tensor and define $A \equiv -\frac{\Lambda}{8\pi}$ so we have:

$$\hat{T}_{\mu\nu} = (\tilde{T}_{\mu\nu} + Ag_{\mu\nu}). \tag{2.1.6}$$

We, therefore, get the EM tensor to be written as in the Hawking-Page paper [6]:

$$T^\mu_\nu = A\delta^\mu_\nu + P_{bb}(T)f(r)^{-2}(\delta^\mu_\nu - 4\delta^\mu_0\delta^0_\nu). \tag{2.1.7}$$

This is the structure of the EM tensor in an AdS background. For $r \gg a$ an integral over the EM tensor will converge so that we have finite total energy.

We will now realize the holographic principle by computing the entropy of a BH in AdS space. The entropy is measured relative to an empty AdS background, and therefore we consider two metrics. This reference metric ensures that we only derive the entropy of the BH and not the AdS space itself. The metric from Eq. (2.0.11) that desribes empty AdS space is used with the metric that describes a Schwarzschild BH in AdS space:

$$ds^2 = -f(r)dt^2 + \frac{dr^2}{f(r)} + r^2 d\Omega^2_{D-2}, \qquad f(r) = 1 - \frac{w_D M}{r^{D-3}} + \frac{r^2}{a^2}, \qquad w_D \equiv \frac{16\pi}{(D-2)A_{D-2}}, \tag{2.1.8}$$

where $A_{D-2} = 2\pi^{(D-1)/2}/\Gamma(\frac{D-1}{2})$ is the surface area on an S^{D-2} unit sphere. We have a horizon at r_0 when $f(r_0) = 0$, which yields the $D-1$ polynomial equation:

$$r_0^{D-1} + a^2 r_0^{D-3} - w_D M a^2 = 0. \tag{2.1.9}$$

Refering to the solution of this equation as r_0 is sufficient for our purposes. We rather solve for the mass of the Schwarzschild AdS:

$$M = \frac{r_0^{D-3}}{w_D}\left(1 + \frac{r_0^2}{a^2}\right). \tag{2.1.10}$$

Then we consider the inverse temperature of the D-dimensional Schwarzschild AdS BH ($SAdS$) and the empty AdS space using the periodicity trick, Appendix A.2:

$$\beta_{AdS} = \frac{4\pi}{f'(r_0)} = \frac{4\pi a^2}{a^2 + r_0^2}, \tag{2.1.11}$$

$$\beta_{SAdS} = \frac{4\pi}{f'(r_0)} = \frac{4\pi r_0 a^2}{(D-3)a^2 + (D-1)r_0^2}. \tag{2.1.12}$$

Considering the Einstein-Hilbert action with a negative cosmological constant:

$$I = -\frac{1}{16\pi}\int d^D x\sqrt{-g}(R + 2\Lambda), \tag{2.1.13}$$

notice the action has a sign in front, due to the Euclidean signature. In any AdS space in D dimensions we have that the Ricci scalar is:

$$R = -\frac{D(D-1)}{a^2}. \tag{2.1.14}$$

Using Einstein's field equations for AdS space with a vanishing EM tensor $T_{\mu\nu} = 0$ we can find a relation between the Ricci scalar and the cosmological constant:

$$R_{\mu\nu} - \frac{1}{2}g_{\mu\nu}R - \Lambda g_{\mu\nu} = 0. \tag{2.1.15}$$

Taking the trace where $g_{\mu\nu}g^{\mu\nu} = D$ yields:

$$R = \frac{D}{1 - D/2}\Lambda, \tag{2.1.16}$$

which implies a relation between the AdS length scale and the cosmological constant:

$$\Lambda = \frac{(\frac{D}{2} - 1)(D-1)}{a^2}. \tag{2.1.17}$$

The volume integral of the action is infinite, so we need to put a regularization parameter L as an upper limit, which should be taken to ∞ at the end of the calculation. Our metric determinant is:

$$g = -r^{2(D-2)}\left(\sin^{D-3}\theta_1 \sin^{D-4}\theta_2 ... \sin^2\theta_{D-4}\sin\theta_{D-3}\right)^2, \tag{2.1.18}$$

with angular coordinate indices $\{\theta_1, \theta_2, ...\}$. The Ricci scalar and cosmological constants are independent of the coordinates so we compute the measure:

$$\begin{aligned}\int d^D x\sqrt{-g} &= \int dt_E dr d\theta_1 d\theta_2 ... d\theta_{D-2} r^{D-2}\sin^{D-3}\theta_1 \sin^{D-4}\theta_2 \times ... \times \sin^2\theta_{D-4}\sin\theta_{D-3} \\ &= \int_0^\beta dt_E \int dr r^{D-2}\int d\Omega_{D-2} = \beta\frac{L^{D-1}}{D-1}A_{D-2}.\end{aligned} \tag{2.1.19}$$

Eq. (2.1.13), Eq. (2.1.16) and Eq. (2.1.19) yields the action:

$$I_{AdS} = \frac{\Lambda A_{D-2} L^{D-1}\beta_{AdS}}{4\pi(D-1)(D-2)}, \tag{2.1.20}$$

$$I_{SAdS} = \frac{\Lambda A_{D-2}\left(L^{D-1} - r_0^{D-1}\right)\beta_{SAdS}}{4\pi(D-1)(D-2)}. \tag{2.1.21}$$

The Euclidean proper time of the two paths should agree when $r = L$. When computing the proper time the metric should only contain the time-component, that yields two versions of the proper time:

$$\Delta t_E = \int \sqrt{g_{\mu\nu} dx^\mu dx^\nu} = \beta_{AdS} \sqrt{\left(1 + \frac{L^2}{a^2}\right)}, \tag{2.1.22}$$

$$\Delta t_E = \int \sqrt{g_{\mu\nu} dx^\mu dx^\nu} = \beta_{SAdS} \sqrt{\left(1 - \frac{w_D M}{L^{D-3}} + \frac{L^2}{a^2}\right)}. \tag{2.1.23}$$

This gives us a relation between the two inverse temperatures, that is expanded for the squareroot:

$$\frac{\beta_{AdS}}{\beta_{SAdS}} = \sqrt{\frac{1 - \frac{w_D M}{L^{D-3}} + \frac{L^2}{a^2}}{1 + \frac{L^2}{a^2}}} \simeq 1 - \frac{w_D M a^2}{2L^{D-3}(a^2 + L^2)}. \tag{2.1.24}$$

Since we are computing the entropy of an AdS BH with a flat AdS reference metric, we should consider the change of the two actions while sending $L \to \infty$:

$$\Delta I = I_{SAdS} - I_{AdS} = \frac{A_{D-2} r_0^{D-2}(a^2 - r_0^2)}{4((D-3)a^2 + (D-1)r_0^2)}. \tag{2.1.25}$$

This change of action and the entropy have also been computed in [20] and in [21], for $D = 4$.
From statistical mechanics, we know that given a partition function in the canonical ensemble we can write up the entropy:

$$S = \beta \langle E \rangle + \ln Z, \qquad \langle E \rangle = -\frac{\partial}{\partial \beta} \ln Z, \tag{2.1.26}$$

while the partition function is given by the path integral:

$$Z[g_{\mu\nu}] = \int \mathcal{D} G_{\mu\nu} e^{-I[g_{\mu\nu}]}. \tag{2.1.27}$$

Computing the logarithm of the partition function gives a decoupling between the action and the partition function integral:

$$\ln Z = -I + \ln \int \mathcal{D} G_{\mu\nu}. \tag{2.1.28}$$

The difference in entropy between the AdS BH and empty AdS space is:

$$\Delta S = \left(\beta_{SAdS} \frac{\partial}{\partial \beta_{SAdS}} - 1\right) \Delta I, \tag{2.1.29}$$

where the partition function integrals over the field $G_{\mu\nu}$ gives the same constant for BH Ads and Ads. Applying the chain rule, we obtain the following derivatives, where the relation between r_0 and M is applied:

$$\frac{\partial r_0}{\partial \beta_{SAdS_D}} = \frac{((D-3)a^2 + (D-1)r_0^2)^2}{4\pi a^2((D-3)a^2 - (D-1)r_0^2)}, \tag{2.1.30}$$

$$\frac{\partial \Delta I}{\partial r_0} = \frac{-A_{D-2}(D-2) r_0^{D-3}(r_0^4(D-1) - a^4(D-3))}{4((D-3)a^2 + (D-1)r_0^2)^2}, \tag{2.1.31}$$

$$\frac{\partial \Delta I}{\partial \beta_{SAdS_D}} = \frac{A_{D-2}}{16\pi}(D-2) w_D M. \tag{2.1.32}$$

Finally we obtain the BH AdS entropy:

$$S_H = \beta_{SAdS_D} \frac{A_{D-2}}{16\pi}(D-2) w_D M - \Delta I = \frac{A_{D-2} r_0^{D-2}}{4}. \tag{2.1.33}$$

This is the same Hawking entropy as found when computing it in a flat background from the Schwarzschild metric. The same relation between the surface area of the BH and the entropy is valid.

The scaling of $S_H \sim A$ for a BH in flat space and AdS space indicates that the information may be stored on the boundary of these spaces. The gauge/gravity duality conjectures that pure gravitational physics in an asymptotic AdS space is a holographic dual to another class of physics, the CFTs. For the holographic principle to hold, one would expect to find the same scaling of entropy by a CFT computation. A CFT does not have any particular length scales, so when introducing a temperature, the scaling of the entropy can only be dependent on the temperature. In the large group dimensional N limit we have large temperatures. Therefore we have a small value of β and the relation to a length scale is $\beta \sim 1/r_0$. For the S^{D-2} sphere, the entropy scaling becomes $S \sim \beta^{-(D-2)}$ and likewise $S \sim r_0^{D-2}$ [21]. The proportionality to the area has been computed in $D = 5$ [22] to be the same as for the black hole. An observable, the entropy has been computed on the AdS side of the theory and motivated the same scaling through CFT arguments which agrees, thus realizing the holographic principle.

Chapter 3

Conformal Field Theories

A CFT is a specific kind of QFT that is invariant under conformal transformations. The CFTs are found at fixed points of the renormalization group flow. The β-function describes the trajectory of the renormalization group flow:

$$\beta(g) = \frac{\partial g}{\partial \log(\mu)}, \tag{3.0.1}$$

where μ is the renormalization scale and g is the coupling strength. When the β-function is vanishing we have a fixed point, and thus a CFT. Given the conformal symmetry at these points, the theory is under strong constraints so that the theory is completely described by the CFT data, without a Lagrange description. We will characterize the CFT data later in this chapter. [23].

The conformal transformations consist of translations, rotations, and boosts which constitute the Poincare group, and dilatations, and the Special Conformal Transformations (SCTs). The dilatation is a scale-changing transformation while it preserves angles. It implies that there is no preferred length scale in a CFT. Unlike a QFT which has DOF realized as particles, a CFT does not contain particles as a consequence of scale invariance. The symmetries under conformal transformations can be found when considering the conformal algebra.

3.1 Conformal Algebra

We will use the notation of a position x^μ in a D-dimensional space where $\mu = 0, 1, 2, 3, ..., D-1$ and $t = x^0$ is a time-like coordinate while $\vec{x} = (x^1, x^2, ..., x^{D-1})$ are space-like coordinates. In total, we have D components for each index. In this section, we will work with an Euclidean signature of the metric on $\mathbb{R}^D$ so that our algebra lives in the $SO(D)$ group. Associated with the global symmetries of the theory we have a current J_μ and a stress tensor $T_{\mu\nu}$ which are conserved quantities:

$$\partial_\mu J^\mu = 0, \qquad \partial_\mu T^{\mu\nu} = 0. \tag{3.1.1}$$

Since the EM tensor is a symmetric tensor, it can be decomposed into a symmetric and traceless part and a trace part. In order to have a conformal invariant theory we must have that the trace of the EM tensor vanishes $T^\mu_\mu = 0$. The Weyl transformation reads:

$$\delta g_{\mu\nu} = c(x)\delta_{\mu\nu}, \tag{3.1.2}$$

with $g_{\mu\nu}$ being the metric, and $\delta_{\mu\nu}$ being the metric of Euclidean space. In general these transformations change the metric from being flat to a curved one. But if we also insist on diffeomorphisms as a small

coordinate change, and likewise change the metric by:

$$x'^{\mu} = x^{\mu} + \epsilon^{\mu}(x), \qquad \delta g_{\mu\nu} = \partial_{\mu}\epsilon_{\nu} + \partial_{\nu}\epsilon_{\mu}, \tag{3.1.3}$$

then we can find a subclass of Weyl transformations where the geometry of spacetime is still flat up to a scale factor $c(x)$, through the Killing equation:

$$\partial_{\mu}\epsilon_{\nu} + \partial_{\nu}\epsilon_{\mu} = c(x)\delta_{\mu\nu}. \tag{3.1.4}$$

This equation has 4 types of solutions [24]:

$$\begin{aligned} &\epsilon^{\mu} = a^{\mu}, && c(x) = 0, \\ &\epsilon^{\mu} = x_{\nu}\omega^{[\nu\mu]} && c(x) = 0, \\ &\epsilon^{\mu} = \lambda x^{\mu}, && c(x) = 2\lambda, \\ &\epsilon^{\mu} = 2a_{\nu}x^{\nu}x^{\mu} - x^2 a^{\mu}, && c(x) = 4a^{\nu}x_{\nu}, \end{aligned} \tag{3.1.5}$$

where λ is a scaling constant and a^{μ} is a constant vector while $\omega_{[\mu\nu]}$ is an antisymmetric symbol, that gives a sign for interchanging the indices $\mu \leftrightarrow \nu$. Using the conformal transformation of Eq. (3.1.3) for a function which is expanded to first order gives:

$$f(x'^{\mu}) = f(x^{\mu} + \epsilon^{\mu}) = e^{-i\epsilon^{\mu}\partial_{\mu}} f(x^{\mu}) \simeq (1 - i\epsilon^{\mu}\partial_{\mu}) f(x^{\mu}). \tag{3.1.6}$$

The generators of the theory are now contracted with some arbitrary constants, and by comparing the expression to a Taylor polynomial we can write up these generators. The algebra of the theory is an extension to the Poincare algebra, in which it contains both generators of tranlations P_{μ}, rotations $M_{\mu\nu}$, dilatations D and SCTs, K_{μ}. These are written as [1]:

$$\begin{aligned} P_{\mu} &= -i\partial_{\mu}, & M_{\mu\nu} &= i(x_{\mu}\partial_{\nu} - x_{\nu}\partial_{\mu}), \\ D &= -ix^{\mu}\partial_{\mu}, & K_{\mu} &= -2ix_{\mu}x^{\nu}\partial_{\nu} + ix^2\partial_{\mu}. \end{aligned} \tag{3.1.7}$$

The generator of translations and SCTs has one index, with D components for each generator. The dilatation operator is a scalar with 1 component. One can represent the rotation generator as a matrix, with generally D^2 components. Due to the antisymmetry one may subtract the diagonal of D components and take half, since the entrances are repeated. This leaves us with $(D^2 - D)/2$ components for the generator of rotations, so that the total amount of DOF for a CFT:

$$N_{CFT} = 2D + 1 + \frac{D(D-1)}{2} = \frac{(D+1)(D+2)}{2}. \tag{3.1.8}$$

Now that we have a representation of the generators we can write up the conformal algebra. It consists of the Poincare algebra:

$$\begin{aligned} &[M_{\mu\nu}, M_{\rho\sigma}] = i(\delta_{\nu\rho}M_{\mu\sigma} - \delta_{\mu\sigma}M_{\rho\nu} - \delta_{\nu\sigma}M_{\mu\rho} + \delta_{\mu\rho}M_{\sigma\nu}), \\ &[P_{\mu}, P_{\nu}] = 0, \qquad [P_{\rho}, M_{\mu\nu}] = i(\delta_{\mu\rho}P_{\nu} - \delta_{\nu\rho}P_{\mu}), \end{aligned} \tag{3.1.9}$$

and the extended algebra [17, 24]:

$$\begin{aligned} [D, P_{\mu}] &= iP_{\mu}, & [D, K_{\mu}] &= -iK_{\mu}, \\ [K_{\mu}, P_{\nu}] &= 2i(\delta_{\mu\nu}D - M_{\mu\nu}), & [K_{\rho}, M_{\mu\nu}] &= i(\delta_{\rho\mu}K_{\nu} - \delta_{\rho\nu}K_{\mu}), \\ [D, M_{\mu\nu}] &= 0, \qquad [D, D] = 0, & [K_{\mu}, K_{\nu}] &= 0. \end{aligned} \tag{3.1.10}$$

One can view the SCT as a combination of inversions, R and translations of the form:

$$K_{\mu} = RP_{\mu}R. \tag{3.1.11}$$

[1] Notice that we are using D both for spacetime dimensions and the dilatation operator

An inversion transforms the positions by:

$$R : x^\mu \to x'^\mu = \frac{x^\mu}{x^2}. \tag{3.1.12}$$

By the following way, one can obtain the new coordinate x'^μ after a SCT is performed. Starting with an inversion and translate it by a^μ:

$$\frac{x^\mu}{x^2} - a^\mu = \frac{x^\mu - x^2 a^\mu}{x^2}, \tag{3.1.13}$$

we then apply an inversion of that vector:

$$\frac{(x^\mu + x^2 - a^\mu)/x^2}{(x^\mu + x^2 - a^\mu)^2/x^4} = \frac{x^2(x^\mu - x^2 a^\mu)}{x^2 + x^2 a^2 - 2x^2 x \cdot a}. \tag{3.1.14}$$

Yielding the special conformal transformed coordinates:

$$K_\mu : x^\mu \to x'^\mu = \frac{x^\mu - x^2 a^\mu}{1 + a^2 - 2x \cdot a}. \tag{3.1.15}$$

We have now written up the conformal algebra in D dimensions. Specifically for $D = 2$, the algebra is isomorphic to the Virasoro algebra and has thus been used in the development of ST, see Appendix B.2 for more on this.

3.2 Quantization

Quantization of a theory, in general, implies that states are living on surfaces of Hilbert spaces called leaves. When they are on the same surface the overlap between the initial and final state is given by a correlation function:

$$\langle \Psi_{Final} | \Psi_{Initial} \rangle . \tag{3.2.1}$$

If the states live on two different surfaces one needs a unitary evolution operator, U to consider the overlap:

$$\langle \Psi_{Final} | U | \Psi_{Initial} \rangle . \tag{3.2.2}$$

The arrangement of the surfaces is called a foliation. We apply the radial quantization, meaning that the foliation of S^{D-1} spheres are all centered at the origin of the Euclidean D-dimensional space, shown in Figure 3.1

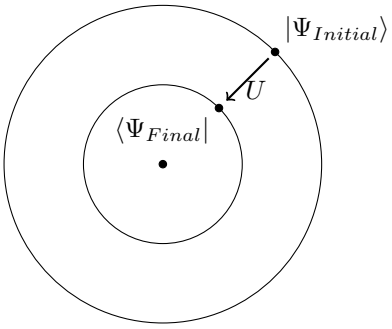

Figure 3.1: *The foliation of radial quantization, with the evolution operator U taking the initial state from one surface to another where the final state lives.*

The evolution operator is in general given by a Hamiltonian. In the radial quantization, the Hamiltonian is given by the dilatation operator. Meaning that the energies are the eigenvalues of the dilatation operator, hence the conformal scaling dimension. The evolution operator takes the form [2]:

$$U = e^{iD\Delta\tau}, \qquad \tau = \log r, \tag{3.2.3}$$

[2] $\Delta\tau$ is here the change in the τ coordinate

which yields that the radial quantization configuration gives conformal scaling dimensions Δ as the eigenvalue to the dilatation operator, while the eigenvalue of the rotation operator is the spin matrices, with spin indices $\{t\}, \{s\}$:

$$D\left|\Delta, l\right\rangle = i\Delta\left|\Delta, l\right\rangle, \qquad M_{\mu\nu}\left|\Delta, l\right\rangle_{\{s\}} = (\Sigma_{\mu\nu})^{\{t\}}_{\{s\}}\left|\Delta, l\right\rangle_{\{t\}}, \tag{3.2.4}$$

while l is the $SO(D)$ spin and $\Sigma_{\mu\nu}$ is a finite dimensional matrix. One may view the translation operator as a raising operator, and the operator for SCTs as a lowering operator:

$$P_\mu\left|\Delta\right\rangle = \left|\Delta + 1\right\rangle, \qquad K_\mu\left|\Delta\right\rangle = \left|\Delta - 1\right\rangle, \tag{3.2.5}$$

while the ground state level, hence the vacuum $|0\rangle$, will be annihilated by the SCT:

$$K_\mu\left|0\right\rangle = 0. \tag{3.2.6}$$

This is a result of commutators of Eq. (3.1.10) applied on the action of the dilatation operator, see Appendix B.1.

A primary field $\mathcal{O}_{(0)}$ has the conformal scaling dimension Δ while the descendants' fields $\mathcal{O}_{(n)}$ have $\Delta + n$. In this way we can see that n'th descendant state is given by acting with P_μ, n times. Since $(P_\mu)^n \sim (\partial_\mu)^n$ we say that descendant states are derivatives of primary states:

$$\mathcal{O}_{(n)} = \partial_{\mu_1}\partial_{\mu_2}...\partial_{\mu_n}\mathcal{O}_{(0)}. \tag{3.2.7}$$

We will expand the notation for the quantized theory to how conformal operators act on the fields. The general action, G of all CFT generators on the field $\mathcal{O}(x)$ is [24]:

$$G\mathcal{O}(x) = \Delta\partial_\mu\epsilon^\mu\mathcal{O}(x) + \epsilon^\mu\partial_\mu\mathcal{O}(x), \tag{3.2.8}$$

where ϵ^μ is given from Eq. (3.1.5) and the action of $G\mathcal{O}(x)$ can be written as the commutator $[G, \mathcal{O}(x)]$ for each generator:

$$\begin{aligned}
[P_\mu, \mathcal{O}(x)] &= -i\partial_\mu\mathcal{O}(x), \\
[D, \mathcal{O}(x)] &= -i(\Delta + x^\mu\partial_\mu)\mathcal{O}(x), \\
[M_{\mu\nu}, \mathcal{O}(x)] &= -i(\Sigma_{\mu\nu} + x_\mu\partial_\nu - x_\nu\partial_\mu)\mathcal{O}(x), \\
[K_\mu, \mathcal{O}(x)] &= -i(2x_\mu\Delta + x^\lambda\Sigma_{\lambda\mu} + 2x_\mu(x^\rho\partial_\rho) - x^2\partial_\mu)\mathcal{O}(x).
\end{aligned} \tag{3.2.9}$$

We now have the conformal algebra, which includes how operators act on fields and states. This quantization and the conformal algebra is needed when deriving the observables of the theory, namely the correlation functions. The algebra and radial quantization can put bounds on and restrict the correlation function. This is seen in the unitarity bound and the Operator Product Expansion (OPE).

3.3 Unitarity Bound

In a quantum theory, we have operators which are unitary $UU^\dagger = I$. Unitarity implies that all matrix elements that can represent a norm of a state constructed by conformal generators must be positive $\lambda \geq 0$. Otherwise, we would have unphysical states. By imposing the unitarity bound, this is avoided. We will now show how unitarity implies some strict constraints on the scaling dimension. Let us consider a state $P_\mu\left|\Delta, l\right\rangle$, and that the SCT operator is the hermitian conjugate of the translation operator $K_\mu = (P_\mu)^\dagger$. Let us consider a matrix element, which is the norm of that state:

$$A_{\nu\{t\},\mu\{s\}} = {}_{\{t\}}\left\langle\Delta, l|K_\nu P_\mu|\Delta, l\right\rangle_{\{s\}}, \tag{3.3.1}$$

with $\{s\}$ and $\{t\}$ being the spin indices. We will call the eigenvalue of this operator λ_A so that it obeys the bound $\lambda_A \geq 0$ by unitarity. Since the operator K_μ annihilates the state, and the translation operator annihilates the hermitian conjugated state:

$$K_\mu\left|\Delta\right\rangle = 0, \qquad \left\langle\Delta\right| P_\mu = 0, \tag{3.3.2}$$

we express the relation as the commutator in the matrix using Eq. (3.1.10):

$$A_{\nu\{t\},\mu\{s\}} = {}_{\{t\}}\langle \Delta, l| K_\nu P_\mu |\Delta, l\rangle_{\{s\}} = {}_{\{t\}}\langle \Delta, l| 2iD\delta_{\mu\nu} - 2iM_{\mu\nu} + P_\mu K_\nu |\Delta, l\rangle_{\{s\}}, \tag{3.3.3}$$

where the last term annihilates the state and vanishes.. The first term gives an eigenvalue of scaling dimension, while the second term is defined as a new matrix element:

$$A_{\nu\{t\},\mu\{s\}} = -2\Delta\delta_{\mu\nu} + 2B_{\mu\{s\}\nu\{t\}}, \qquad B_{\mu\{s\}\nu\{t\}} \equiv -i\langle\{t\}| M_{\mu\nu} |\{s\}\rangle. \tag{3.3.4}$$

One can rewrite the rotation generator in the $\{s\}$ $\{t\}$ space:

$$-iM_{\mu\nu} = -\frac{1}{2}(V^{\alpha\beta})_{\mu\nu}(M_{\alpha\beta})_{\{s\},\{t\}}, \tag{3.3.5}$$

which is analogus to the spin orbit coupling $L \cdot S = \frac{1}{2}((L+S)^2 - L^2 - S^2)$.

The Casimir operator, C, is the one operator that commutes with all elements in the group, hence it commutes with the CFT generators. In section 3.8 we will expres C in terms of the CFT generators. It will act and give the same eigenvalue on every state in an irreducible representation, where the eigenvalue is given by:

$$C_{\Delta,l} = \Delta(\Delta - D) + l(l + D - 2). \tag{3.3.6}$$

The matrix element $B_{\mu\{s\}\nu\{t\}}$ corresponds to a Casimir value of the $SO(D)$ spin representation $C_{0,l} = l(l + D - 2)$ for each operators $V^2 \to C_{0,1}$ and $M^2 \to C_{0,l}$ and $(M + V)^2 \to C_{0,l-1}$:

$$\lambda_B = \frac{1}{2}(C_{0,l} + C_{0,1} - C_{0,l-1}), \tag{3.3.7}$$

giving the eigenvalue of $B_{\mu\{s\}\nu\{t\}}$:

$$\lambda_B = \frac{1}{2}(l(l + D - 2) + D - 1 - (l - 1)(l - 1 + D - 2)) = D + l - 2. \tag{3.3.8}$$

This yields the maximal unitarity bound, when inserting back into $A_{\nu\{t\},\mu\{s\}}$. Specifically for scalars the bound may also be computed. The spin quantum number is $l = 0$ so the state vanishes when acted upon with the generator of rotations $M_{\mu\nu}|\Delta\rangle = 0$. We consider the first level i.e. the norm of the state $P_\mu|\Delta\rangle$:

$$A_{\mu\nu} = \langle\Delta|K_\mu P_\nu|\Delta\rangle, \tag{3.3.9}$$

we write out the commmutator:

$$A_{\mu\nu} = \langle\Delta|2i(\delta_{\mu\nu}D - M_{\mu\nu}) + P_\nu K_\mu|\Delta\rangle = 2i\delta_{\mu\nu}\langle\Delta|D|\Delta\rangle = -2\delta_{\mu\nu}\Delta. \tag{3.3.10}$$

Changing the matrix element to the norm of state $P_\mu|\Delta\rangle$ says that the indices μ, ν should be contracted, this yields the unitarity bound:

$$\lambda_A = -2D\Delta \geq 0 \to \Delta \geq 0. \tag{3.3.11}$$

Considering the second level, i.e. the norm of state $P_\mu P^\mu|\Delta\rangle$ we can find a stronger unitarity bound. This will be the strongest bound so that higher levels do not restrict this bound further [24]. We consider the matrix element:

$$A_{\mu\nu\rho\sigma} = \langle\Delta|K_\mu K_\nu P_\rho P_\sigma|\Delta\rangle, \tag{3.3.12}$$

applying a range of commutator relations so that one can move all translations operators to the left and SCTs to the right one ends up with the expression:

$$A_{\mu\nu\rho\sigma} = -4i(\delta_{\nu\rho}\delta_{\mu\sigma} + \delta_{\nu\sigma}\delta_{\mu\rho} - \delta_{\rho\sigma}\delta_{\mu\nu})\langle\Delta|D|\Delta\rangle - 4(\delta_{\nu\rho}\delta_{\mu\sigma} + \delta_{\mu\rho}\delta_{\nu\sigma})\langle\Delta|D^2|\Delta\rangle. \tag{3.3.13}$$

In order to change this to the norm of the state we need to contract μ, ν and σ, ρ, giving the bound:

$$\lambda_A = \Delta D(2 - D + 2\Delta) \geq 0. \tag{3.3.14}$$

The result is that the unitarity bounds read:

$$\begin{aligned} &\Delta \geq \frac{D}{2} - 1, \quad \text{for} \quad l = 0, \\ &\Delta \geq l + D - 2 \quad \text{for} \quad l \neq 0. \end{aligned} \tag{3.3.15}$$

These unitarity bounds are important for CFTs, since they restrict the scaling dimension, and thus the correlation functions from below. But first, we need to describe the coordinate systems used in D-dimensional CFTs.

3.4 Coordinate Systems in Conformal Field Theories

For a general D-dimensional CFT with 4 operators in different locations x_i^μ, where $i = 1, 2, 3, 4$ and $\mu = 0, 1, ..., D-1$, we can use conformal symmetry to project the locations onto a complex plane plus a point at infinity. We only need a complex variable z and its conjugate to describe their position between two operators, while the remaining two are fixed at certain locations. Specifically, we can imagine a 4-point correlator between 4 operators at generic locations in $\mathbb{R}^D$ Euclidean space. We may then use SCTs to send $|x_4^\mu| \to \infty$. Using translations we can send x_1^μ to the origin $x_1^\mu = (0, 0, ..., 0)$. Using rotations and dilatations we can fix $x_3^\mu = (1, 0, 0, ..., 0)$. The location of the last operator will be at $x_2^\mu = (x, y, 0, ..., 0)$. In other words we have a conformal transformation $T \in SO(D)$ which fixes $T : \{x_1, x_2, x_3, x_4\} \to \{0, z, 1, \infty\}$. The 2-dimensional sheet is depicted in Figure 3.2

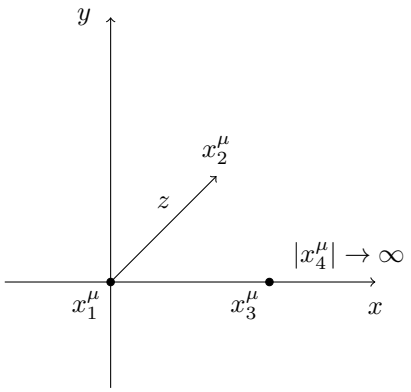

Figure 3.2: *Conformal symmetries may put the locations of operators/fields on this particular configuration in the complex plane. We will refer to this configuration as the z-picture.*

We can describe the location of the second field with respect to the first field by a complex variable z and its complex conjugate $\bar{z}$:

$$z = x + iy, \qquad \bar{z} = x - iy, \tag{3.4.1}$$

we will refer to these coordinates as the Dolan-Osborn coordinates [25, 26].
Another coordinate system is the conformal invariant cross-ratios. They are related to the positions of the operators:

$$u = \frac{x_{12}^2 x_{34}^2}{x_{13}^2 x_{24}^2}, \qquad v = \frac{x_{14}^2 x_{23}^2}{x_{13}^2 x_{24}^2}, \tag{3.4.2}$$

where we have the position differennce $x_{ij}^\mu = x_i^\mu - x_j^\mu$. Notice that the coordinates themselves are related by an interchange of operator positions $v = u_{2 \leftrightarrow 4}$. The connection to the Dolan-Osborn coordinates is:

$$u = z\bar{z}, \qquad v = (1 - z)(1 - \bar{z}), \tag{3.4.3}$$

The connection to the 2D sheet Cartesian variables is:

$$u = x^2 + y^2, \qquad v = (x - 1)^2 + y^2. \tag{3.4.4}$$

In both Lorentzian and Euclidean CFTs the conformal cross-ratios are restriced to positive values [27]:

$$0 \leq u, v \leq \infty. \tag{3.4.5}$$

The extra bound for an Euclidean CFT is [27]:

$$(1-\sqrt{u})^2 < v < (1+\sqrt{u})^2, \tag{3.4.6}$$

which has a special interpretation in radial/angular coordinates, that we will comment on soon when introducing these coordinates. We may divide the $\{u, v\}$-plane into three regions

$$\begin{aligned} & 0 \leq u, v \leq 1, && \text{Region A}, \\ 1 \leq u, \quad & 0 \leq v \leq u, && \text{Region B}, \\ 1 \leq v, \quad & 0 < u \leq v, && \text{Region C}. \end{aligned} \tag{3.4.7}$$

We will refer to region A as the unit box, while it has also been referred to as the diamond in $\{z, \bar{z}\}$ coordinates [28]. Using Eq. (3.4.2) one may interchange the location of two operators $x_i \leftrightarrow x_j$. Such an interchange of operators will induce the transformations, in the specific situations:

$$u \to \frac{u}{v}, \quad v \to \frac{1}{v}, \qquad x_1 \leftrightarrow x_2, \qquad A \leftrightarrow C, \tag{3.4.8}$$

$$u \to v, \quad v \to u, \qquad x_1 \leftrightarrow x_3, \qquad B \leftrightarrow C, \tag{3.4.9}$$

$$u \to \frac{1}{u}, \quad v \to \frac{v}{u}, \qquad x_1 \leftrightarrow x_4, \qquad A \leftrightarrow B. \tag{3.4.10}$$

An interchange of $x_1 \leftrightarrow x_2$ is equivalent to interchanging $x_1 \leftrightarrow x_4$ and then $x_1 \leftrightarrow x_3$. These symmetries can be used in a mapping between region A,B and C as shown. With the mapping in mind, we can restrict ourselves to the unit box. The relation between the $\{u, v\}$ coordinates and $\{z, \bar{z}\}$ in Eq. (3.4.3) imposes the range of the diamond:

$$0 \leq z, \bar{z} \leq 1. \tag{3.4.11}$$

A direction that we will explore in this thesis will be to express this sheet in radial and angular coordinates. One can do this by writing the complex variables as:

$$z = se^{i\phi}, \qquad \bar{z} = se^{-i\phi}, \tag{3.4.12}$$

so that s is a radial coordinate and $\phi = arg(z)$ is an angular:

$$s = |z| = \sqrt{z\bar{z}}, \qquad \xi = \cos\phi = \frac{z+\bar{z}}{2\sqrt{z\bar{z}}}. \tag{3.4.13}$$

We may think of $\cos(\arg(z))$ as a vector in the unit circle which is projected down to the x-axis. This yields a range of ξ, while the range for s follows from the ranges of $\{z, \bar{z}\}$:

$$0 \leq s \leq 1, \qquad -1 \leq \xi \leq 1. \tag{3.4.14}$$

Another way to view these Euclidean unit box bounds is that the u bounds imply a unit circle in the complex plane centered at the origin and that the v bounds imply a unit circle around 1 in the complex plane, which is given when writing the box bounds in cartesian coordinates e.g. $(x-1)^2 + y^2 < 1$. The overlapping region of the two unit circles corresponds to where both of these bounds are satisfied. The Euclidean regime is therefore mapped from a box in $\{u, v\}$ coordinates to an overlapping region of unit circles in $\{s, \phi\}$ coordinates.
The Euclidean bounds can also be viewed as a constraint coming from the unit circle. One can write:

$$\cos\phi = \frac{1+u-v}{2\sqrt{u}}. \tag{3.4.15}$$

where the angle is restricted within $-1 < \cos\phi < 1$. Solving for $\{u, v\}$ implies the Euclidean bounds in Eq. (3.4.6).

These coordinate bounds are important when dicussing the crossing relation of the 4-point correlation functions. We will dicuss crossing relations further in the next sections.

3.5 The Operator Product Expansion

The OPE is an important method that simplifies and constrains our correlation functions. One can determine the 3-point correlation function as a sum over 2-point correlation functions using the OPE. Likewise, 4-point correlation functions can be fixed up to a sum over conformal blocks and OPE coefficients using the OPE. Therefore it is a needed method to our CFT toolbox.

One is able to replace two local operators when they are very close to each other by a series of operators at the midpoint. If we have a state $|\Psi\rangle$ and two fields ϕ within the sphere of state $|\Psi\rangle$, it generates the state:

$$|\Psi\rangle = \phi(x)\phi(y=0)\,|0\rangle\,, \tag{3.5.1}$$

where x, y and later z are operator locations, equivalent to x_i^μ with a change of notation. We have that a state can be expanded in a basis of energies, which in the radial quantization corresponds to dilatations:

$$|\Psi\rangle = \sum_n c_n\,|E_n\rangle\,. \tag{3.5.2}$$

These energy states corresponds to operators, so using Eq. (3.5.1) and Eq. (3.5.2) we can write an expansion over the fields at $y = 0$:

$$\phi(x)\phi(y=0)\,|0\rangle = \sum_{\mathcal{O}} \lambda_{\mathcal{O}} C_{\mathcal{O}}(x,\partial_y)\mathcal{O}(y=0)\,|0\rangle\,, \tag{3.5.3}$$

where $\mathcal{O}$ is a primary operator, and $C_{\mathcal{O}}$ is a power series in ∂_y. Conformal invariance can fix the power series up to the prefactor $\lambda_{\mathcal{O}}$ called the OPE coefficient. Let us apply the OPE to the 3-point correlation function:

$$\langle\phi_1(x)\phi_2(y=0)\phi_3(z)\rangle = \sum_{\mathcal{O}} \lambda_{\mathcal{O}} C_{\mathcal{O}}(x,\partial_y)\,\langle\mathcal{O}(y)\phi(z)\rangle\,. \tag{3.5.4}$$

In Appendix B.3 we show how to determine the first terms in OPE coefficient expansion, which for a scalar field is:

$$C_\phi(x,\partial_y) = \frac{1}{|x|^{2\delta-\Delta}}\left(1 + \frac{1}{2}x^\mu\partial_\mu + \frac{\Delta+2}{8(\Delta+1)}x^\mu x^\nu\partial_\mu\partial_\nu + \frac{-\Delta}{16(\Delta-D/2+1)(\Delta+1)}x^2\partial^2 + ...\right). \tag{3.5.5}$$

3.6 Correlation Functions and the Bootstrap Equation

The n-point correlation function is defined as a functional expectation value of operators $\mathcal{O}_i$ at different locations x_i written as:

$$\langle\mathcal{O}_1(x_1)\mathcal{O}_2(x_1)...\mathcal{O}_n(x_n)\rangle\,. \tag{3.6.1}$$

These correlation functions are the observables of a CFT. The operators to be considered in the theory are scalars ϕ, vector fields J_μ and stress tensor $T_{\mu\nu}$. The symmetries of CFT fix the 2-point function. Translation and rotation invariance say that it must be given by some function that is only dependent on the length between operators $\sim f(|x_1 - x_2|)$. Then scale invariance fixes the structure of the 2-point correlation function:

$$\langle\mathcal{O}_1(x_1)\mathcal{O}_2(x_2)\rangle = \frac{\delta_{12}}{|x_{12}|^{\Delta_1+\Delta_2}}, \tag{3.6.2}$$

where $x_{ij} = x_i - x_j$, and δ_{12} is the Kronecker δ, while Δ_1 and Δ_2 are the conformal scaling dimensions with respect to operator 1 and operator 2.

We observe such a dependency in the Ising model. Here we have a chain of magnets that react to an applied magnetic field. These magnets will have a spin σ and be at some distance r. The operators of interest in the correlation function are among others the spins, and the correlation function for a non-interacting theory will follow the structure of a CFT 2-point function [24]:

$$\langle\sigma(r)\sigma(0)\rangle \sim \frac{1}{r^{2\Delta}}, \tag{3.6.3}$$

where Δ is the dimension that is dependent on the spin.

This structure is closely related to critical points in phase transitions. A critical point is when a system is at the critical temperature T_C and at the critical pressure P_C, so that the system is undergoing a second order phase transition/continuous phase transition [29]. In such a system the magnetic susceptibility χ will be dependent on a critical exponent α by the following relation:

$$\chi \propto |T_C - T|^{-\alpha}, \tag{3.6.4}$$

where T is the temperature. When studying CFT correlation functions we also study the Ising model and the critical points in phase transitions.

The CFT symmetries can also fix the 3-point function:

$$\langle \mathcal{O}_1(x_1)\mathcal{O}_2(x_2)\mathcal{O}_3(x_3)\rangle = \frac{\lambda_{123}}{|x_{12}|^{\Delta_1+\Delta_2-\Delta_3}|x_{23}|^{\Delta_2+\Delta_3-\Delta_1}|x_{13}|^{\Delta_1+\Delta_3-\Delta_2}}, \tag{3.6.5}$$

the constant λ_{123} can be fixed depending on which operators are chosen. If we specifically consider the 3-point function of some operators with the same scaling dimension Δ and the stress tensor with scaling dimension $\Delta_T = D-2$, we have the following structure of the 3-point function:

$$\langle \mathcal{O}(x_1)\mathcal{O}(x_2)T^{\mu\nu}(x_3)\rangle = \lambda_{\mathcal{O}\mathcal{O}T}\frac{H^{\mu\nu}(x_1,x_2,x_3)}{|x_{12}|^{2\Delta-D+2}|x_{13}|^{D-2}|x_{23}|^{D-2}}, \tag{3.6.6}$$

where the OPE coefficient can be fixed to be [17, 30]:

$$\lambda_{\mathcal{O}\mathcal{O}T} = -\frac{D\Delta}{D-1}\frac{\Gamma(D/2)}{2\pi^{D/2}}. \tag{3.6.7}$$

In the large D limit using the Stirling approximation this scales as:

$$\lambda_{\mathcal{O}\mathcal{O}T} \sim -2^{-D/2}\pi^{(D+1)/2}e^{-D/2}\Delta D^{(D-1)/2}. \tag{3.6.8}$$

This D^D scaling is striking in the context of large D CFTs and could well be important for future work on the subject. For large D Schwarzschild BHs one can find that the power also scales with $P_{bb} \sim D^D$ [31]. This scaling suggests that methods of bound restrictions from [31] can be applied for 3-point correlation functions.

The 4-point function cannot be fixed completely by conformal symmetries, instead it depends on some conformal partial wave function $\mathcal{A}(u,v)$. This function is expanded into an irreducible representation of the conformal algebra i.e. conformal blocks. The OPE fixes the structure of the 4-point correlation function:

$$\langle \mathcal{O}(x_1)\mathcal{O}(x_2)\mathcal{O}(x_3)\mathcal{O}(x_4)\rangle = \frac{\mathcal{A}(u,v)}{(x_{12}^2x_{34}^2)^{\Delta}}, \qquad \mathcal{A}(u,v) = \sum_{\mathcal{O}'} P_{\mathcal{O}'}G_{\Delta_{\mathcal{O}'},l_{\mathcal{O}'}}(u,v), \tag{3.6.9}$$

where $P_{\mathcal{O}'}$ is the conformal block coefficient, which is closely related to the OPE coefficent $P_{\mathcal{O}'} = |\lambda_{\mathcal{O}'}|^2$, and $G_{\Delta_{\mathcal{O}'},l_{\mathcal{O}'}}(u,v)$ is the conformal block. The sum is over $\mathcal{O}'$s which are the possible operators for the propagator. Schematically we can write the correlation function as in Figure 3.3. The $\mathcal{O}'$ operators have different spins l and scaling dimensions Δ, so we assume the sum to decompose into a sum over these two physical objects.

The simplest correlator is for identical scalars, which will have the main focus in this project. Due to the fields being identical this lets us put constraints on the correlation function by the bootstrap method. For identical scalars ϕ and corresponding scaling dimension Δ_ϕ we have the following structure:

$$\langle \phi(x_1)\phi(x_2)\phi(x_3)\phi(x_4)\rangle = \frac{\mathcal{A}(u,v)}{(x_{12}^2x_{34}^2)^{\Delta_\phi}}, \tag{3.6.10}$$

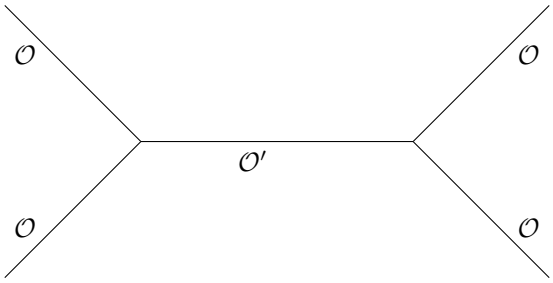

Figure 3.3: *Schematical representation of the 4-point correlation function of identical fields $\mathcal{O}$ which sums over the propagator fields $\mathcal{O}'$. This is equivalent to a Feynman diagram from QFT for a CFT.*

The 4-point correlation function is the most interesting in CFTs because it can put constraints on the irreducible representation of the conformal algebra, where the 2-point and 3-point functions are too simple.

Concerning the 4-point correlation function, conformal invariance and the fact that we work with identical scalars let us interchange the positions of the operators to 3 types of configurations called channels, which are comparable to the Mandelstam variables of the s, t, u channels. These 3 different computation channels of the same correlation function let us put a condition on the conformal block, known as the conformal bootstrap. If one interchanges the position of the operators $1 \leftrightarrow 2$ or $3 \leftrightarrow 4$ we get the symmetry [17]:

$$\mathcal{A}(u,v) = \mathcal{A}\left(\frac{u}{v}, \frac{1}{v}\right), \tag{3.6.11}$$

while interchanging $1 \leftrightarrow 3$ and $2 \leftrightarrow 4$ yields the bootstrap equation:

$$\mathcal{A}(u,v) = \left(\frac{u}{v}\right)^{\Delta_\phi} \mathcal{A}(v,u). \tag{3.6.12}$$

The sum over conformal blocks includes a unit operator when the scaling dimension and spin is 0. This enables us to write:

$$\mathcal{A}(u,v) = 1 + \sum_{\Delta,l} P_{\Delta,l} G_{\Delta,l}(u,v), \tag{3.6.13}$$

applying this to the conformal bootstrap Eq. (3.6.12) yields the crossing function, which is by construction equal to 1:

$$F(u,v) \equiv \sum_{\Delta,l} P_{\Delta,l} \frac{v^{\Delta_\phi} G_{\Delta,l}(u,v) - u^{\Delta_\phi} G_{\Delta,l}(v,u)}{u^{\Delta_\phi} - v^{\Delta_\phi}} = 1 \tag{3.6.14}$$

The crossing function is useful when checking whether the crossing constraints are consistent for a particular OPE coefficient or conformal block. We will specifically use this when reviewing a paper on conformal blocks in a large D limit, and comparing this crossing function to the exact D-dimensional block in the case of $D = 4$.

One may further reduce any n-point function to a 1-point function. To do this one has to know the CFT data. The CFT data consists of the scaling dimensions Δ and the irreducible representations of all primary operators, and the OPE coefficients λ_{ijk}. This data defines the particular CFT. The CFT data must obey the unitarity bound, the bootstrap equation, and that the EM tensor $T_{\mu\nu}$ must obey Ward identities. The Ward identities will not be applied in this thesis, and we have therefore excluded them from this CFT overview.

3.7 Embedding Space Formalism

In this section, we introduce the embedding space formalism. This is a natural space in which to write the CFT algebra since it compares nicely to the AdS algebra. We will also use this formalism when introducing

the Casimir operator, which is important for getting the structure of the conformal blocks. The conformal group with Euclidean signature $SO(D)$ is isomorphic to the Lorentz group of $SO(D+1,1)$. The conformal group thereby lives in a $\mathbb{R}^D$ space that can be mapped to an embedding Minkowski space $\mathbb{R}^{D+1,1}$. We, therefore, include new indices with capital roman letters $A = 0, \mu, D+1$. The new embedding space coordinates X^A are related to the $SO(D)$ algebra by [30]:

$$X^0 = \frac{1+x^2}{2}, \qquad X^\mu = x^\mu, \qquad X^{D+1} = \frac{1-x^2}{2}. \tag{3.7.1}$$

This is a natural choice since $(X^A)^2 = -(X^0)^2 + (X^\mu)^2 + (X^{D+1})^2 = 0$ so that they are on the light-cone. This leaves a Minkowski metric on the mostly plus form $\eta_{AB} = diag(-1, 1, ..., 1)$. The generator of the CFT algebra in our embedding space is then:

$$J_{AB} = -i\left(X_A \frac{\partial}{\partial X^B} - X_B \frac{\partial}{\partial X^A}\right), \tag{3.7.2}$$

which is antisymmetric $J_{AB} = -J_{BA}$ in its indices. The commutator of the generator with itself is:

$$[J_{AB}, J_{CD}] = i(\eta_{AC}J_{BD} + \eta_{BD}J_{AC} - \eta_{BC}J_{AD} - \eta_{AD}J_{BC}). \tag{3.7.3}$$

One can identify the CFT algebra as the projection from the embedding space $SO(D+1,1)$ to the target space:

$$D = -iJ_{0,D+1}, \qquad P_\mu = J_{\mu,0} - J_{\mu,D+1}, \qquad M_{\mu\nu} = J_{\mu\nu}, \qquad K_\mu = J_{\mu,0} + J_{\mu,D+1}, \tag{3.7.4}$$

establishing the same algebra as the $SO(D)$ CFT. The particular fascinating thing about this embedding space formalism is that the structure of the generators and coordinates are very similar to that of AdS space. With a slight change of notation, chapter 2 had the structure of an $SO(D+1,1)$ space with a choice of coordinates $-(Y^0)^2 + (Y^\mu)^2 + (Y^{D+1})^2 = -a^2$, with a being the AdS length scale. The generators in this space are given as:

$$I_{AB} = -i\left(Y_A \frac{\partial}{\partial Y^B} - Y_B \frac{\partial}{\partial Y^A}\right), \tag{3.7.5}$$

and obey the same commutation relation as Eq. (3.7.3). Since the conformal group with Euclidean signature $SO(D)$ is isomorphic to $SO(D+1,1)$ and equivalent to the generator of AdS, we have a natural correspondence between the CFT and the AdS algebra.

3.8 Casimir Operator and Conformal Blocks

In section 3.3 we introduced the Casimir operator. We will now introduce a method to derive the conformal blocks using this operator. The embedding space formalism is isomorphic to the conformal algebra, so we can write the Casimir in $SO(D+1,1)$ as:

$$C = \frac{1}{2}J_{AB}J^{AB}. \tag{3.8.1}$$

Acting with the Casimir on a state $C\phi(x_1)\phi(x_2)\left|0\right\rangle = \mathcal{D}\phi(x_1)\phi(x_2)\left|0\right\rangle$ gives the differential operator at position 1 and 2:

$$\mathcal{D} = \frac{1}{2}(J^1_{AB} + J^2_{AB})(J_1^{AB} + J_2^{AB}). \tag{3.8.2}$$

Due to symmetry this is equivalent to an operator at position 3 and 4. When acting on a conformal block, we get an eigenvalue equation:

$$\mathcal{D}G_{\Delta,l} = C_{\Delta,l}G_{\Delta,l}. \tag{3.8.3}$$

with the Casimir eigenvalue $C_{\Delta,l}$ defined in Eq. (3.3.6). We will now write the differential operator in terms of the generators. Notice that the metric in the embedding formalsim is:

$$\eta_{00} = -1, \quad \eta_{\mu\mu} = \eta_{D+1,D+1} = 1, \tag{3.8.4}$$

with indices A, B going from 0 to $D+1$. The operators J_{AB} can be identified as:

$$J_{0,D+1} = D, \quad J_{\mu\nu} = M_{\mu\nu}, \quad J_{D+1,\mu} = \frac{1}{2}(P_\mu + K_\mu), \quad J_{0\mu} = \frac{1}{2}(P_\mu - K_\mu), \tag{3.8.5}$$

which yields the Casimir:

$$C = \frac{1}{2}M_{\mu\nu}M^{\mu\nu} - D^2 + \frac{1}{2}(P_\mu K^\mu + K_\mu P^\mu). \tag{3.8.6}$$

One may use the differential operator of Eq. (3.8.2) and act with this on the 4-point correlation functions in the radial quantization. Using this one can re-write this differential operator in the Dolan-Osborn coordinates or conformal invariant cross-ratios [17, 26]:

$$\frac{\mathcal{D}(z,\bar{z})}{2} = z^2(1-z)\partial_z^2 - z^2\partial_z + (z \rightleftarrows \bar{z}) + (D-2)\frac{z\bar{z}}{z-\bar{z}}((1-z)\partial_z - (z \rightleftarrows \bar{z})), \tag{3.8.7}$$

$$\begin{aligned}\frac{\mathcal{D}(u,v)}{2} &= [(1-v)^2 - u(1+v)]v\partial_v^2 + (1-u+v)u^2\partial_u^2 - (1+u-v)u\partial_u + [(1-v)^2 - u(1+v)]\partial_v \\ &\quad - 2(1+u-v)uv\partial_u\partial_v - (D-2)u\partial_u.\end{aligned} \tag{3.8.8}$$

In Appendix B.4 we show the connection between $\{z, \bar{z}\} \to \{u, v\}$ differential operators.
The solution, hence the conformal blocks, to these conformal Casimir equations have been found by Dolan-Osborn in dimensions $D = 2, 4, 6$ [17, 26]:

$$\begin{aligned}
G_{\Delta,l}^{D=2} &= k_{\Delta+l}(z)k_{\Delta-l}(\bar{z}) + k_{\Delta-l}(z)k_{\Delta+l}(\bar{z}), \\
G_{\Delta,l}^{D=4} &= \frac{z\bar{z}}{z-\bar{z}}(k_{\Delta+l}(z)k_{\Delta-l-2}(\bar{z}) - k_{\Delta-l-2}(z)k_{\Delta+l}(\bar{z})), \\
G_{\Delta,l}^{D=6} &= \left(-\frac{1}{2}\right)^l \frac{(z\bar{z})^3}{(z-\bar{z})^3}[k_{\Delta+l}(z)k_{\Delta-l-6}(\bar{z}) - \frac{(\Delta-4)(\Delta+l)^2}{16(\Delta-2)(\Delta+l-1)(\Delta+l+1)}k_{\Delta+l+2}(z)k_{\Delta-l-4}(\bar{z}) \\
&\quad - \frac{l+3}{l+1}k_{\Delta+l-2}(z)k_{\Delta-l-4}(\bar{z}) + \frac{(\Delta-4)(l+3)(\Delta-l-4)^2}{16(\Delta-2)(l+1)(\Delta-l-5)(\Delta-l-3)}k_{\Delta+l}(z)k_{\Delta-l-2}(\bar{z}) - z \leftrightarrow \bar{z}], \\
k_\beta(x) &= x^{\beta/2}{}_2F_1(\beta/2, \beta/2, \beta, x),
\end{aligned} \tag{3.8.9}$$

where ${}_2F_1(a,b,c,x)$ is the hypergeometric function that we will describe in the coming chapter 4. The conformal blocks have not been constructed in $D > 6$. And a general closed expression has neither been written up. The natural generalization to D must come from solving the Casimir equation in a simplifying coordinate system. This method is used to find conformal blocks in general dimensions for specific coordinate systems. We will therefore be using the differential operator of Eq. (3.8.7) extensively.

Chapter 4

Radial/Angular Decomposition of the Conformal Block

In this chapter, we review [28] which studies a radial/angular decomposition of 4-point correlation functions and their associated conformal blocks in general dimensions. Their study is motivated by a search for a more transparent set of variables that capture the most important physics. Both the physical interpretation and the mathematical description indeed simplifies in the new variable set. The paper suggests a new symmetric configuration, called the ρ-picture, of operator locations instead of the operator location configuration used by Dolan-Osborn, called the z-picture. These two pictures are related by a conformal transformation of operator locations. The analysis of the conformal block is carried out in both the symmetric configuration and the z-picture so that they are comparable. Later in chapter 7, it will shown that the coordinates of the ρ-picture are essentially the same as the ones used in a large D limit of chapter 5. Conformal blocks are written in a multipole expansion of spherically harmonic functions which relate to the spin structure and dimensional dependency of the block. The coefficients in the multipole expansion are solved by a recursion method.

4.1 Conformal Block in the Cylinder Representation

In this section, we will introduce a radial/angular decomposition of the 4-point correlation function by writing the conformal blocks as a linear combination of a spherically harmonic function over descendants and spin. Starting with the radial quantization and representing the operator locations on a cylinder we obtain the structure of the linear combination, and we determine the coefficients, i.e. the levels by a recursion method so that the conformal blocks satisfy the Casimir equation.

The configuration of operators in Dolan-Osborn coordinates on $\mathbb{R}^D$ can be mapped to a cylinder $S^{D-1} \times \mathbb{R}$ using a Weyl transformation. This gives us a bunch of time slices from the initial state $|\phi\rangle$ to the final state $\langle\phi|$. On this mapping the z complex variable is related to the unit vectors n_2 and n_3 on each time slice:

$$n_2 \cdot n_3 = \cos\theta, \qquad \theta = \arg z. \tag{4.1.1}$$

The time τ is related to the complex variable z shown in Figure 4.1 The 4-point correlation function of identical scalars in the radial quantization can be written as:

$$\langle\phi|\phi(\tau_3, n_3)\phi(\tau_2, n_2)|\phi\rangle\,, \tag{4.1.2}$$

We then insert a complete set of energies E and write the time evolution for τ_2 and τ_3:

$$\sum_E \langle\phi|e^{\tau_3 H}\phi(0, n_3)e^{-\tau_3 H}|E\rangle\,\langle E|e^{\tau_2 H}\phi(0, n_2)e^{-\tau_2 H}|\phi\rangle\,, \tag{4.1.3}$$

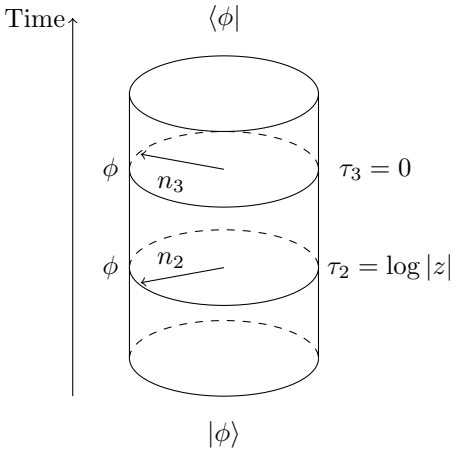

Figure 4.1: *The cylinder representation of operator locations*

where H is the Hamiltonian. Acting with the Hamiltonian on the energy states $|E\rangle$ we get the eigenvalue E and if we act with H on $|\phi\rangle$ we get a factor that cancels with the prefactor $(x_{12}^2 x_{34}^2)^{\Delta_\phi}$ from the 4-point correlation function [32]. The radial distance on the flat space is given by $|z|$ which is transformed to the cylinder by a relation to the time, in general terms $r = e^\tau$. The cylinder must then be of a unit circle, hence n_2 and n_3 are unit vectors. One obtains a factor that is related to the complex variable $e^{-E(\tau_3-\tau_2)} = |z|^E$, giving the sum over conformal blocks $\mathcal{A}$:

$$\mathcal{A}(z, n_2, n_3) = \sum_E |z|^E \langle\phi|\phi(0, n_3)|E\rangle \langle E|\phi(0, n_2)|\phi\rangle . \tag{4.1.4}$$

The matrix elements will have a tensor-structure given by the spin j, hence a j-rank tensor constructed by n_2 and n_3. From representation theory we have that one can split a representation into a symmetric traceless part, an antisymmetric part and a trace part. The matrix element can only consist of either n_2 or n_3 so the anti-symmetric contribution must be vanishing. Therefore we have each matrix element of the schematic form:

$$\langle E|\phi(0, n_2)|\phi\rangle \sim n_2^{\mu_1} n_2^{\mu_2} ... n_2^{\mu_j} - \text{trace}. \tag{4.1.5}$$

The product of the two matrix elements must be proportional to a contraction between the spin indices, i.e. a Gegenbauer polynomial $C_j^\nu(\xi)$:

$$(n_2^{\mu_1} n_2^{\mu_2} ... n_2^{\mu_j} - \text{trace})(n_3^{\mu_1} n_3^{\mu_2} ... n_3^{\mu_j} - \text{trace}) \propto C_j^\nu(n_2 \cdot n_3), \tag{4.1.6}$$

where ν defined from the dimension $\nu \equiv (D-2)/2$. Gegenbauer polynomials are spherically harmonic functions for a D-dimensional space that generalize the Legendre polynomials, $P_j(\xi)$ that is the harmonic function in $D = 3$. They can be defined in terms of the generating function:

$$\frac{1}{(1 - 2\xi t + t^2)^\nu} = \sum_j^\infty C_j^\nu(\xi) t^j. \tag{4.1.7}$$

Gegenbauer polynomials are defined on the interval $-1 < \xi < 1$ and are orthogonal to each other with respect to a weight function $(1-\xi^2)^{\nu-1/2}$. They are a particular solution to the Gegenbauer differential equation:

$$(1-\xi^2)\partial_\xi^2 C_j^\nu(\xi) - (2\nu+1)\xi\partial_\xi C_j^\nu(\xi) + j(j+2\nu)C_j^\nu(\xi) = 0. \tag{4.1.8}$$

Gegenbauer polynomials are an effective way of describing the spin contributions to the conformal block. For specific dimensions $D = 2, 3, 4$ we see that they simplify respectively:

$$\lim_{\nu\to 0} \frac{1}{\nu} C_j^\nu(\cos\theta) = \frac{2}{j}\cos(j\theta), \qquad C_j^{1/2}(\cos\theta) = P_j(\cos\theta), \qquad C_j^1(\cos\theta) = \frac{\sin((j+1)\theta)}{\sin\theta}, \tag{4.1.9}$$

while for the strict $D \to \infty$ limit we have the simplification:

$$\lim_{\nu\to\infty} \frac{1}{(2\nu)_j} C_j^\nu(\cos\theta) = \frac{\cos^j\theta}{j!}. \tag{4.1.10}$$

where $(p)_n$ are Pochhammer symbols defined by:

$$(p)_n \equiv p(p+1)...(p+n-1), \tag{4.1.11}$$

and related to the Γ-functions by $(p)_n = \Gamma(p+n)/\Gamma(p)$. The relations of Eq. (4.1.9) and Eq. (4.1.10) have been proven in Appendix C.1 and we comment on the $D = 4$ relation to the character of the $SU(2)$ representation.

The Gegenbauer polynomials are related to the hypergeometric function:

$$C_j^\nu(\xi) = \frac{(2\nu)_j}{j!} {}_2F_1\left(-j, 2\nu+j, \nu+1/2, \frac{1-\xi}{2}\right). \tag{4.1.12}$$

The hypergeometric function is generally defined by a power series for $|x| < 1$:

$${}_2F_1\left(a,b,c,x\right) = \sum_{n=0}^{\infty} \frac{(a)_n (b)_n}{(c)_n} \frac{x^n}{n!}. \tag{4.1.13}$$

The hypergeometric functions solve Euler's hypergeometric differential equation term by term:

$$x(1-x)\partial_x^2 {}_2F_1(a,b,c,x) + (c-(a+b+1)x)\partial_x {}_2F_1(a,b,c,x) - ab\,{}_2F_1(a,b,c,x) = 0. \tag{4.1.14}$$

The relation between the Gegenbauer polynomial and the hypergeometric functions let us pick a natural normalization:

$$C_j^\nu(1) = \frac{(2\nu)_j}{j!}, \tag{4.1.15}$$

which for $\xi = 1$ only has the first term in the hypergeometric sum contributing, which is a 1 leaving only the factor in front as the normalization.

Writing up the partial wave function from Eq. (3.6.13) in the radial/angular representation:

$$\mathcal{A}(u,v) = 1 + \sum_{E,j} p_{E,j} |z|^E C_j^\nu(\cos\theta), \tag{4.1.16}$$

where $p_{E,j}$'s are coefficents. In the radial quantization we have that the energies are given as $E = \Delta + n$, where we have primary operators for $n = 0$. We can redefine the coefficient in front of the Gegenbauer polynomial, so that using our normalization such that the conformal block becomes [28]:

$$G_{\Delta,l} = \sum_{n=0}^{\infty} |z|^{\Delta+n} \sum_j A_{n,j} \frac{C_j^\nu(\cos\theta)}{C_j^\nu(1)}, \tag{4.1.17}$$

where $A_{n,j}$'s are the coefficients or levels that we want to solve so that we have complete expression for the conformal block. Applying the radial/angular coordinates from section 3.4:

$$s = |z| = \sqrt{z\bar{z}}, \qquad \xi = \cos\theta = \frac{z+\bar{z}}{2\sqrt{z\bar{z}}}, \tag{4.1.18}$$

and the normalization from Eq. (4.1.15) we can write the conformal block as:

$$G_{\Delta,l}(s,\xi) = \sum_{n=0}^{\infty} \sum_j A_{n,j} \mathcal{P}_{\Delta+n,j}(s,\xi), \qquad \mathcal{P}_{E,j}(s,\xi) \equiv s^E \frac{j!}{(2\nu)_j} C_j^\nu(\xi). \tag{4.1.19}$$

We have now expanded the conformal block in Gegenbauer polynomials, so if we want to compute the concrete expressions for the conformal blocks we will need to determine the $A_{n,j}$ coefficients. The block satisfies the conformal Casimir equation, so by making a coordinate transformation from Eq. (3.8.7) we can write the differential operator as:

$$\begin{aligned}\mathcal{D} &= \mathcal{D}_0 + \mathcal{D}_1,\\ \mathcal{D}_0 &= s^2\partial_s^2 + (2\nu+1)(\xi\partial_\xi - s\partial_s) - (1-\xi^2)\partial_\xi^2,\\ \mathcal{D}_1 &= s(-\xi s^2\partial_s^2 + 2(1-\xi^2)s\partial_s\partial_\xi - \xi s\partial_s - (2\nu+\xi^2)\partial_\xi + \xi(1-\xi^2)\partial_\xi^2),\end{aligned} \tag{4.1.20}$$

which is derived in Appendix C.2. We will refer to $\mathcal{D}_0$ as the homogeneity preserving part and $\mathcal{D}_1$ as the homogeneity increasng part. Using the fact that the homogeneity preserving part solves the Gegenbauer differential equation, we find that the action of $\mathcal{D}_0$ is:

$$\mathcal{D}_0 P_{E,j} = C_{E,j}\mathcal{P}_{E,j}, \qquad C_{E,j} \equiv E(E-D) + j(j+D-2), \tag{4.1.21}$$

which has the same form as the Casimir eigenvalue. One can show that the action of the homogeneity increasing part is:

$$\begin{aligned}\mathcal{D}_1\mathcal{P}_{E,j} =& -\gamma^+_{E,j}\mathcal{P}_{E+1,j+1} - \gamma^-_{E,j}\mathcal{P}_{E+1,j-1},\\ \gamma^+_{E,j} =& \frac{(E+j)^2(j+2\nu)}{2(j+\nu)}, \qquad \gamma^-_{E,j} = \frac{(E-j-2\nu)^2 j}{2(j+\nu)}.\end{aligned} \tag{4.1.22}$$

Since this operator changes the energy and spin, one cannot directly set up a closed expression, but instead build up a recursion relation for the $A_{n,j}$ levels. We have that the conformal block also satisfies the Casimir equation, and setting this eigenvalue equal to the action of the homogeniety preserving and increasing operator, we can write the recursion as:

$$(C_{\Delta+n,j} - C_{\Delta,l})A_{n,j} = A_{n-1,j-1}\gamma^+_{\Delta+n-1,j-1} + A_{n-1,j+1}\gamma^-_{\Delta+n-1,j+1}. \tag{4.1.23}$$

We have an initial normalization condition:

$$A_{0,j} = \delta_{j,l}. \tag{4.1.24}$$

For the first level $n=1$ we find the results:

$$A_{1,l+1} = \frac{\gamma^+_{\Delta,l}}{C_{\Delta+1,l+1} - C_{\Delta,l}} = \frac{(\Delta+l)(l+2\nu)}{4(l+\nu)}, \qquad A_{1,l-1} = \frac{\gamma^-_{\Delta,l}}{C_{\Delta+1,l-1} - C_{\Delta,l}} = \frac{(\Delta-l-2\nu)l}{4(l+\nu)}, \tag{4.1.25}$$

while for the second level $n=2$ we find:

$$\begin{aligned}A_{2,l+2} =& \frac{\gamma^+_{\Delta+1,l+1}A_{1,l+1}}{C_{\Delta+2,l+2} - C_{\Delta,l}} = \frac{(\Delta+l)(\Delta+l+2)^2(l+2\nu)(l+2\nu+1)}{32(\Delta+l+1)(l+\nu)(l+\nu+1)},\\ A_{2,l-2} =& \frac{\gamma^-_{\Delta+1,l-1}A_{1,l-1}}{C_{\Delta+2,l-2} - C_{\Delta,l}} = \frac{(\Delta-l-2\nu)(\Delta-l-2\nu+2)^2 l(l-1)}{32(l+\nu)(l+\nu-1)(\Delta-l-2\nu+1)},\\ A_{2,l} =& \frac{\gamma^+_{\Delta+1,l-1}A_{1,l-1} + \gamma^-_{\Delta+1,l+1}A_{1,l+1}}{C_{\Delta+2,l} - C_{\Delta,l}} = \frac{(\Delta+l)(\Delta-l-2\nu)[(\Delta-\nu)l(l+2\nu) + (\Delta-2\nu)(\nu-1)]}{16(\Delta-\nu)(l+\nu+1)(l+\nu-1)}.\end{aligned} \tag{4.1.26}$$

The first two expressions can only depend on one another, while the third is a linear combination of the previous two $A_{1,l+1}$, $A_{1,l-1}$, since only these two $A_{n,j}$'s exist at the first level. Therefore we can generalize the expressions for the highest and lowest spin:

$$\begin{aligned}A_{n,l+n} =& \frac{\gamma^+_{\Delta,l}\gamma^+_{\Delta+1,l+1}\gamma^+_{\Delta+2,l+2,}\times\ldots\times\gamma^+_{\Delta+n-1,l+n-1}}{(C_{\Delta+1,l+1} - C_{\Delta,l})(C_{\Delta+2,l+2} - C_{\Delta,l})\times\ldots\times(C_{\Delta+n,l+n} - C_{\Delta,l})} = \frac{(\frac{\Delta+l}{2})_n^2(l+2\nu)_n}{n!(l+\nu)_n(\Delta+l)_n},\\ A_{n,l-n} =& \frac{\gamma^-_{\Delta,l}\gamma^-_{\Delta+1,l-1}\gamma^-_{\Delta+2,l-2,}\times\ldots\times\gamma^-_{\Delta+n-1,l-n+1}}{(C_{\Delta+1,l-1} - C_{\Delta,l})(C_{\Delta+2,l-2} - C_{\Delta,l})\times\ldots\times(C_{\Delta+n,l-n} - C_{\Delta,l})} = \frac{(\frac{\Delta-l-2\nu-2n+2}{2})_n^2(l-n+1)_n}{n!(l+\nu-n+1)_n(\Delta-l-2\nu)_n}.\end{aligned} \tag{4.1.27}$$

A closed expression for the general spin level is still to be found. We discuss further why we have the decoupling of the levels for the highest and lowest spin in section 7.1.

4.2 ρ-Configuration

We will build up a similar recursion method as seen in the previous section, but for a different operator location configuration. Using conformal transformations we can describe the positions of the operators of the 4-point function by a new variable ρ. This has the advantage that it is a more symmetric configuration of the operators around the origin in Figure 4.2 which converges more rapidly for the conformal blocks. The ρ-configuration is related to the z-configuration by the following set of transformations:

$$x^\mu_{(\rho)} \xrightarrow{I} \xrightarrow{P_\mu} \xrightarrow{I} \xrightarrow{P_\mu} \xrightarrow{M_{\mu\nu}} \xrightarrow{P_\mu} \xrightarrow{D} x^\mu_{(z)}, \tag{4.2.1}$$

which is applied on all operator locations. First, we apply a SCT that is decomposed of inversions and a translation. It is chosen in a particular way so that under the translation x_4 is send to $(0,0)$ on the plane, then the inversion takes $x_4 \to \infty$. The next translation is then based on sending x_3 to the origin. Then one can use a rotation to fix x_1 to the x-axis. The last translation is based on measuring all coordinates with respect to x_1 hence sending x_1 to the origin. The final transformation is scaling the system so that we fix x_3 to be at $(1,0)$, then we have obtained the z-configuration. This conformal transformation is considered in Appendix C.3 where the operations are directly applied.

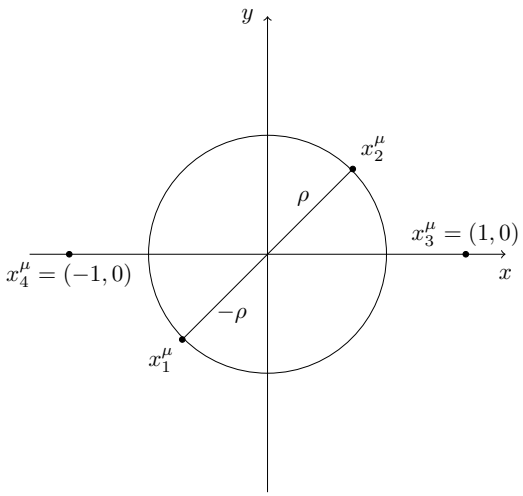

Figure 4.2: *The ρ-configuration where operators of the 4-point correlation function is located at x_i^μ, using conformal transformations.*

One can relate the variables of the ρ and z-picture, derived in Appendix C.4:

$$\rho = \frac{z}{(1+\sqrt{1-z})^2}, \qquad z = \frac{4\rho}{(1+\rho)^2}, \tag{4.2.2}$$

where a complex conjugated variable $\bar{\rho}$ is defined by the conjugated $\bar{z}$ as $\bar{\rho} \equiv \rho(\bar{z})$. Its relation to the $\{z, \bar{z}\}$ coordinates yields the range of the Euclidean unit box CFT:

$$0 \leq \rho, \bar{\rho} \leq 1. \tag{4.2.3}$$

The ρ-configuration lets us write the conformal block based on ρ instead of z defining new coordinates:

$$r = |\rho| = \sqrt{\rho\bar{\rho}}, \quad \eta = \cos\theta = \frac{\rho + \bar{\rho}}{2\sqrt{\rho\bar{\rho}}}, \qquad \theta = \arg(\rho). \tag{4.2.4}$$

Analogous to the $\{s, \xi\}$ coordinates, the ranges for these new coordinates in the Euclidean unit box will be:

$$0 \leq r \leq 1, \qquad -1 \leq \eta \leq 1. \tag{4.2.5}$$

With these coordinates and the normalization we can write the conformal block as:

$$G_{\Delta,l}(r,\eta)=\sum_{n=0}^{\infty}\sum_{j}B_{n,j}\mathcal{P}_{\Delta+n,j}(r,\eta),\qquad \mathcal{P}_{E,j}(r,\eta)\equiv r^{E}\frac{j!}{(2\nu)_j}C_j^{\nu}(\eta). \tag{4.2.6}$$

We have the same setup as in the z-picture, where we will determine $B_{n,j}$ coefficients. The $\{s,\xi\}$ and $\{r,\eta\}$ coordinates are related by:

$$s=\frac{4r}{1+2\eta r+r^2},\qquad \xi=\frac{\eta(1+r^2)+2r}{1+2\eta r+r^2}. \tag{4.2.7}$$

Using this relation one can transform the differential operator to be:

$$\mathcal{D}=\mathcal{D}_0+\tilde{\mathcal{D}}, \tag{4.2.8}$$

$$\mathcal{D}_0=r^2\partial_r^2+(2\nu+1)(\eta\partial_\eta-r\partial_r)-(1-\eta^2)\partial_\eta^2, \tag{4.2.9}$$

$$\tilde{\mathcal{D}}=4r^2\left(\left[\frac{r^2-(2\eta^2-1)}{1+r^4-2r^2(2\eta^2-1)}-\frac{\nu}{1-r^2}\right]r\partial_r+\frac{2\eta(1-\eta^2)}{1+r^4-2r^2(2\eta^2-1)}\partial_\eta\right). \tag{4.2.10}$$

The homogeneity preserving part gives a Casimir value like we have seen in the $\{s,\xi\}$ coordinates:

$$\mathcal{D}_0\mathcal{P}_{E,j}(r,\eta)=C_{E,j}\mathcal{P}_{E,j}(r,\eta),\qquad C_{E,j}=E(E-D)+j(j+D-2). \tag{4.2.11}$$

We then consider the action of the homogeneity increasing part $\tilde{\mathcal{D}}\mathcal{P}_{E,j}$. To do this we have some useful relations:

$$(2\eta^2-1)\mathcal{P}_{E,j}=a_j^-\mathcal{P}_{E,j-2}+a_j^0\mathcal{P}_{E,j}+a_j^+\mathcal{P}_{E,j+2}, \tag{4.2.12}$$

$$2\eta(1-\eta^2)\partial_\eta\mathcal{P}_{E,j}=b_j^-\mathcal{P}_{E,j-2}+b_j^0\mathcal{P}_{E,j}+b_j^+\mathcal{P}_{E,j+2}, \tag{4.2.13}$$

with:

$$\begin{aligned}
a_j^-&=\frac{j(j-1)}{2(j+\nu)(j+\nu-1)},\qquad a_j^0=\frac{\nu(1-\nu)}{(j+\nu+1)(j+\nu-1)},\qquad a_j^+=\frac{(j+2\nu+1)(j+2\nu)}{2(j+\nu+1)(j+\nu)},\\
b_j^-&=\frac{j(j-1)(j+2\nu)}{2(j+\nu)(j+\nu-1)},\qquad b_j^0=\frac{j(j+2\nu)\nu}{(j+\nu+1)(j+\nu-1)},\qquad b_j^+=-\frac{(j+2\nu+1)(j+2\nu)j}{2(j+\nu+1)(j+\nu)},
\end{aligned} \tag{4.2.14}$$

while $r\partial_r$ acting on the conformal block changes the dimensional dependency through the energy:

$$r\partial_r\mathcal{P}_{E,j}=E\mathcal{P}_{E,j}. \tag{4.2.15}$$

We apply the geometric series to expand the denominators:

$$\frac{1}{1-r^2}=\sum_{k=0}^{\infty}r^{2k},\qquad \frac{1}{1+r^4-2r^2(2\eta^2-1)}=\sum_{k=0}^{\infty}(2(2\eta^2-1)-r^2)^k r^{2k}. \tag{4.2.16}$$

This enables us to write the operator in the geometric series expansion as:

$$\tilde{\mathcal{D}}=4r^2\sum_{k=0}^{\infty}\Big((2(2\eta^2-1)-r^2)^k r^{2k}(1-2\eta^2+r^2)r\partial_r-\nu r^{2k}r\partial_r+(2(2\eta^2-1)-r^2)^k 2\eta(1-\eta^2)\partial_\eta\Big). \tag{4.2.17}$$

For now, we are only interested in the two lowest levels $n=0,2$. It is sufficient to take $k=0$ for these first two levels, since we arrange the expressions by the n dependency in $\mathcal{P}_{E+n}$. For order $n=2$ the action is:

$$\begin{aligned}
\tilde{\mathcal{D}}\mathcal{P}_{E,j}&=-\Gamma_{E,j}^{E+2,j-2}\mathcal{P}_{E+2,j-2}-\Gamma_{E,j}^{E+2,j}\mathcal{P}_{E+2,j}-\Gamma_{E,j}^{E+2,j+2}\mathcal{P}_{E+2,j+2},\\
\Gamma_{E,j}^{E+2,j-2}&=4(Ea_j^--b_j^-),\qquad \Gamma_{E,j}^{E+2,j}=4[E(a_j^0+\nu)-b_j^0],\qquad \Gamma_{E,j}^{E+2,j+2}=4(Ea_j^+-b_j^+).
\end{aligned} \tag{4.2.18}$$

Compactly this can be written as:

$$\tilde{\mathcal{D}}\mathcal{P}_{E,j}=-\sum_{j'=j-2,j,j+2}\Gamma_{E,j}^{E+2,j'}\mathcal{P}_{E+2,j'}, \tag{4.2.19}$$

while for general orders of n we have:

$$\tilde{\mathcal{D}}\mathcal{P}_{E,j} = -\sum_{n=2,4,\ldots}\sum_{j'}\Gamma_{E,j}^{E+n,j'}\mathcal{P}_{E+n,j'=j-n,j-n+2,\ldots,j+n}. \tag{4.2.20}$$

By applying the differential operator on the conformal block and comparing it to the eigenvalue of the Casimir equation one can build up the recursion relation:

$$(C_{\Delta+n,j} - C_{\Delta,l})B_{n,j} = \sum_{n=0,2,4,\ldots}^{n-2}\sum_{j'}\Gamma_{\Delta+n',j'}^{\Delta+n,j}B_{n',j'}. \tag{4.2.21}$$

For $n = 0$ we take the initial condition:

$$B_{0,j} = k\delta_{jl}, \tag{4.2.22}$$

coming from the RHS of Eq. (4.2.21) which has no levels for $j = l$ up to some normalization k, which for now is $k = 1$. We then move on to the next level $n = 2$, where $n' = 0$ so that we only have one sum over $j' = j-2, j, j+2$ giving us the recursion relation:

$$(C_{\Delta+2,j} - C_{\Delta,l})B_{2,j} = \Gamma_{\Delta,j-2}^{\Delta+2,j}\delta_{l,j-2} + \Gamma_{\Delta,j}^{\Delta+2,j}\delta_{l,j} + \Gamma_{\Delta,j+2}^{\Delta+2,j}\delta_{l,j+2}, \tag{4.2.23}$$

for the 3 possible spins $j = l-2, l, l+2$ we get the second level:

$$\begin{aligned}
B_{2,l-2} &= \frac{\Gamma_{\Delta,l}^{\Delta+2,l-2}}{(C_{\Delta+2,l-2} - C_{\Delta,l})} = \frac{l(l-1)(\Delta-l-2\nu)}{2(l+\nu-1)(l+\nu)(\Delta-l-2\nu+1)},\\
B_{2,l} &= \frac{\Gamma_{\Delta,l}^{\Delta+2,l}}{(C_{\Delta+2,l} - C_{\Delta,l})} = \nu\frac{\Delta(1-\nu)+(l+\nu+1)(l+\nu-1)-l(l+2\nu)}{(\Delta-\nu)(l+\nu+1)(l+\nu-1)} = \nu\frac{\Delta\nu(\nu-1)+(\Delta-1)l(l+2\nu)}{(\Delta-\nu)(l+\nu+1)(l+\nu-1)},\\
B_{2,l+2} &= \frac{\Gamma_{\Delta,l}^{\Delta+2,l+2}}{(C_{\Delta+2,l+2} - C_{\Delta,l})} = \frac{(\Delta+l)(l+2\nu)(l+2\nu+1)}{2(\Delta+l+1)(l+\nu)(l+\nu+1)}.
\end{aligned} \tag{4.2.24}$$

Compared to the $A_{n,j}$'s the $B_{n,j}$'s only have levels for even integers of n, making the conformal block a more rapid converging expression.

4.3 Decoupling of Descendants for the Leading Twist

In this section, we consider a special case where the recursion of Eq. (4.1.23) simplifies massively, and argue why this happens. In this case, only one level has a non-zero coefficient that is the maximal spin $j = l + n$. The twist τ is defined by the difference of the conformal scaling dimension and spin $\tau \equiv \Delta - l$. The operators for the leading twist are of scaling dimension $\Delta = l + D - 2 = l + 2\nu$, which saturates the unitarity bound. The maximal twist thus has scaling dimensions that matches the operators in free field theories. One can use Eq. (4.1.27) to write the only non-zero contribution i.e. the general n'th level for the leading twist:

$$A_{n,l+n} = \frac{(l+\nu)_n^2(l+2\nu)_n}{n!(l+\nu)_n(2(l+\nu))_n} = \frac{(l+\nu)_n(l+2\nu)_n}{n!(2l+2\nu)_n}, \tag{4.3.1}$$

which we will refer to as the decoupling. This decoupling from other descendants can be understood when considering a primary operator $\mathcal{O}_{(0)}$ and its descendants $\mathcal{O}_{(n)}$ given by:

$$\mathcal{O}_{(n)} = \partial_{\mu_1}\partial_{\mu_2}\ldots\partial_{\mu_n}\mathcal{O}_{(0)}. \tag{4.3.2}$$

The scaling dimension of the primary is $\Delta_{\mathcal{O}}$ while it is $\Delta_{\mathcal{O}} + n$ for the descendants. If a contraction between two indices would be applied one would obtain a Laplican operator ∂^2 that appears in the EOM for scalar

fields when acted upon a primary operator. The ∂^2 operators have scaling dimension less than $l+n$, and these states decouple. Given the scalar field EOM we can see that the following 3-point function will vanish:

$$\lim_{x_4\to\infty} |x_4|^{2\Delta_\phi} \langle \phi(x_4)\phi(x_1)\partial_{x_2}^2 \mathcal{O}_{(0)}(x_2)\rangle = 0, \tag{4.3.3}$$

where these coordinates are operator locations with the conformal configuration from the z-picture. The 3-point function is explicitly:

$$\langle \phi(x_4)\phi(0)\mathcal{O}_{(0)}(x_2)\rangle = \frac{\lambda_\mathcal{O}}{|x_4|^{2\Delta_\phi-\Delta_\mathcal{O}}|x_4-x_2|^{\Delta_\mathcal{O}}|x_2|^{\Delta_\mathcal{O}}}, \tag{4.3.4}$$

with external scaling dimensions for $\Delta_4=\Delta_1=\Delta_\phi$ and according to the z-picture $x_1\to 0$. For large values of x_4, we have that $|x_4-x_2|\simeq|x_4|$, which yields:

$$\lim_{x_4\to\infty} |x_4|^{2\Delta_\phi} \langle \phi(x_4)\phi(x_1)\mathcal{O}_{(0)}(x_2)\rangle = \frac{\lambda_\mathcal{O}}{|x_2|^{\Delta_\mathcal{O}}}. \tag{4.3.5}$$

The scaling dimension for the primary operator is $\Delta_\mathcal{O}=l+D-2$ and when a descendant operator is on the form $\mathcal{O}_{\mu_1\mu_2\ldots\mu_l}$ with l indicies we have:

$$\lim_{x_4\to\infty} |x_4|^{2\Delta_\phi} \langle \phi(x_4)\phi(x_1)\mathcal{O}_{\mu_1\mu_2\ldots\mu_l}(x_2)\rangle = \lambda_\mathcal{O}\frac{(x_2)_{\mu_1}(x_2)_{\mu_2}\ldots(x_2)_{\mu_l}}{|x_2|^{D-2+2l}}, \tag{4.3.6}$$

up to some trace terms. In Appendix B.3 we showed that:

$$\partial_\mu \frac{1}{|x_2|^{D-2}} = (D-2)\frac{(x_2)_\mu}{|x_2|^D}. \tag{4.3.7}$$

If we then apply l derivatives we have:

$$\partial_{\mu_1}\partial_{\mu_2}\ldots\partial_{\mu_l}\frac{1}{|x_2|^{D-2}} = 2^l\left(\frac{D}{2}-1\right)_l \frac{(x_2)_{\mu_1}(x_2)_{\mu_2}\ldots(x_2)_{\mu_l}}{|x_2|^{D-2+2l}}, \tag{4.3.8}$$

up to some extra trace terms given when taking the derivative of each $(x_2)_\mu$ in the numerator. From this fact we can see that our 3-point function is actually given by acting with l derivatives on $1/|x_2|^{D-2}$. This function is harmonic in D meaning that it solves the Laplace equation. For each ∂^2 a solution exists to the Laplace equation, which decouples the level. In Appendix C.5 we show how the partition functions are affected by the structure of primary and descendant operators, for both scalar fields and gauge fields. This is to give an overview of the decoupling procedure in general for several kinds of fields.

4.4 Mapping of the Euclidean Unit Box Region in the ρ-Picture

Throughout the thesis, we have commented on the ranges of the coordinates. Due to the crossing symmetry when exchanging two operator locations we have a specific region of interest called the unit box. We will now consider the mapping of the unit box to the ρ-picture and see how it plays out in these coordinates. The relation between the $\{u,v\}$ and $\{r,\eta\}$ or $\{\rho,\bar\rho\}$ coordinate sets are:

$$u=\frac{16\rho\bar\rho}{(1+\rho)^2(1+\bar\rho)^2}, \qquad v=\frac{(1-\rho)^2(1-\bar\rho)^2}{(1+\rho)^2(1+\bar\rho)^2}, \tag{4.4.1}$$

$$u=\frac{16r^2}{(1+2\eta r+r^2)^2}, \qquad v=\frac{(1+r^2-2r\eta)^2}{(1+r^2+2r\eta)^2}, \tag{4.4.2}$$

Notice that the symmetry $\rho\to\rho^{-1}$ leaves the coordinates invariant $u(\rho)=u(1/\rho)$ and $v(\rho)=v(1/\rho)$. That symmetry corresponds to sending $r\to 1/r$ and $\eta\to\eta$. An exchange of operator positions $x_1\leftrightarrow x_2$

corresponds to a change in $\rho \to -\rho$. That same exchange leaves r invariant $r \to r$ and changes $\eta \to -\eta$. In other words the exchange between $x_1 \leftrightarrow x_2$ rotates the unit box region by π around the origin. For the $\{z, \bar{z}\}$ coordinates the operator exchange corresponds to $z \to z/(z-1)$.

If we insist on $0 \leq u, v, \leq 1$ we get a series of bounds in the new coordinates, these are:

$$0 \leq r, \qquad r \leq g_-(\eta), \qquad r \geq g_+(\eta), \qquad g_\pm(\eta) \equiv 2 - \eta \pm \sqrt{(2-\eta)^2 - 1}, \qquad 0 < \eta. \tag{4.4.3}$$

Notice that these do not have any upper bound on r, so we can be either inside or outside of the unit circle. If we force $r \leq g_-(\eta)$ the r is confined within the unit circle and $r \geq g_+(\eta)$ confines r outside of the unit circle. Using the transformation $r \to r^{-1}$ one can access the other region. The relation $\eta = \cos\theta$ lets us represent this region in Figure 4.3. This region in the ρ-picture is equivalent to the two overlapping circles discussed in section 3.4 for the z-picture. The conformal blocks are represented as a power series that will only converge for $|\rho| < 1$. This motivates the question to what happens in the rest of the unit circle. This restiction in $\{u, v\}$ coordinates is:

$$r \leq 1 \quad \to \quad \sqrt{u} - \sqrt{v} \leq 1. \tag{4.4.4}$$

It is now possible to do a mapping of the remaining sections of the ρ-picture to the conformal invariant cross-ratio space. This is shown in Figure 4.4. A part of the crossing symmetry section from Eq. (3.4.7) is mapped to the remaining part of the unit circle. Values of $x < 0$ in the ρ-picture are constrained by the $\{r, \eta\}$ coordinates. For the region where $v < 0$ the relation between $r(\eta)$, takes values outside the real numbers. And for $u < 0$ we have the radius $r < 0$ which is unphysical. We notice that if we are in the unit box region of $\{u, v\}$ then we only cover a part of the ρ-picutre, while the rest can be mapped by crossing symmetry.

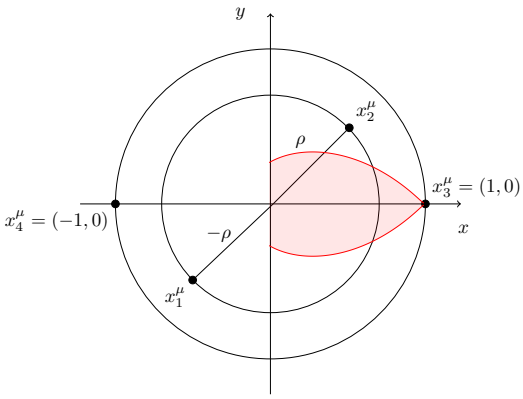

Figure 4.3: *The ρ-picture of operator locations, with the Euclidean unit box region within the unit circle in red.*

We have studied the crossing symmetry in the ρ-picture and seen that the Euclidean unit box is mapped to the ρ-picture in a non-trivial way. These regions may be used in the future to explore the crossing symmetry of the conformal blocks in the radial/angular decomposition. A possibility is that the crossing symmetry can be studied in the same framework as [33] for large dimensions which we will explore in chapter 6. To get there we will now turn the attention to conformal blocks in large D limits in chapter 5.

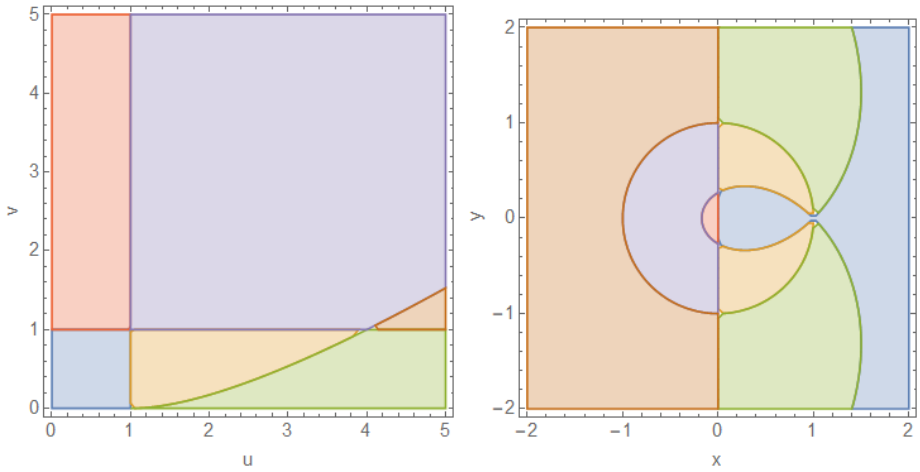

Figure 4.4: *A mapping between the $\{u, v\}$ coordinate system (left) and the ρ-configuration (right) is shown. Each color is mapped to the corresponding same color. In (blue) we have the unit box region from the constraint $0 < u, v < 1$, in (orange) we have the region within the unit circle and in (green) we have the region outside the unit circle. Note that the green, red, brown and purple regions in the $\{u, v\}$ coordinates extends to $\{u, v\} \to \infty$.*

Chapter 5

Scalar Block Suggested Variables for Conformal Blocks in Large Dimensions

In this chapter, we will make a review of [34] which introduces a new set of coordinates that is established by a large D approximation of the scalar conformal block. The main motivation for this paper is to study whether CFTs become trivial at large D.

The coordinates introduced will be related in chapter 7 to those from chapter 4. Further, we derive a symmetric conformal block in Δ and $1-l$ from the Casimir equation method introduced in section 3.8. We will further compare the structure of these large D conformal blocks with the radial/angular decomposition of the blocks and the exact dimensional solution to the blocks. We further check whether the large D blocks satisfy the crossing function.

5.1 Deriving the Large Dimensional Conformal Block

It is often instructive to look at the scalar conformal block, where the spin is $l = 0$ since the expression is simpler and therefore easier to manipulate. The exact D-dimensional scalar block with conformal cross-ratios $\{u, v\}$ is given by [34]:

$$G_{\Delta,0}(u,v) = \sum_{n,m=0}^{\infty} \frac{(\frac{\Delta}{2})_n^2 (\frac{\Delta}{2})_{n+m}^2}{(\Delta+1-\frac{D}{2})_n (\Delta)_{2n+m}} \frac{u^{\frac{\Delta}{2}+n}}{n!} \frac{(1-v)^m}{m!}. \tag{5.1.1}$$

It is technically productive to note that this particular infinite sum of the D-dimensional scalar block resembles that of the hypergeometric function:

$${}_2F_1(a,b,c;x) = \sum_{n=0}^{\infty} \frac{(a)_n (b)_n}{(c)_n} \frac{x^n}{n!}, \tag{5.1.2}$$

where $(p)_n$ is the Pochhammer functions defined in Eq. (4.1.11). We will apply a saddle-point integral over an integral representation of this hypergeometric function. In general a saddle-point integral is written on the form:

$$I \equiv \int_a^b dx f(x) e^{Dg(x)}. \tag{5.1.3}$$

When D is large the integral is dominated by the point, hence the saddle-point x^*, where $g(x)$ takes its maximum value. When the dominant point is within the integration range, the solution, valid in large D, to the integral is:

$$I \simeq \sqrt{\frac{2\pi}{-Dg''(x^*)}} f(x*) e^{Dg(x*)}. \tag{5.1.4}$$

Using this method, and applying a range of identities for the Pochhammer and Γ-function, and further using the Stirling approximation on the Γ-functions we end up with the following scalar block in large D, derived in Appendix D.1:

$$G_{\Delta,0}(u,v) \approx 2^{\Delta-1} \frac{1+\sqrt{v}}{v^{\frac{1}{4}}} \left(\frac{u}{(1+\sqrt{v})^2}\right)^{\frac{\Delta}{2}} {}_2F_1\left(\frac{\Delta-1}{2}, \frac{\Delta}{2}, \Delta - \frac{D}{2}+1, \frac{u}{(1+\sqrt{v})^2}\right). \tag{5.1.5}$$

This hypergeometric function suggests a new variable y_+, we therefore define the new set of variables:

$$y_\pm = \frac{u}{(1\pm\sqrt{v})^2}. \tag{5.1.6}$$

This brings the scalar block on the form [34]:

$$G_{\Delta,0}(y_+,y_-) \approx \frac{2^\Delta y_-^{1/2} y_+^{\Delta/2}}{\sqrt{y_- - y_+}} {}_2F_1\left(\frac{\Delta-1}{2}, \frac{\Delta}{2}, \Delta - \frac{D}{2}+1, y_+\right). \tag{5.1.7}$$

To achieve the spin dependent part we must look at the Casimir equation. The conformal block satisfies the Casimir differential equation:

$$\mathcal{D} G_{\Delta,l} = \frac{1}{2} C_{\Delta,l} G_{\Delta,l}, \tag{5.1.8}$$

with $\mathcal{D}$ being the differential operator from Eq. (3.8.7), and $C_{\Delta,l}$ the Casimir eigenvalue. Notice the convention of $1/2$ in the Casimir equation, which is used in [34] while for the radial/angular block we used a convention of 1. The differential operator can be found by making a transformation from the Dolan-Osborn coordinates to the $\{y_+, y_-\}$ coordinates:

$$\begin{gathered}\mathcal{D} = \mathcal{D}_{y_+} + \mathcal{D}_{y_-} + \mathcal{D}_{y_0}, \\ \mathcal{D}_{y_\pm} = 2y_\pm^2(1-y_\pm)\partial_{y_\pm}^2 - y_\pm(y_\pm + D - 2)\partial_{y_\pm}, \qquad \mathcal{D}_{y_0} = \frac{2}{y_+ - y_-}(y_+^2(1-y_+)\partial_{y_+} - y_-^2(1-y_-)\partial_{y_-}).\end{gathered} \tag{5.1.9}$$

The conformal block is written in a form where the conformal scaling dimension appears as u^Δ. Therefore if one applies a derivative ∂_u on the conformal block it pulls down a Δ and since $\Delta \propto D$ we count it as a dimension. Given the new coordinates, the extra scaling dimension is obtained by either acting with ∂_{y_+} or ∂_{y_-}. Given the unitarity bound the scaling dimension is proportional to the dimension. When we consider the large D limit we, therefore, have to count the derivatives of y_+ and y_-. We notice that $\mathcal{D}_{y_\pm}$ is at leading order in D as long as the denominator in $\mathcal{D}_{y_0}$ does not contribute to the dimension. Specifically, the approximation is valid when $y_+ - y_- \geq D^{-1}$ which equivalently in cross-ratios is $v \geq D^{-2}$. We can therefore neglect the mixed term and its differential operator $\mathcal{D}_{y_0}$. When the mixed term vanishes it allows for a separable solution with a spin-dependent block part and a scaling dimension block part. With this transformation the conformal Casimir equation is then neatly solved by the following simple and highly factorized result [34]:

$$G_{\Delta,l}(y_+,y_-) = \frac{2^{\Delta+l}}{\sqrt{y_- - y_+}} A_\Delta(y_+) A_{1-l}(y_-), \tag{5.1.10}$$

where

$$\begin{aligned} A_\Delta(y_+) &\equiv y_+^{\Delta/2} {}_2F_1\left(\frac{\Delta-1}{2}, \frac{\Delta}{2}, \Delta - \frac{D}{2}+1, y_+\right), \\ A_{1-l}(y_-) &\equiv y_-^{(1-l)/2} {}_2F_1\left(-\frac{l}{2}, \frac{1-l}{2}, -l - \frac{D}{2}+2, y_-\right). \end{aligned} \tag{5.1.11}$$

This solution is tested in Appendix D.2. The factor $2^{\Delta+l}$ is a normalization convention of the conformal block when one looks at the corner of parameter space where $u \to 0$ and $v \to 1$.
We will now compare this large D approximated conformal block to the exact conformal block for different values of the spin, scaling dimensions and conformal cross-ratios evaluated at $D = 4$. For the exact conformal block in $D = 4$ we have the expression [25]:

$$G_{\Delta,l}(u,v) = \frac{u^{\Delta/2}}{\sqrt{(u-v+1)^2-4u}}\left(\frac{z^{l/2+1}}{\bar{z}^{l/2}}{}_2F_1\left(\frac{\Delta+l}{2},\frac{\Delta+l}{2},\Delta+l,z\right)\right. \\ \left.\times{}_2F_1\left(\frac{\Delta-l-2}{2},\frac{\Delta-l-2}{2},\Delta-l-2,\bar{z}\right)-z\leftrightarrow\bar{z}\right), \tag{5.1.12}$$

$$\bar{z}(u,v) = \frac{u-v+1-\sqrt{(u-v+1)^2-4u}}{2}, \qquad z(u,v) = \frac{u-v+1+\sqrt{(u-v+1)^2-4u}}{2}. \tag{5.1.13}$$

From this, we can generate a plot over the absolute value of the conformal block and see how it behaves. Indeed, in Figure 5.1 we see for specific slices of $\{u, v\}$ space, that these large D blocks reproduce many of the specific features of the exact $D = 4$ conformal block. This qualitative match hints that $D = 4$ might be close to this large D limit. Then we test whether the crossing relation is satisfied by the large D block

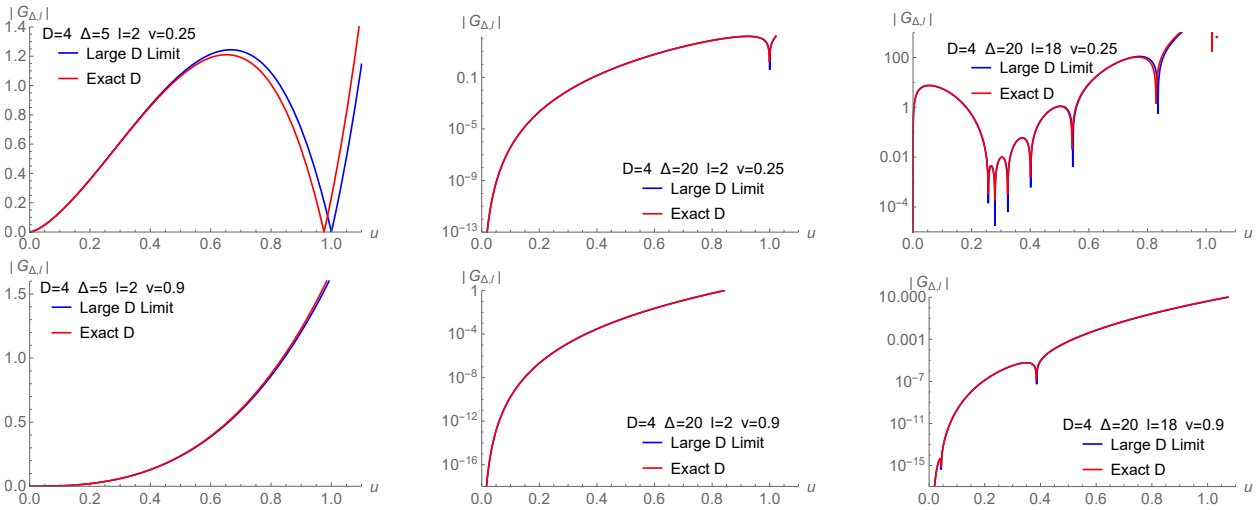

Figure 5.1: *The absolute value of the conformal block $|G_{\Delta,l}(u,v)|$ in the large D limit (blue) plotted with the exact conformal block (red), both evaluated at $D = 4$ and as functions of the cross-ratio u. Both blocks are evaluated at different fixed values of scaling dimension Δ, spin l and cross-ratio v. One observes that the structure of the conformal block in the large D approximation is very close to that of exact D.*

by comparing it to the exact D case from [25] and putting the expressions into the crossing functions Eq. (3.6.14). More specifically, the crossing function in our case for a particular external scaling dimension reads:

$$F_{\Delta_\phi}(u,v) = \sum_{n=0}^{n_{max}}\sum_{l=0}^{l_{max}} P_{n,l,\Delta_\phi}\frac{v^{\Delta_\phi}G_{2\Delta_\phi+2n+l,l}(u,v)-u^{\Delta_\phi}G_{2\Delta_\phi+2n+l,l}(v,u)}{u^{\Delta_\phi}-v^{\Delta_\phi}}. \tag{5.1.14}$$

Here we put an upper bound on the sums i.e. n_{max} and l_{max} so that the sum can be evaluated numerically. The external scaling dimension Δ_ϕ is dependent on the scaling dimension of the block Δ. The OPE for a Generalized Free Field theory (GFFT)/mean-field theory is [35]:

$$P_{n,l,\Delta_\phi} = \frac{(1+(-1)^l)(\Delta_\phi-D/2+1)_n^2(\Delta_\phi)_{n+l}^2}{l!n!(l+D/2)_n(2\Delta_\phi+n-D+1)_n(2\Delta_\phi+2n+l-1)_l(2\Delta_\phi+n+l-D/2)_n}, \tag{5.1.15}$$

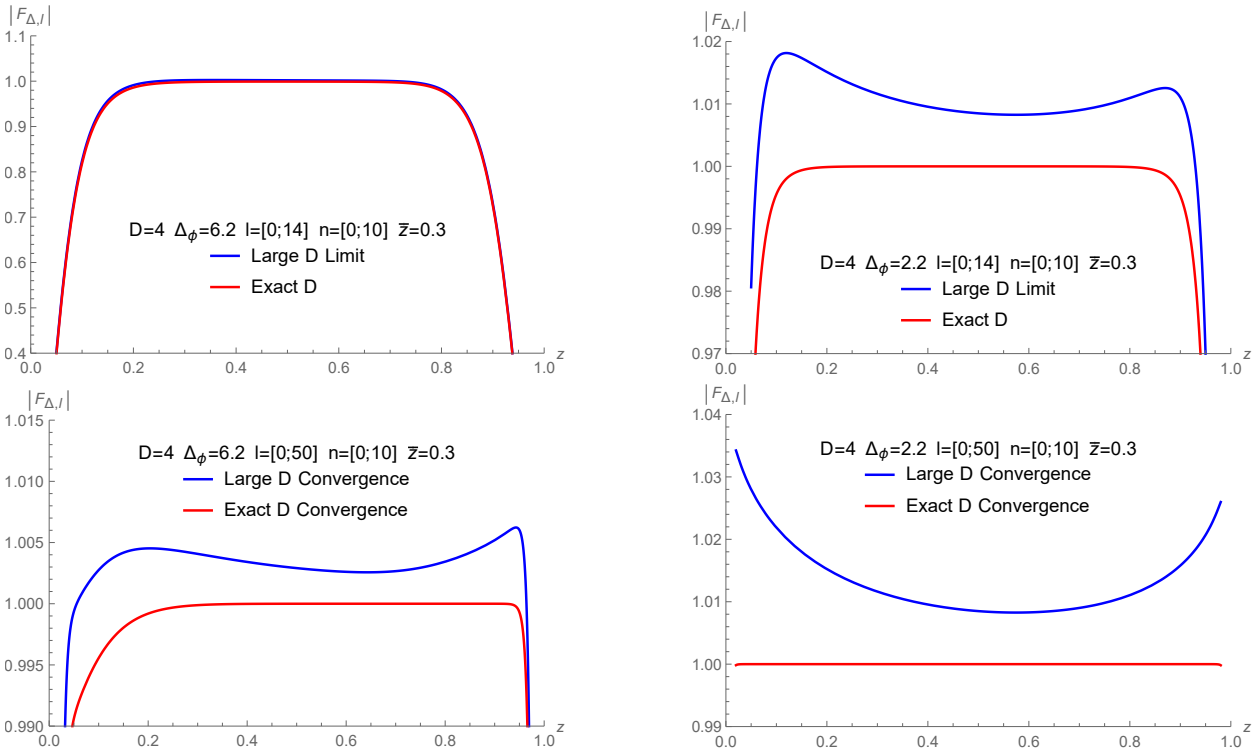

Figure 5.2: *The absolute value of the crossing function $|F_{\Delta_\phi}(z,\bar{z})|$ for the large D conformal block (blue) and exact conformal block (red) in $D=4$ as a function of the parameter z. Both crossing functions are evaluated for different values of Δ_ϕ and for different maximum values of the level n_{max} and spin l_{max}.*

The plot converges for $\Delta_\phi = 2.2$ but not for $\Delta_\phi = 6.2$ compared to [34]. If it should converge then one needs to add more terms to the sum. Doing so we can see that these conformal blocks obey the bootstrap equation in Figure 5.2

5.2 Plotting the Radial/Angular Conformal Block Function

We have compared the large D conformal block with the exact D conformal block at $D=4$. It could be interesting to see how the radial/angular decomposed conformal block turns out in this comparison. Therefore, we would like to bring the radial/angular conformal block from chapter 4 in a form that is comparable to the large D block. The block decomposition is written in the form:

$$G_{\Delta,l}(r,\eta) = \sum_{n=0}^{\infty}\sum_{j} B_{n,j} r^{\Delta+n} \frac{j!}{(2\nu)_j} C_j^{\nu}(\eta). \tag{5.2.1}$$

In order to do a $\{u,v\}$ plot we have to find $r(u,v)$ and $\eta(u,v)$. We can find that by transforming $\{r,\eta\} \to \{\rho,\bar{\rho}\} \to \{z,\bar{z}\} \to \{u,v\}$, giving:

$$r = \frac{\sqrt{u}}{1+\sqrt{v}+\sqrt{(1+\sqrt{v})^2-u}}, \qquad \eta = \frac{1-v+\sqrt{(1-v)^2-u(1-\sqrt{v})^2}}{\sqrt{u}(1+\sqrt{v}+\sqrt{(1+\sqrt{v})^2-u})}. \tag{5.2.2}$$

The $B_{n,j}$'s have a normalization constant which has been set to $k=1$. They note in [28] that $k=4^{\Delta}$ for section 2 in [28], so for the $\{u,v\}$ coordinates we have multiplied with this constant on the conformal block to use the same normalization convention. Another footnote from [28] section 2 is that if we wanted to relate

it to the Dolan-Osborn convention we have to multiply with $(-2)^l \frac{(\nu)_l}{(2\nu)_l}$. The $B_{n,j}$'s are found by a recursion, and we have only computed the first few terms. We therefore consider the following expression for the first two levels $n = 0, 2$ of the block:

$$\begin{aligned} G_{\Delta,l}(r,\eta) = \frac{4^\Delta(-2)^l(\nu)_l}{(2\nu)_l}(B_{0,l}r^\Delta \frac{l!}{(2\nu)_l}C_l^\nu(\eta) + B_{2,l-2}r^{\Delta+2}\frac{(l-2)!}{(2\nu)_{l-2}}C_{l-2}^\nu(\eta) \\ + B_{2,l}r^{\Delta+2}\frac{l!}{(2\nu)_l}C_l^\nu(\eta) + B_{2,l+2}r^{\Delta+2}\frac{(l+2)!}{(2\nu)_{l+2}}C_{l+2}^\nu(\eta)), \end{aligned} \tag{5.2.3}$$

where each $B_{n,j}$ is normalized to 1 after pulling out the normalization. This block has been plotted in Figure 5.3. In Figure 5.4 we compare this expression of the block to that of the large D block [34] and the exact D block [25]. The behavior seems to resemble the same structure as these two other blocks in the case of $D = 4$. If more terms were included in the infinite sum over levels n, the block would most likely converge to the same behavior as the other two. In Figure 5.5 we plot the structure of each individual term of Eq. (5.2.3) at $D = 4$ with different scaling dimensions and spins. We conclude from these plots that the most dominating terms seem to be dependent on the value of Δ and l. The lowest level $n = 0$ seems to be more dominant in the case for low Δ and l. For large l the second level is the most dominant, while for low spins and large scaling dimensions, the terms seem equally dominant. From this analysis there appears to be no way to neglect some terms and thus simplify the sum over levels and spins in Eq. (5.2.1).

From this chapter, we have found that the large D version of the conformal block resembles the same features of the exact D blocks even for relatively small dimensions such as $D = 4$. The structure is similarly resembled by the radial/angular decomposed block, even for the first 4 terms in the series, presumably because of the use of a faster convergent ρ-configuration than z-configuration.

Now that we have verified that the different compositions of the conformal blocks resemble the exact D block we will consider a new type of large D limit in chapter 6 that can be used to consider the crossing relation and constrain the CFT data.

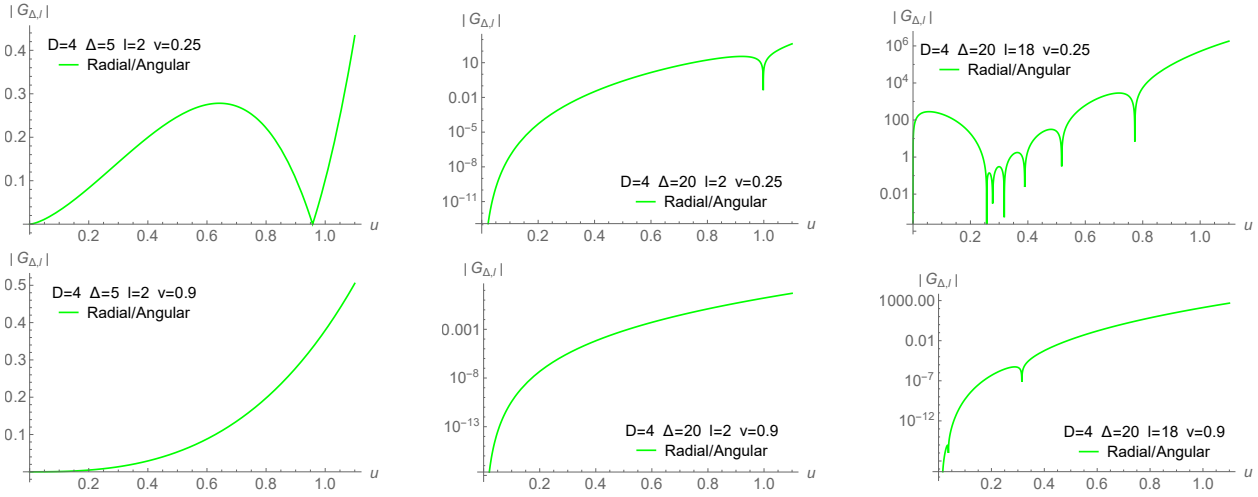

Figure 5.3: *The absolute value of the radial/angular composed conformal block $|G_{\Delta,l}(u,v)|$ (green) evaluated at $D = 4$ and as a function of the cross-ratio u. The block is evaluated at different fixed values of scaling dimension Δ, spin l and cross-ratio v*

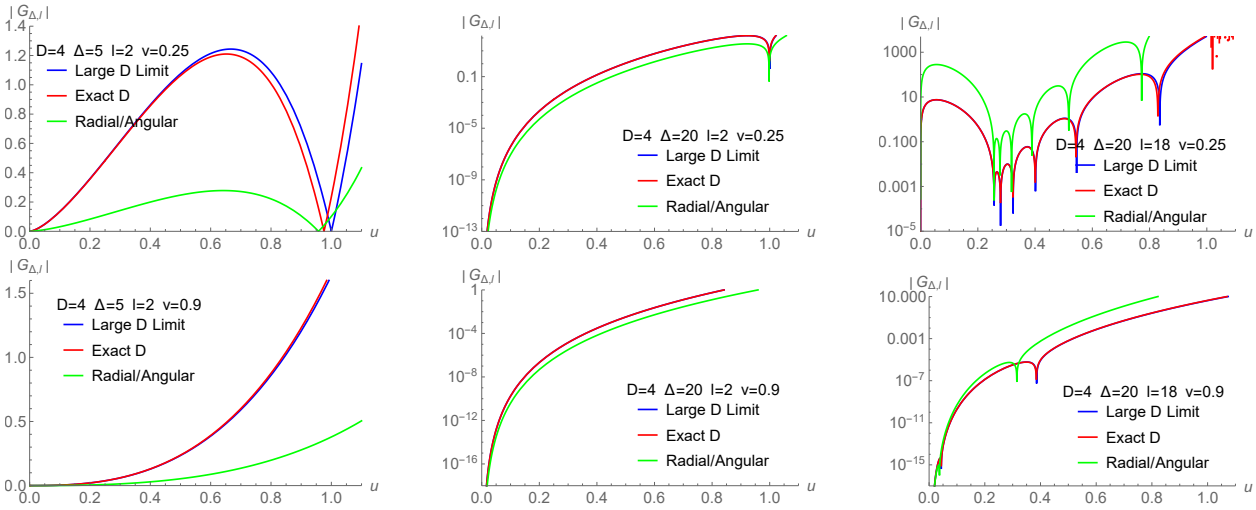

Figure 5.4: *The absolute value of the radial/angular composed conformal block* $|G_{\Delta,l}(u,v)|$ *(green) plotted with the exact conformal block (red) and the large D conformal block (blue), all evaluated at* $D = 4$ *and as functions of the cross-ratio* u*. All blocks are evaluated at different fixed values of scaling dimension* Δ*, spin* l *and cross-ratio* v

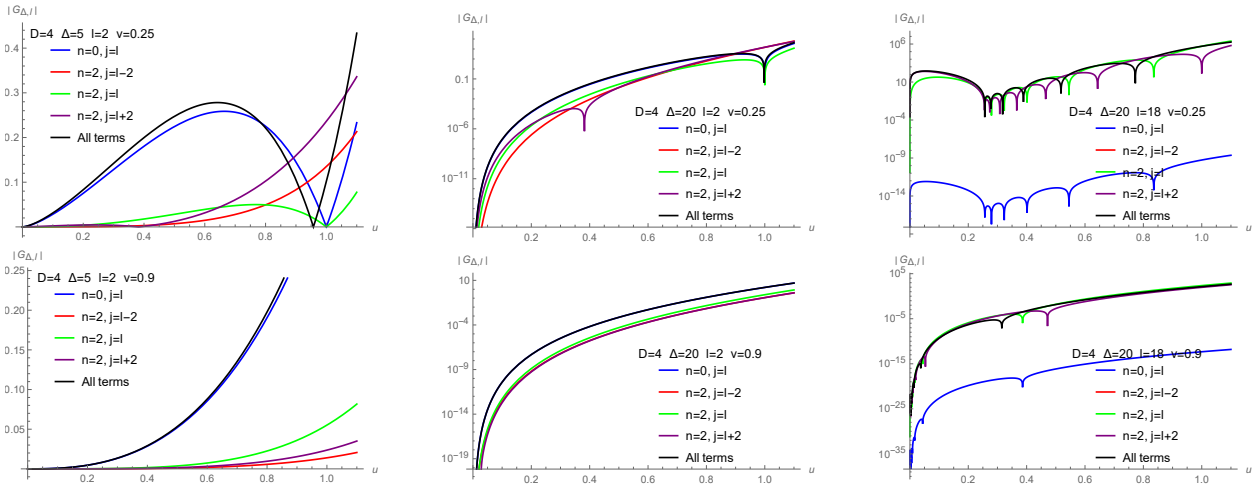

Figure 5.5: *The absolute value for each term of the radial/angular composed conformal block* $|G_{\Delta,l}(u,v)|$ *in* $D = 4$*. The first* $n = 0$ *level is (blue), the second level with spin* $j = l - 2$ *is (red), the second level with spin* $j = l$ *is (green) and the second level with spin* $j = l + 2$ *is (purple) while all terms added together are (black)*

Chapter 6

Constraints on Large Dimensional Conformal Theories

In this chapter, we will make a review of [33] which builds on [34] and investigates whether one can construct a consistent CFT in higher dimensions and whether we can put bounds on the CFT data of these theories. Conformal blocks up to $D = 6$ have been computed [26], but seem to be relatively un-studied in $D > 6$. This large D constraint analysis will be important for large D CFTs, to know whether one can build a consistent theory besides the GFFT. The starting point is the conformal block derived in chapter 5 and further simplifies this expression by assuming a linear scaling of spin and scaling dimension.

6.1 Large Dimensional Linear Scaling of the Conformal Block and the 4-Point Correlation Function

We consider the conformal block from equation (5.1.10) using a linear scaling between the scaling dimension Δ and the spacetime dimension D by relating $\Delta = \delta D$ and similarly for the spin $l = \omega D$. The justification for the scaling dimension is that through the unitarity bound it scales linearly with dimension. If spins shall be represented as well on equal footing, then we must assume a similar linear scaling for the spin. Using the Euler integral representation of the hypergeometric function the two factorized functions with spin and scaling dimensions can be written on the form:

$$A_{\delta D}(y_+) = \frac{y_+^{\delta D/2}\Gamma(D(\delta-\frac{1}{2})+1)}{\Gamma(\frac{\delta D}{2})\Gamma(D\frac{\delta-1}{2}+1)}\int_0^1 dt\frac{\sqrt{1-y_+t}}{t}\exp\left(D\ln\left(\frac{t^{\delta/2}(1-t)^{(\delta-1)/2}}{(1-y_+t)^{\delta/2}}\right)\right), \tag{6.1.1}$$

$$A_{1-\omega D}(y_-) = \frac{y_-^{(1-\omega D)/2}\Gamma(2-D(\omega+\frac{1}{2}))}{\Gamma(\frac{1-\omega D}{2})\Gamma(\frac{3}{2}-D\frac{\omega+1}{2})}\int_0^1 dt\sqrt{\frac{1-t}{t}}\exp\left(D\ln\left(\frac{(1-y_-t)^{\omega/2}}{t^{\omega/2}(1-t)^{(\omega-1)/2}}\right)\right). \tag{6.1.2}$$

Given the structure of the integral, it is natural to use the saddle-point approximation of the integral for large values of D. We, therefore, define the functions:

$$S_\delta(t) \equiv \ln\left(\frac{t^{\delta/2}(1-t)^{(\delta-1)/2}}{(1-y_+t)^{\delta/2}}\right), \qquad S_\omega(t) \equiv \ln\left(\frac{(1-y_-t)^{\omega/2}}{t^{\omega/2}(1-t)^{(\omega-1)/2}}\right). \tag{6.1.3}$$

The saddle-point is where $S(t)$ has the most dominant point, and this is found when the incline of $S(t)$ is flat hence $\partial_t S(t_{\delta,\omega}) = 0$:

$$t_\delta^\pm = \frac{2\delta - 1 \pm A}{2(\delta-1)y_+}, \qquad A \equiv \sqrt{1 + 4\delta(\delta-1)(1-y_+)}, \tag{6.1.4}$$

$$t_\omega^\pm = \frac{2\omega + 1 \pm B}{2(\omega+1)y_-}, \qquad B \equiv \sqrt{1 + 4\omega(\omega+1)(1-y_-)}. \tag{6.1.5}$$

The saddle-point must lie in the integration range $t \in [0,1]$ in order to use the saddle-point approximation. The unitarity bound with the linear scaling assumption can be written as:

$$\left(\frac{1}{2} - \delta\right) \leq \frac{1}{D}, \qquad \frac{1+\omega-\delta}{2} \leq \frac{1}{D}. \tag{6.1.6}$$

For values of $D \gg 1$, unitarity is only ensured when $\delta > 1/2$ for scalars and $\omega < \delta$ for non scalars. It is stated in [33] that when these bounds are obeyed the integration range is indeed in $t \in [0,1]$, but only for the negative solutions t_δ^- and t_ω^-.

Then we need to compute the curvature of $S(t)$ at the saddle-point:

$$\begin{aligned}
\beta_\delta \equiv \partial_t^2 S(t_\delta^-) &= \frac{(\delta-1)(A-1)^2(2\delta-1-A)^2 + \delta(2(\delta-1)y_+ - 2\delta + 1 + A)((A-1)^2 - (2\delta-1-A)^2)}{(2(\delta-1)^2 y_+^2)^{-1}(A-1)^2(2\delta-1-A)^2(2(\delta-1)y - 2\delta + 1 + A)}, \\
\beta_\omega \equiv \partial_t^2 S(t_\omega^-) &= \frac{(2\omega+1-B)^2((1+B)^2(\omega+1)+\omega) + 2(\omega+1)\omega y_-(2\omega+1-B)((1+B)^2-1)}{(2(\omega+1)^2 y_-^2)^{-1}(2\omega+1-B)^2(2(\omega+1)y_- - (2\omega+1-B))^2(1+B)^2}.
\end{aligned} \tag{6.1.7}$$

The saddle-point approximation puts the functions on the form:

$$2^{\delta D} A_{\delta D}(y_+) \simeq \frac{\Gamma(D(\delta - \frac{1}{2}) + 1)}{\Gamma(\frac{\delta D}{2})\Gamma(D\frac{\delta-1}{2} + 1)} \frac{\sqrt{1 - y_+ t_\delta^-}}{t_\delta^-} \sqrt{\frac{2\pi}{-D\beta_\delta}} \exp\left(D \ln\left(\frac{2^\delta y_+^{\delta/2}(t_\delta^-)^{\delta/2}(1-t_\delta^-)^{(\delta-1)/2}}{(1-y_+t_\delta^-)^{\delta/2}}\right)\right), \tag{6.1.8}$$

$$2^{\omega D} A_{1-\omega D}(y_-) \simeq \frac{y_-^{1/2}\Gamma(2 - D(\omega + \frac{1}{2}))}{\Gamma(\frac{1-\omega D}{2})\Gamma(\frac{3}{2} - D\frac{\omega+1}{2})} \sqrt{\frac{1-t_\omega^-}{t_\omega^-}} \sqrt{\frac{2\pi}{-D\beta_\omega}} \exp\left(D \ln\left(\frac{2^\omega y_-^{-\omega/2}(1-y_-t_\omega^-)^{\omega/2}}{(t_\omega^-)^{\omega/2}(1-t_\omega^-)^{(\omega-1)/2}}\right)\right). \tag{6.1.9}$$

Applying the Stirling approximation for the Γ-function and some algebra we can write the conformal block in the linear scaling large D limit:

$$G_{\delta,\omega}(y_+, y_-) = \frac{f_\delta(y_+)e^{Dg_\delta(y_+)} f_\omega(y_-)e^{Dg_\omega(y_-)}}{\sqrt{y_- - y_+}}. \tag{6.1.10}$$

Notice that we have pulled out the $(y_- - y_+)^{-1/2}$ dependency from the f_ω when comparing to [33] in order

to give a more symmetric expression:

$$f_\delta(y_+) = \sqrt{\frac{(\delta-1)^{-3}(A-1)^3\delta(2\delta-1)(2(\delta-1)y_+-2\delta+1+A)^2}{2(16\delta(\delta-1)^2(A-\delta)y_+^2+16\delta(\delta-1)(A-\delta)(A-2\delta+1)y_++(2\delta-1-A)^2((A-1)^2+4\delta A-4\delta^2))}}, \tag{6.1.11}$$

$$g_\delta(y_+) = \log\left(\sqrt{\frac{2(\delta-1)^2y_+}{(2\delta-1)(2(\delta-1)y_+-2\delta+1+A)}}\left(\frac{2(2\delta-1)^2(2\delta-1-A)(2(\delta-1)y_+-2\delta+1+A)}{y_+\delta(\delta-1)^2(A-1)}\right)^{\delta/2}\right), \tag{6.1.12}$$

$$f_\omega(y_-) = \sqrt{\frac{(4y_-)^{-1}(\omega+1)^{-5}(B+1)^2(2\omega+1)^3(2\omega+1-B)(2(\omega+1)y_--(2\omega+1-B))^3}{16\omega(B-\omega)(\omega+1)^2y_-^2-16(\omega+1)^2(2\omega+1-B)\omega(B-\omega)y_-+(2\omega+1-B)^2(4B\omega+(B+1)^2-4\omega^2)}}, \tag{6.1.13}$$

$$g_\omega(y_-) = \log\left(\sqrt{\frac{2(\omega+1)^2y_-}{(2\omega+1)(2(\omega+1)y_--2\omega-1+B))}}\left(\frac{y_-(2\omega+1)^2(2\omega+1-B)(2(\omega+1)y_--2\omega-1+B)}{8\omega(\omega+1)^2(B+1)}\right)^{-\omega/2}\right). \tag{6.1.14}$$

Notice that if one changes $\delta \to -\omega$ and $y_+ \to y_-$ the structure of the g-functions above have very similar expressions up to a few factors. This approximation of the conformal block has been plotted and compared to the $D = 4$ case in Figure 6.1.

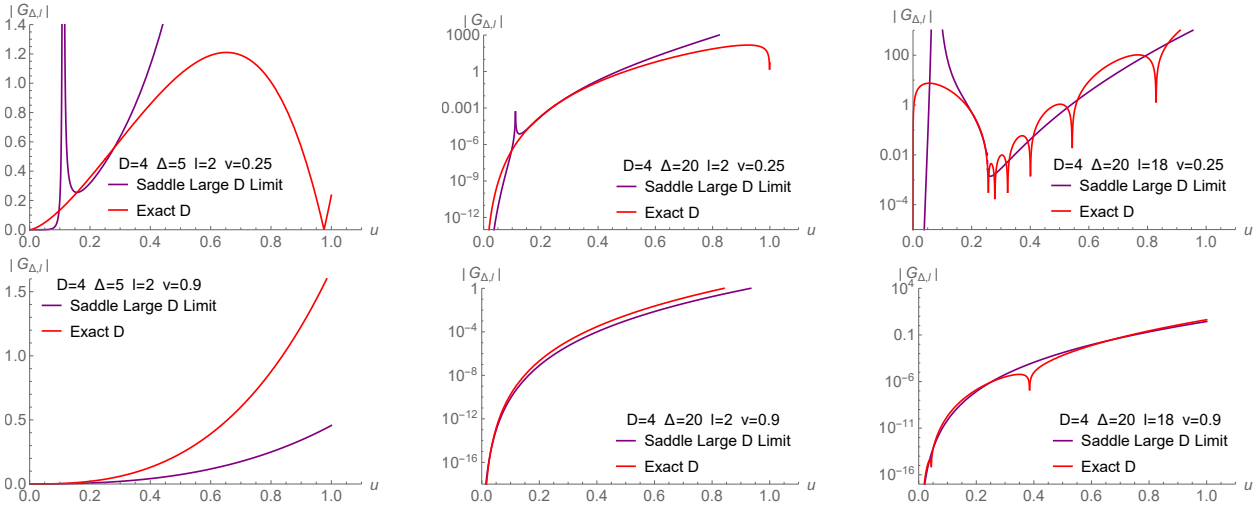

Figure 6.1: *The absolute value of the further approximated linear scaling large D conformal block $|G_{\Delta,l}(u,v)|$ (purple) plotted with the exact conformal block (red), both evaluated at $D = 4$ and as functions of the cross-ratio u. Both blocks are evaluated at different fixed values of scaling dimension Δ, spin l and cross-ratio v.*

The approximation to the conformal blocks from [33] does not seem to resemble the same structure of the conformal blocks as those from [25] for a low amount of dimensions and specifically $D = 4$ from Figure 6.1. Even when comparing to the large D case by using the large D approximation from [34] the structure is not similar, as seen in Figure 6.2. Therefore, either the saddle-point approximation method to the blocks applied in [34] should be doubted, or the linear scaling of both spin and scaling dimension. From the unitarity bound we have that the scaling dimension scales linearly with dimension, so that $\Delta = \delta D$ seems to be a fine assumption. But there is no indication that $l = \omega D$ should be a meaningful approximation.

One can be studying the scaling of $1 - l = \omega D$ to make the factorized parts of the conformal block completely symmetric. Likewise in [36] another symmetry is explored, which has some similarities to this large D conformal block discussion. The Casimir eigenvalue is invariant under the light transform L. The

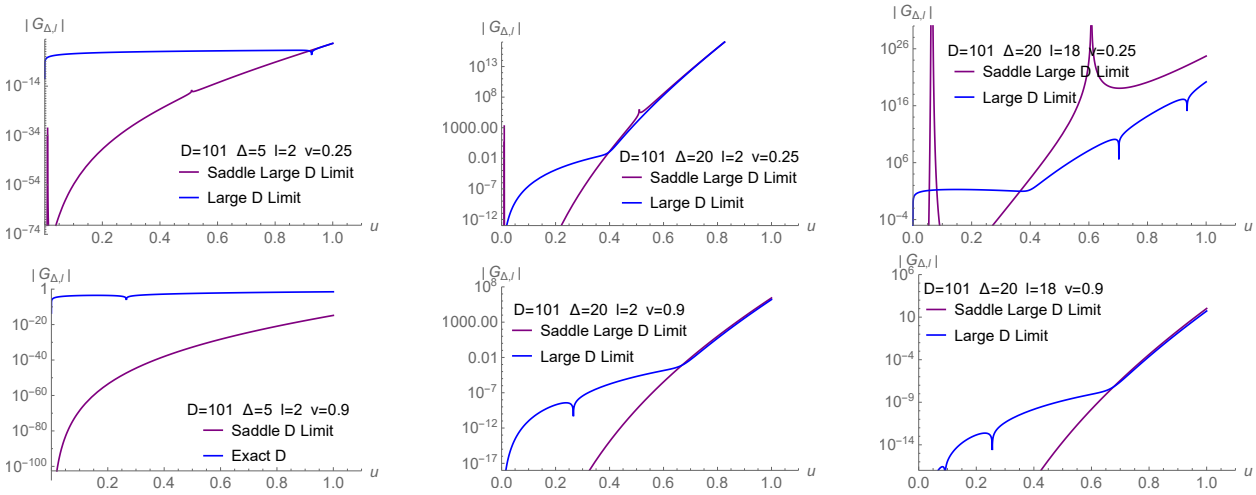

Figure 6.2: *The absolute value of the further approximated linear scaling large D conformal block $|G_{\Delta,l}(u,v)|$ (purple) plotted with the conformal block of the usual large D limit (blue), both evaluated at $D = 101$ and as functions of the cross-ratio u. Both blocks are evaluated at different fixed values of scaling dimension Δ, spin l and cross-ratio v. The choice of $D = 101$ should fit into the large D approximation so that the conformal blocks behave similarly. If evaluated at larger D the numerical code cannot represent extremely small numbers anymore leading to divergences, and a plot that cannot be trusted.*

light transform changes the scaling dimension and spin by:

$$L : (\Delta, l) \to (1 - l, 1 - \Delta), \tag{6.1.15}$$

so that the Casimir eigenvalue is invariant under this transformation:

$$LC_{\Delta,l} = C_{1-l,1-\Delta} = C_{\Delta,l}. \tag{6.1.16}$$

This light transform and how it can be applied in this context may be a path to pursue, but it is outside the scope of this thesis.

We will now introduce a new set of coordinates, which we will refer to as the Gadde-Sharma coordinates that are related to the conformal cross-ratios:

$$u = a^2 e^{\sigma/D}, \qquad v = b^2 e^{\tau/D}, \tag{6.1.17}$$

where a, b shall be thought of as constants. We will then relate the Gadde-Sharma coordinates to the $\{y_+, y_-\}$ coordinates:

$$y_\pm = \frac{u}{(1+\sqrt{v})^2} = \frac{a^2 e^{\sigma/D}}{(1 \pm b e^{\tau/2D})^2}. \tag{6.1.18}$$

The approximation for the conformal block is for the leading order in D, therefore we make a $1/D$ expansion of $\{y_+, y_-\}$:

$$y_\pm = \hat{y}_\pm \left(1 + \frac{\sigma}{D} - \frac{\tau}{D}\frac{b}{b \pm 1} + \mathcal{O}(1/D^2)\right), \qquad \hat{y}_\pm = \frac{a^2}{(1 \pm b)^2}. \tag{6.1.19}$$

This implies that the conformal block written in Eq. (6.1.10) is in the leading D order when $y_+ \to \hat{y}_+$. If we want an expansion for the next to leading order in D the conformal block factorizes. Applying the next to leading order in the expansion brings the conformal block on the form:

$$G_{\delta,\omega}(\sigma,\tau) = \mathcal{N}_{\delta,\omega}(a^2,b^2)\mathcal{B}_{\delta,\omega,a,b}(\sigma,\tau), \tag{6.1.20}$$

$$\mathcal{N}_{\delta,\omega}(a^2,b^2) \equiv \frac{f_\delta(\hat{y}_+)e^{Dg_\delta(\hat{y}_+)} f_\omega(\hat{y}_-)e^{Dg_\omega(\hat{y}_-)}}{\sqrt{\hat{y}_- - \hat{y}_+}}, \tag{6.1.21}$$

$$\mathcal{B}_{\delta,\omega,a,b}(\sigma,\tau) \equiv e^{k_+(a,b,\delta)\left((1+\frac{1}{b})\sigma-\tau\right)} e^{k_-(a,-b,1+\omega)\left((1-\frac{1}{b})\sigma-\tau\right)}, \tag{6.1.22}$$

where

$$k_{\pm}(a,b,x) \equiv \frac{b(1+b)}{4((1+b)^2-a^2)}\left(1 \pm \sqrt{1+4x(x-1)\left(1-\frac{a^2}{(1+b)^2}\right)}\right). \tag{6.1.23}$$

The structure of these next to leading order terms are complicated to compute using the $\{y_+, y_-\}$ expansion. Therefore it is instructive to look at the scalar block from Eq. (5.1.1) and apply the large D approximation to obtain the $k_\pm$ associated with the scaling dimensional part of the block. This has been computed in Appendix E.

We are interested in the behavior of the 4-point correlation function when we have to consider crossing in section 6.2, therefore we want to apply the $\mathcal{A}(u,v)$ function from Eq. (3.6.13) to the linear scaled large D conformal block. Together with the unitarity bounds we can write the structure of the 4-point correlation function as:

$$\mathcal{A}(u,v) = 1 + \sum_{\frac{D-2}{2}\leq\Delta, l=0} P_{\Delta,0}G_{\Delta,0}(u,v) + \sum_{l+D-2\leq\Delta, 0\neq l} P_{\Delta,l}G_{\Delta,l}(u,v). \tag{6.1.24}$$

We write out specifically the scalar $l=0$ case for the second term leaving a factor $(1+(-1)^l)$ that picks out the even terms. Then one should include values for $\Delta < D-2$ in the first term, to avoid double counting:

$$\mathcal{A}(u,v) = 1 + \sum_{\frac{D-2}{2}\leq\Delta<D-2, l=0} P_{\Delta,0}G_{\Delta,0}(u,v) + \sum_{l+D-2\leq\Delta, 0\leq l} (1+(-1)^l)P_{\Delta,l}G_{\Delta,l}(u,v). \tag{6.1.25}$$

We call the first sum over a domain $\mathcal{D}_1$ and the second sum over a domain $\mathcal{D}_2$. Including that $\Delta = \delta D$ and $l = D\omega$ and taking the large D limit we have the domains of integration:

$$\mathcal{D}_1 \equiv \{(\delta,\omega) : \omega = 0, \frac{1}{2} \leq \delta < 1\}, \qquad \mathcal{D}_2 \equiv \{(\delta,\omega) : \omega > 0, \delta \geq \omega + 1\}. \tag{6.1.26}$$

Using these domains for Eq. (6.1.25) we can change the sums to integrals, which is well approximated for large D, and apply the Gadde-Sharma coordinates:

$$\mathcal{A}(\sigma,\tau) = 1 + D\int_{\mathcal{D}_1} d\delta P_{\delta,0}\mathcal{N}_{\delta,0}(a^2,b^2)\mathcal{B}_{\delta,0,a,b}(\sigma,\tau) + D^2\int_{\mathcal{D}_2} d\delta d\omega P_{\delta,\omega}\mathcal{N}_{\delta,\omega}(a^2,b^2)\mathcal{B}_{\delta,\omega,a,b}(\sigma,\tau), \tag{6.1.27}$$

while the factor $(1+(-1)^l)$, that have been neglected in that above, will give some rapid oscillations for the block when going to large D since the dependency $(-1)^l = e^{i\pi D\omega}$ gives rotations in the complex plane. The OPE coefficient $P_{\Delta,l}$ is convergent when we restrict ourselves to the unit box/diamond region of parameter space:

$$0 < z, \bar{z} < 1, \qquad 0 < u, v < 1, \qquad 0 < a, b < 1 \quad \text{and} \quad a + b < 1. \tag{6.1.28}$$

The approximation which allowed us to re-cast $\mathcal{A}(u,v)$ in terms of a saddle-point evaluation for large values of D enables us to consider crossing symmetry in section 6.2. The crossing symmetry can further restrict our CFT data.

6.2 Constraints by Crossing Symmetry

Concerning crossing symmetry we apply the conformal bootstrap of Eq. (3.6.12) on the linear scaled Δ and l versions of the large D conformal blocks:

$$1 + \sum_{\mathcal{D}_1\cup\mathcal{D}_2} (1+(-1)^l)P_{\Delta,l}G_{\Delta,l}(u,v) = \left(\frac{u}{v}\right)^{\Delta_\phi}\left(1 + \sum_{\mathcal{D}_1\cup\mathcal{D}_2} (1+(-1)^l)P_{\Delta,l}G_{\Delta,l}(v,u)\right). \tag{6.2.1}$$

Notice that $u \leftrightarrow v$ is interchanged in the conformal block on the RHS, according to the bootstrap. The LHS is referred to as the s-channel while the RHS is referred to as the t channel. The sums are then replaced with integrals for large values of D as we showed for the $\mathcal{A}(u,v)$ function in the previous section 6.1. The

integral over domain $\mathcal{D}_1$ has a D dependene and the integral over domain $\mathcal{D}_2$ has a D^2 dependence. The union over these two domains can therefore be represented with two integrals. For compactness we suppres these D dependencies. We change to the Gadde-Sharma coordinates and use the linear scaling for external scaling dimension $\Delta_\phi = \delta_\phi D$:

$$\begin{aligned} &1 + \int_{\mathcal{D}_1 \cup \mathcal{D}_2} d\delta d\omega (1 + e^{i\pi\omega D}) P_{\delta,\omega} \mathcal{N}_{\delta,\omega}(a^2, b^2) \mathcal{B}_{\delta,\omega,a,b}(\sigma, \tau) \\ = &\left(\frac{a^2}{b^2}\right)^{\delta_\phi D} e^{(\sigma-\tau)\delta_\phi} \left(1 + \int_{\mathcal{D}_1 \cup \mathcal{D}_2} d\delta d\omega (1 + e^{i\pi\omega D}) P_{\delta,\omega} \mathcal{N}_{\delta,\omega}(b^2, a^2) \mathcal{B}_{\delta,\omega,b,a}(\tau, \sigma)\right). \end{aligned} \tag{6.2.2}$$

Notice again that $\sigma \leftrightarrow \tau$ and $a \leftrightarrow b$ have been interchanged on the RHS by the bootstrap condition.
Now let us focus on the σ and τ dependency. This behavior is contained in $\mathcal{B}_{\delta,\omega,a,b}(\sigma, \tau)$ functions and the prefactor for the t-channel. We assume there are some globally dominant saddle-points in the $\{a, b\}$-space defined in the s-channel to be (δ_s^*, ω_s^*) and the t-channel to be (δ_t^*, ω_t^*). The dominant saddle-points will be bounded within the integration regions for the t- and s-channels. These integration regions will be satisfying unitarity and crossing symmetry between the channels for us to have a consistent theory. We will in the following check under which conditions these are satisfied. The exponential dependency of Eq. (6.2.2) using Eq. (6.1.22) is specifically for σ and τ:

$$k_{s+}\left(1 + \frac{1}{b}\right) + k_{s-}\left(1 - \frac{1}{b}\right) = \delta_\phi - k_{t+} - k_{t-}, \qquad -k_{s+} - k_{s-} = -\delta_\phi + k_{t+}\left(1 + \frac{1}{a}\right) + k_{t-}\left(1 - \frac{1}{a}\right), \tag{6.2.3}$$

where we have defined the functions, $k_{s-}, k_{s+}, k_{t-}, k_{t+}$ which are related to the $k_\pm$ function by evaluating them at the dominant point for the s- and t-channel respectively:

$$k_{s+} \equiv k_+(a, b, \delta_s^*), \quad k_{s-} \equiv k_-(a, -b, 1 + \omega_s^*), \quad k_{t+} \equiv k_+(b, a, \delta_t^*), \quad k_{t-} \equiv k_-(b, -a, 1 + \omega_t^*). \tag{6.2.4}$$

The goal is now to consider the domains $\mathcal{D}_1$ and $\mathcal{D}_2$ in the k_{s-} and k_{s+} variables for the dominant point. The k_{t-} and k_{t+} will be related through crossing symmetry. This will enable us to consider how the s-channel and t-channel domains overlap each other and thus see how our theory is constrained.

Eq. (6.2.3) contains two coupled equations. Solving these for k_{t-} and k_{t+}:

$$k_{t+} = \frac{a-1}{2b}(k_{s+} - k_{s-}) - \frac{1}{2}(k_{s+} + k_{s-} - \delta_\phi), \quad k_{t-} = -\frac{a+1}{2b}(k_{s+} - k_{s-}) - \frac{1}{2}(k_{s+} + k_{s-} - \delta_\phi). \tag{6.2.5}$$

We would like to investigate the unions of the domains in the s- and t-channels. To do so, we invert the $k_\pm$ functions so that we solve for δ in k_+ and ω for k_-:

$$\delta = \zeta(a, b, k_+), \quad \omega = -\zeta(a, -b, k_-), \tag{6.2.6}$$

$$\zeta(a, b, y) = \frac{1}{2} \pm \frac{1}{2b}\sqrt{(4y(1+b) - b)^2 - (4ya)^2}. \tag{6.2.7}$$

Applying the relations of $\delta(k_+)$ and $\omega(k_-)$ in Eq. (6.2.6) on the domains from Eq. (6.1.26) we can write up the domains in the s-channel:

$$\begin{aligned} \mathcal{D}_1^s &= \{(k_{s+}, k_{s-}) : k_{s-} = k_-(a, -b, 1), \quad k_+\left(a, b, \frac{1}{2}\right) \leq k_{s+} < k_+(a, b, 1)\}, \\ \mathcal{D}_2^s &= \{(k_{s+}, k_{s-}) : k_{s-} > k_-(a, -b, 1), \quad k_{s+} \geq k_+(a, b, \omega + 1)\}. \end{aligned} \tag{6.2.8}$$

The bounds are functions, which we define according to [33] and evaluate them:

$$\mathcal{Q}_{\omega_s}(k_{s+}, a, b) \equiv k_-(a, -b, 1) = 0, \tag{6.2.9}$$

$$\tilde{\mathcal{Q}}_{\delta_s, min}(k_{s-}, a, b) \equiv k_+\left(a, b, \frac{1}{2}\right) = \frac{b}{4(1 - a + b)}, \tag{6.2.10}$$

$$\tilde{\mathcal{Q}}_{\delta_s, max}(k_{s-}, a, b) \equiv k_+(a, b, 1) = \frac{b(1+b)}{2((1+b)^2 - a^2)}, \tag{6.2.11}$$

$$Q_{\delta_s}(k_{s-}, a, b) \equiv k_+(a, b, 1 + \omega(k_{s-})) = \frac{b(1+b) + \sqrt{\gamma(k_{s-})}}{4((1+b)^2 - a^2)}, \tag{6.2.12}$$

where:

$$\gamma(k_{s-}) = b^2(1+b)^2 + 8b(1-b)((1+b)^2-a^2)k_{s-} + 16((b+1)^2-a^2)((1-b)^2-a^2)k_{s-}^2. \tag{6.2.13}$$

Let us then consider the t-channel. These will have a similar structure of bounds as the s-channel, but including the crossing symmetry between a and b it will take the form:

$$\begin{aligned}\mathcal{D}_1^t &= \{(k_{t+},k_{t-}) : k_{t-} = k_-(b,-a,1), \quad k_+\left(b,a,\frac{1}{2}\right) \leq k_{t+} < k_+(b,a,1)\},\\ \mathcal{D}_2^t &= \{(k_{t+},k_{t-}) : k_{t-} > k_-(b,-a,1), \quad k_{t+} \geq k_+(b,a,\omega+1)\}.\end{aligned} \tag{6.2.14}$$

In order to compare the domains, the t-channel domains have to be changed into the $\{k_{s+},k_{s-}\}$ variables. The relation of $k_{t\pm}$ in terms of $k_{s\pm}$ is written in (6.2.5). Inverting that expression:

$$\begin{aligned}k_{s+} =& \frac{(a+b-1)k_{s-} + 2bk_{t+} - b\delta_\phi}{a-b-1},\\ k_{s-} =& \frac{-b\delta_\phi + (1+a+b)k_{s+} + 2bk_{t-}}{1+a-b}.\end{aligned} \tag{6.2.15}$$

This can bring the t-channel domains on the form:

$$\begin{aligned}\mathcal{D}_1^t &= \{(k_{ts+},k_{s-}) : k_{s-} = \mathcal{Q}_{\omega_t}(k_{s+},a,b), \quad \tilde{\mathcal{Q}}_{\delta_{t,min}}(k_{s-},a,b), \leq k_{s+} < \tilde{\mathcal{Q}}_{\delta_{t,max}}(k_{s-},a,b)\},\\ \mathcal{D}_2^t &= \{(k_{s+},k_{s-}) : k_{s-} > \mathcal{Q}_{\omega_t}(k_{s+},a,b), \quad k_{s+} \geq \mathcal{Q}_{\delta_t}(k_{s-},a,b)\},\end{aligned} \tag{6.2.16}$$

where the bounds are defined by the $\mathcal{Q}$-functions:

$$\mathcal{Q}_{\omega_t}(k_{s+},a,b) \equiv \frac{-b\delta_\phi + (1+a+b)k_{s+}}{1+a-b}, \tag{6.2.17}$$

$$\tilde{\mathcal{Q}}_{\delta_{t,min}}(k_{s-},a,b) \equiv \frac{2k_{s-}((1-b)^2-a^2) + 2b(1+a-b)\delta_\phi - ab}{2(1-(a-b)^2)}, \tag{6.2.18}$$

$$\tilde{\mathcal{Q}}_{\delta_{t,max}}(k_{s-},a,b) \equiv \frac{(2\delta_\phi-1)a^2 - 2\delta_\phi(b+1)^2 + b + 1 + \sqrt{\zeta}}{4(a-b-1)(a+b+1)}, \tag{6.2.19}$$

$$\mathcal{Q}_{\delta_t}(k_{s-},a,b) \equiv \frac{(2\delta_\phi-1)a^2 - 2\delta_\phi(b+1)^2 + b + 1 + \sqrt{\rho(k_{s-})}}{4(a-b-1)(a+b+1)}, \tag{6.2.20}$$

where:

$$\zeta \equiv a^2(1-2\delta_\phi)(4b^2\delta_\phi + 2\delta_\phi - 2b - 1) + (2\delta_\phi(b^2-1) + b + 1)^2 \tag{6.2.21}$$

$$\begin{aligned}\rho(k_{s-}) \equiv& 16(a^4 - 2a^2(b^2+1) + (b^2-1)^2)k_{s-}^2 - 8(a-b-1)(a+b+1)((2\delta_\phi-1)a^2 - 2\delta_\phi(b-1)^2 - b + 1)k_{s-}\\ &+ a^2(1-2\delta_\phi)(4b^2\delta_\phi + 2\delta_\phi - 2b - 1) + (2\delta_\phi(b^2-1) + b + 1)^2.\end{aligned} \tag{6.2.22}$$

Notice that the inequalities change direction from the s- to the t-channel, because when we solve for k_{s+} and k_{s-} we have a change in sign, which changes the inequality.

Besides the regions, we would like to categorize the different kinds of overlap types between these regions for general values of $\{a,b\}$. They are categorized by defining the extremum points and then looking at the placement of those points. We find the start and end points of the domain regions in the s- and t-channels. These are found by solving the coupled equations from the domains' upper and lower bounds of

$\mathcal{D}_1$.

$$\begin{aligned}
&\text{Minimum of} \quad \mathcal{D}_1^s \quad k_{s-} = \mathcal{Q}_{\omega_s} \wedge k_{s+} = \tilde{\mathcal{Q}}_{\delta_s,min} \to (k_{s-}^P, k_{s+}^P) = \left(0, \frac{b}{4(1-a+b)}\right), \\
&\text{Maximum of} \quad \mathcal{D}_1^s \quad k_{s-} = \mathcal{Q}_{\omega_s} \wedge k_{s+} = \mathcal{Q}_{\delta_s} \to (k_{s-}^B, k_{s+}^B) = \left(0, \frac{b(1+b)}{2((1+b)^2-a^2)}\right), \\
&\text{Minimum of} \quad \mathcal{D}_1^t \quad k_{s-} = \mathcal{Q}_{\omega_t} \wedge k_{s+} = \tilde{\mathcal{Q}}_{\delta_t,min} \to (k_{s-}^O, k_{s+}^O) = \left(\frac{\delta_\phi}{2} - \frac{a+b+1}{8(1+a-b)}, \frac{4\delta_\phi - 1}{8}\right), \\
&\text{Maximum of} \quad \mathcal{D}_1^t \quad k_{s-} = \mathcal{Q}_{\omega_t} \wedge k_{s+} = \mathcal{Q}_{\delta_t} \to (k_{s-}^R, k_{s+}^R) = \left(\frac{\delta_\phi}{2} - \frac{a+1}{4(1+a-b)}, \frac{\delta_\phi}{2} - \frac{a+1}{4(1+a+b)}\right),
\end{aligned} \tag{6.2.23}$$

where P, B, O, R and in the following equation G refers to the colors in the plot. The last point is the intersection between the $\mathcal{D}_1^s$ and $\mathcal{D}_1^t$ domains. These domains are lines so we will have a specific intersection at:

$$\mathcal{D}_1^s \cap \mathcal{D}_1^t \quad k_{s-} = \mathcal{Q}_{\omega_s} \wedge \mathcal{Q}_{\omega_t} \to (k_{s-}^G, k_{s+}^G) = \left(0, \frac{b\delta_\phi}{1+a+b}\right). \tag{6.2.24}$$

We are now able to represent the domains of the s- and t-channel in $\{k_{s-}, k_{s+}\}$ coordinates. These have been shown in Figure 6.3 for different values of the constants a, b, δ_ϕ. Here the blue regions show the s-channel and the orange regions show the t-channel domain. Meanwhile it is of interest to plot the minimum, maximum and intersection points on these plots as well. We categorize the overlap of domains as follows:

$$\text{Type-I}: \quad \mathcal{D}_1^s \cap \mathcal{D}_1^t, \qquad \text{Type-II}: \quad \mathcal{D}_2^s \cap \mathcal{D}_1^t, \qquad \text{Type-III}: \quad \mathcal{D}_1^s \cap \mathcal{D}_2^t, \qquad \text{Type-IV}: \quad \mathcal{D}_2^s \cap \mathcal{D}_2^t. \tag{6.2.25}$$

According to Figure 6.3(a), we have a Type-IV overlap, combined with a Type-II overlap and a Type-III overlap. For Figure 6.3(b) we have a Type-III overlap and Figure 6.3(c) is a Type-II overlap while Figure 6.3(d) is a Type-I overlap. The points of interest in e.g. Figure 6.3(a) is blue and red, since their placement with respect to each other defines when we no longer have this type of overlap. We would therefore like to find what these boundary values are for all overlap types. This enables us to produce a plot which can represent where we can find the different type of unions of the domains for general values of $\{a, b\}$. This is shown in Figure 6.4.

We will now elaborate on how Figure 6.4 is produced for each overlap type. When producing the $\{a, b\}$ plane of Type-IV overlap, we consider the blue and red point and edges of integration domains. The $\mathcal{Q}$-function correspond to the edges of the domains. We have that the red points should be above the blue edges in Figure 6.4(a) leading to:

$$k_{s-}^R \geq \mathcal{Q}_{\omega_s}(k_+^R, a, b) \cap k_{s+}^R \geq \mathcal{Q}_{\delta_s}(k_-^R, a, b), \tag{6.2.26}$$

while we have that the blue point should be inside the orange region:

$$k_{s-}^B \geq \mathcal{Q}_{\omega_t}(k_{s+}^B, a, b) \cap k_{s+}^B \leq \mathcal{Q}_{\delta_t}(k_{s-}, a, b). \tag{6.2.27}$$

The bounds are evaluated to specific lines that constrain the overlap region. We plug in the values of $\{k_{s-}, k_{s+}\}$ evaluated at the points, giving us these functions:

$$k_{s-}^R \geq \mathcal{Q}_{\omega_s}(k_+^R, a, b) \qquad \to b = \frac{(1+a)(2\delta-1)}{2\delta}, \tag{6.2.28}$$

$$k_{s+}^R \geq \mathcal{Q}_{\delta_s}(k_-^R, a, b) \qquad \to a = 2\delta - 1, \tag{6.2.29}$$

$$k_{s-}^B \geq \mathcal{Q}_{\omega_t}(k_{s+}^B, a, b) \qquad \to b = \frac{1-2\delta+2a\delta}{2\delta-1}, \tag{6.2.30}$$

$$k_{s+}^B \leq \mathcal{Q}_{\delta_t}(k_{s-}, a, b) \qquad \to b = 2\delta - 1. \tag{6.2.31}$$

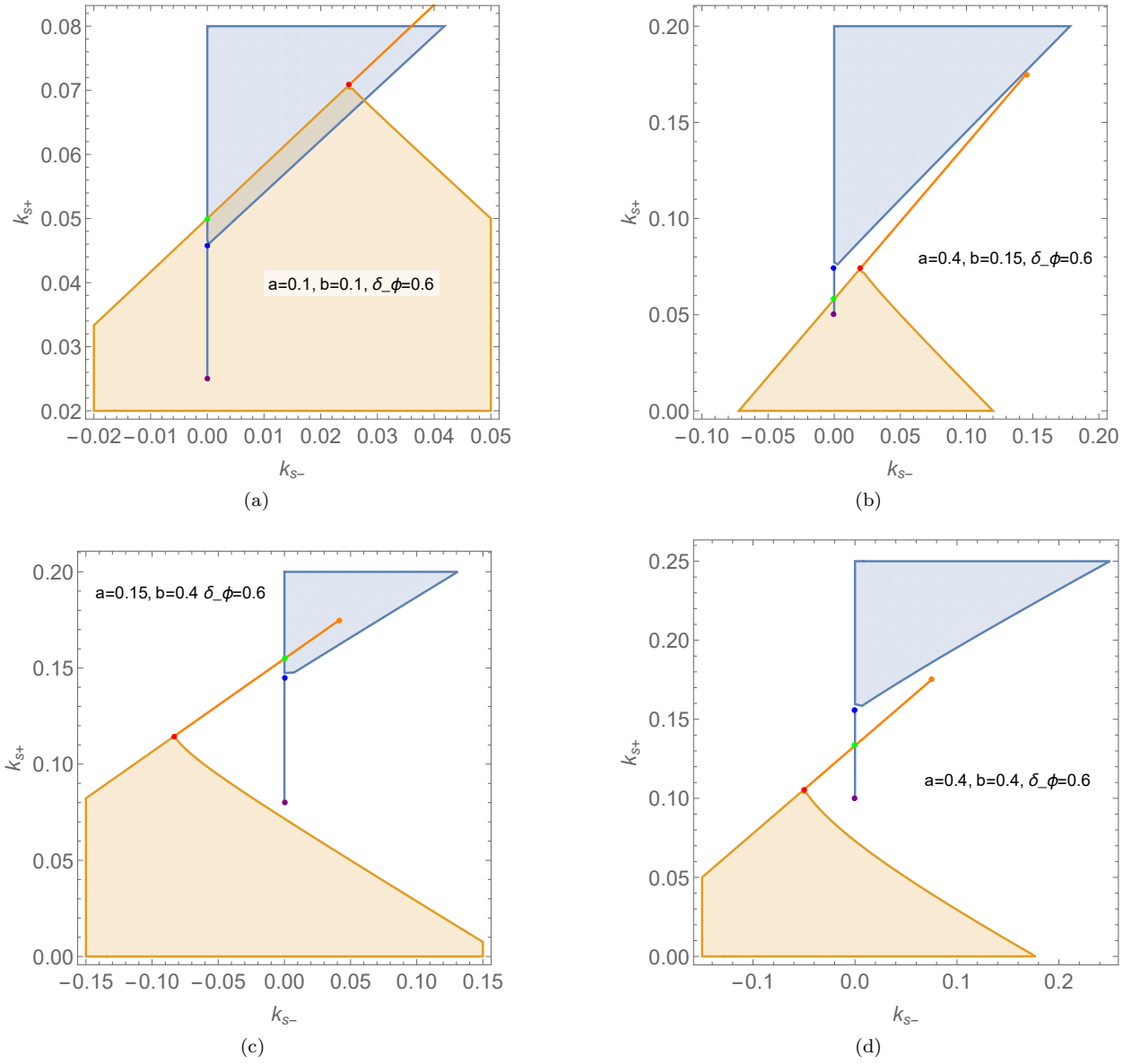

Figure 6.3: *Integration domains in the $\{k_{s-}, k_{s+}\}$ variable space. The blue regions are the s-channel domains $\mathcal{D}^s$ and the orange regions are the t-channel domains $\mathcal{D}^t$. The external scaling dimension is fixed at $\delta_\phi = 0.6$ for all subfigures, and different values of $\{a, b\}$ are presented. The purple, blue, orange, red and green dots show the maximum value of $\mathcal{D}^s_1$, minimum value of $\mathcal{D}^s_1$, maximum value of $\mathcal{D}^t_1$, minimum value of $\mathcal{D}^t_1$ and intersection between $\mathcal{D}^s_1 \cap \mathcal{D}^t_1$ respectively. The values of $\{a, b\}$ are chosen so that there is a subfigure representing each overlap type.*

these inequlities constrain the Type-IV integration domain in the $\{a, b\}$-plane to be in the red square given in Figure 6.4(a). For Type-III we have that the purple point should not leave the orange region in Figure 6.3(b), which we split into a statement whether the purple point is to the right or left of the red point, thus:

$$k^P_{s-} \leq k^R_{s-} \cap k^P_{s-} \geq \mathcal{Q}_{\omega_t}(a, b, k^P_{s+}) \qquad k^P_{s-} \geq k^R_{s-} \cap k^P_{s+} \leq \mathcal{Q}_{\delta_t}(a, b, k^P_{s-}). \tag{6.2.32}$$

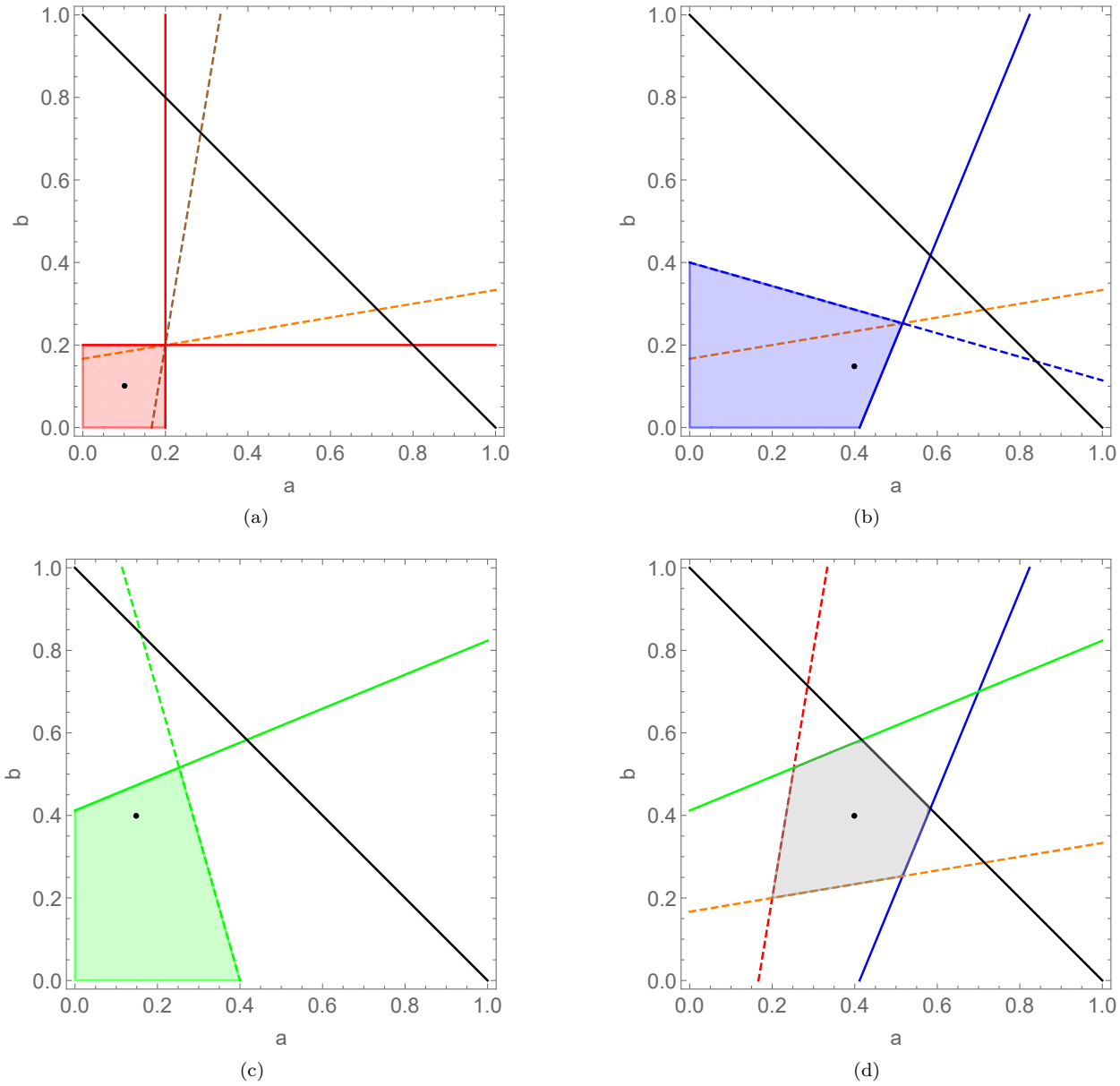

Figure 6.4: *Regions that show how the overlap types are constrained by the choice of* $\{a, b\}$*, with* $\delta_\phi = 0.6$*. Subfigure (a) represents the Type-IV overlap, subfigure (b) is the Type-III overlap, subfigure (c) is the Type-II overlap and subfigure (d) is the Type-I overlap. The black dot represents the choice for* $\{a, b\}$ *in Figure 6.3.*

This translates into the lines:

$$k^P_{s-} \leq k^R_{s-} \qquad \rightarrow b = \frac{2\delta - 1 - a + 2a\delta}{2\delta}, \tag{6.2.33}$$

$$k^P_{s-} \geq \mathcal{Q}_{\omega_t}(a, b, k^P_{s+}) \qquad \rightarrow b = \frac{1 + a - 4\delta + 4a\delta}{4\delta - 1}, \tag{6.2.34}$$

$$k^P_{s-} \geq k^R_{s-} \qquad \rightarrow b = \frac{2\delta - 1 - a + 2a\delta}{2\delta}, \tag{6.2.35}$$

$$k^P_{s+} \leq \mathcal{Q}_{\delta_t}(a, b, k^P_{s-}) \qquad \rightarrow b = \frac{2(1 + a - 6\delta - 2a\delta + 8\delta^2)}{4\delta - 1}. \tag{6.2.36}$$

This leads to the domain in Figure 6.4(b). For Type-II we have that the orange point should not leave the blue region, which leads to the statement:

$$k^O_{s-} \geq \mathcal{Q}_{\omega_s}(a,b,k^O_{s+}) \cap k^O_{s+} \geq \mathcal{Q}_{\delta_s}(a,b,k^O_{s-}). \tag{6.2.37}$$

This translates into the lines:

$$k^O_{s-} \geq \mathcal{Q}_{\omega_s}(a,b,k^O_{s+}) \qquad \to b = \frac{(1+a)(4\delta-1)}{1+4\delta}, \tag{6.2.38}$$

$$k^O_{s+} \geq \mathcal{Q}_{\delta_s}(a,b,k^O_{s-}) \qquad \to b = \frac{(1-4\delta)(2+a-4\delta)}{2(2\delta-1)}, \tag{6.2.39}$$

which leads to Figure 6.4(c). For Type-I we have that the green point should be in between the blue and the purple points and it should be in between the red and the orange points, this leads to the statement:

$$k^G_{s+} \leq k^B_{s+} \cap k^G_{s+} \geq k^P_{s+}, \qquad k^G_{s+} \geq k^R_{s+} \cap k^G_{s+} \leq k^O_{s+}, \tag{6.2.40}$$

giving us the lines:

$$k^G_{s+} \leq k^B_{s+} \qquad \to b = \frac{1-2\delta+2a\delta}{2\delta-1}, \tag{6.2.41}$$

$$k^G_{s+} \geq k^P_{s+} \qquad \to b = \frac{1+a-4\delta+4\delta}{4\delta-1}, \tag{6.2.42}$$

$$k^G_{s+} \geq k^R_{s+} \qquad \to b = \frac{(1+a)(2\delta-1)}{2\delta}, \tag{6.2.43}$$

$$k^G_{s+} \leq k^O_{s+} \qquad \to b = \frac{(1+a)(4\delta-1)}{4\delta+1}. \tag{6.2.44}$$

This leads to the lines in Figure 6.4 (d). All of these types of overlap regions are also constrained by a black line $b = 1-a$, this comes from the fact that $\{a,b\}$ coordinates are confined by the diamond Eq. (6.1.28).

In Figure 6.5 we have shown all of the overlap regions on the same plot for different values of δ_ϕ. The figure shows that the overlap types depend on the value of δ_ϕ and the choice of $\{a,b\}$. One can even have multiple types of overlaps for a specific choice of these parameters. This is why it was not possible to show Type-IV overlap in Figure 6.3(a) without Type-II and Type-III. The red box, i.e. Type-IV overlap always lies on top of other overlap types, and when increasing δ_ϕ we see that this type of overlap becomes more dominant.

If the unitary domain somewhere does not have a solution, it means that one cannot make a consistent theory on top of the GFFT. According to Figure 6.5, solutions of the union domains are lacking for values of $\delta_\phi < 3/4$ since a pink region exists here, which represents no overlaps. This argument can be extended to $\delta_\phi < 1$. The dominant point lies in the $\mathcal{D}^s_1$ and $\mathcal{D}^t_1$ domains. Since there is a discontinuity between the $\mathcal{D}_1$ and $\mathcal{D}_2$ domains, one cannot move this dominant point to the $\mathcal{D}_2$ domains. This means that if the dominant points should agree one needs to match either $\mathcal{D}^s_2$ with $\mathcal{D}^t_2$ or $\mathcal{D}^s_1$ with $\mathcal{D}^t_1$. This is only possible for overlaps of Type-I or Type-IV. Therefore we can extend the argument, that we only find GFFT for $\delta_\phi < 1$, and that a consistent unitary CFT in large dimensions must have that $\delta_\phi > 1$.

The conformal bootstrap program, which consists partly of this crossing symmetry for 4-point correlation functions is used to put bounds on the CFT data. This method has successfully been applied for the specific large D limit of this chapter to obtain the bound on the external scaling dimension $\Delta_\phi/D > 1$. Conformal symmetry imposes a lot of constraints on the correlation functions without the use of a Lagrange description, where this is one of the constraints. But we have to doubt the validity of this analysis since the comparison between these linearly scaled large D conformal blocks in both a relatively small dimension $D = 4$ and a relatively large $D = 101$ dimension with that of the large D limit from [34] does not seem to resemble the same features of the $\{u,v\}$ slices. This mismatch was not pointed out in [33]. For future work, it could be interesting to see whether the crossing symmetry could be effectively applied to the conformal blocks of [28] in a similar manner as in [33]. For the coming chapters, we will study how the coordinates and conformal blocks of [34] and [28] are related.

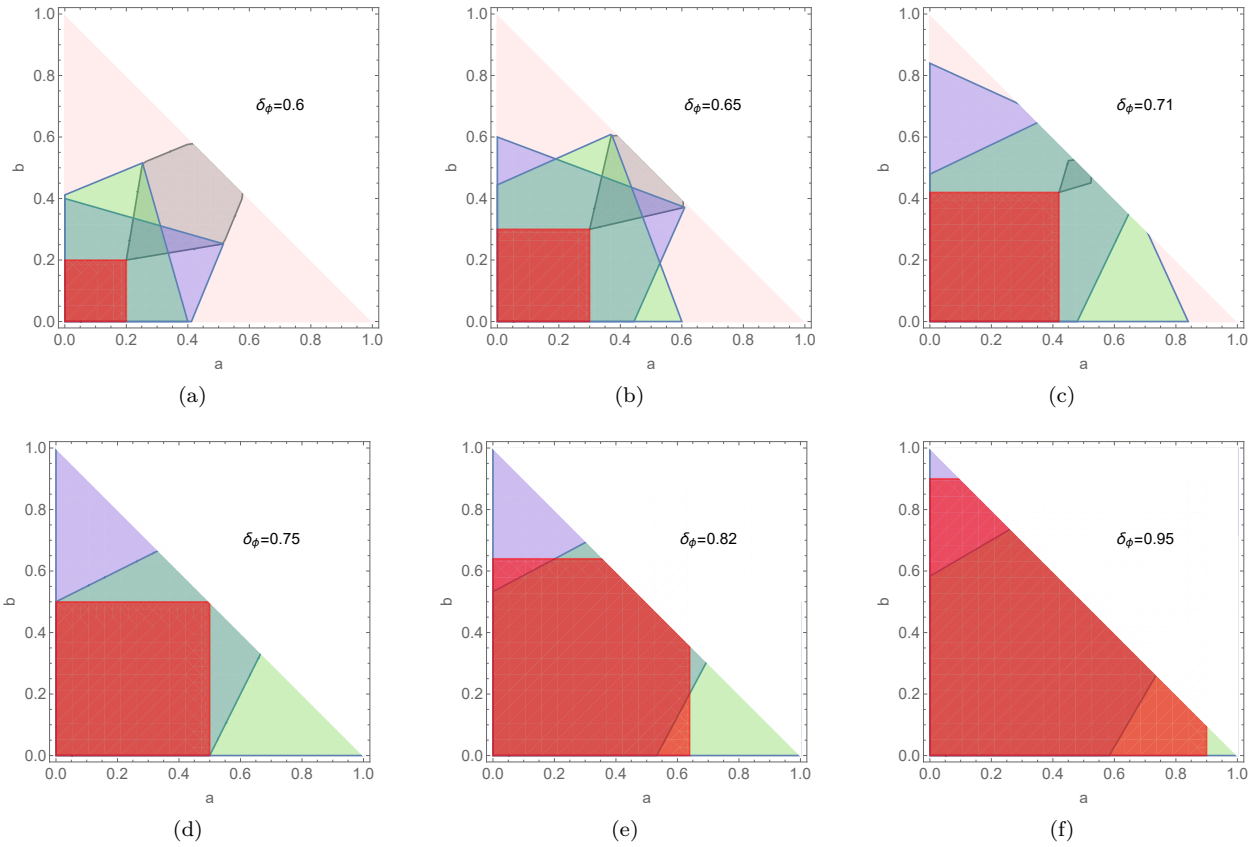

Figure 6.5: *A representation of the different types of overlap regions in the* $\{a, b\}$ *space are given with different values of* δ_ϕ*. Lightpink is no overlap between the s- and t-channel, grey is Type-I, green is Type-II, blue is Type-III and red is Type-IV, preserving the same colors as for Figure 6.4. For* $\delta_\phi > 3/4$ *the whole* $\{a, b\}$ *is covered with overlap types, while for* $\delta_\phi > 1$*, Type-IV covers the whole plane satisfying the crossing constraint.*

Chapter 7

Coordinates and Casimir Operator of Large Dimensional Conformal Field Theories

In this chapter, we find an interesting relation between the $\{y_+, y_-\}$ and $\{r, \eta\}$ coordinates, which essentially says that the y_+ coordinate is a radial coordinate and that y_- is an angular coordinate. This relates to the languages of the papers which are reviewed in chapter 4 and chapter 5. It indicates that a large D conformal block would be comparable to a radial/angular conformal block. We will further see that the Casimir differential operator in $\{y_+, y_-\}$ and $\{r, \eta\}$ can be related so that we can investigate the same large D limit. We also comment on how the large D limits of the Casimir equation may differ and motivate different types of large D limits.

7.1 Radial/Angular Connection to the Large Dimensional Scalar Block Suggested Coordinates

We can relate the $\{y_+, y_-\}$ coordinates to the $\{r, \eta\}$ coordinates by appying several transformations through the different coordinate systems introduced throughout the thesis, i.e. $\{y_+, y_-\} \to \{z, \bar{z}\} \to \{s, \xi\} \to \{r, \eta\}$:

$$y_\pm = \frac{u}{(1 \pm \sqrt{v})^2} = \frac{z\bar{z}}{(1 \pm \sqrt{(1-z)(1-\bar{z})})^2} = \frac{s^2}{(1 \pm \sqrt{1 - 2\xi s + s^2})^2} = \frac{16r^2}{(1 + r^2 + 2r\eta \pm \sqrt{(1 + r^2 - 2r\eta)^2})^2}, \tag{7.1.1}$$

each coordinate decouples from $y_\pm(r, \eta)$ into a dependency of $y_+(r)$ and $y_-(\eta)$:

$$y_+ = \frac{4r^2}{(1 + r^2)^2}, \qquad y_- = \frac{1}{\eta^2}. \tag{7.1.2}$$

This is in agreement with the notation from [34] that y_+ resembles a radial coordinate and y_- resembles an angular coordinate. In [34] y_- was related to the angular coordinate σ by $\sigma^2 \simeq 1/y_-$, which this calculation is consistent with. One can obtain the same decoupling and dependency using another series of transformations through $\{y_+, y_-\} \to \{z, \bar{z}\} \to \{\rho, \bar{\rho}\} \to \{r, \eta\}$.

There is a symmetry associated to the $y_+(r)$ relation of Eq. (7.1.2), that is seen when inverting the relation to $r(y_+)$, which has two solutions:

$$r = \frac{1 \pm \sqrt{1 - y_+}}{\sqrt{y_+}}. \tag{7.1.3}$$

If one reinstates $y_+(r)$ into that expression one obtains:

$$r = \frac{1 + r^2 \pm (1 - r^2)}{2r} = \frac{1}{r} \wedge r. \tag{7.1.4}$$

In order to leave r invariant when inverting twice, one must take the negative solution of Eq. (7.1.3). The transformation of $r \to \frac{1}{r}$ leaves y_+ invariant. In physical terms, we can map the coordinates between the inside and outside of the unit circle of radius $r = 1$ by an inversion.

7.2 Connecting the Casimir Equation between the $\{y_+, y_-\}$ and $\{r, \eta\}$ Coordinates

In this section, we consider the mapping of the Casimir differential operator from the large D scalar suggested variables $\{y_+, y_-\}$ and the radial/angular composed variables $\{r, \eta\}$. Specifically, we would like to map the operator of Eq. (5.1.9) to that of Eq. (4.2.8). As discussed in section 7.1 it is important to take the negative solution of $r(y_+)$ in this mapping. This choice will be needed when finding the derivatives ∂_{y_+}, ∂_{y_-} in terms of ∂_r and ∂_η by the chain rule:

$$\partial_{y_+} = \frac{(1+r^2)^3}{8r(1-r^2)}\partial_r, \qquad \partial^2_{y_+} = -\frac{(1+r^2)^5(3r^4 - 8r^2 + 1)}{64r^3(1-r^2)^3}\partial_r + \frac{(1+r^2)^6}{64r^2(1-r^2)^2}\partial_r^2, \tag{7.2.1}$$

$$\partial_{y_-} = -\frac{1}{2}\eta^3\partial_\eta, \qquad \partial^2_{y_-} = \frac{3}{4}\eta^5\partial_\eta + \frac{1}{4}\eta^6\partial_\eta^2. \tag{7.2.2}$$

The Casimir differential operator for the $\mathcal{D}_{y_+}$, $\mathcal{D}_{y_-}$ and the mixed operator $\mathcal{D}_{y_0}$ reads:

$$\mathcal{D}_{y_+} = \left(\frac{3}{2}r - \frac{2r}{1+r^2} - \nu r - \frac{2\nu r^3}{1-r^2}\right)\partial_r + \frac{r^2}{2}\partial_r^2, \tag{7.2.3}$$

$$\mathcal{D}_{y_-} = \frac{3}{2}\eta\partial_\eta - \frac{1}{\eta}\partial_\eta + \nu\eta\partial_\eta - \frac{1}{2}(1-\eta^2)\partial_\eta^2, \tag{7.2.4}$$

$$\mathcal{D}_{y_0} = \frac{-4r^3\eta^3(1-r^2)\partial_r + (1+r^2)^3(\eta^2-1)\partial_\eta}{\eta(1+r^2)(1+r^4-2r^2(2\eta^2-1))}. \tag{7.2.5}$$

The differential operators in these two different coordinate systems equal the Casimir differential operator up to a factor of 2:

$$\mathcal{D}_{r,\eta}G_{\Delta,l} = C_{\Delta,l}G_{\Delta,l}, \qquad \mathcal{D}_{y_+,y_-}G_{\Delta,l} = \frac{1}{2}C_{\Delta,l}G_{\Delta,l}, \qquad \to \mathcal{D}_{r,\eta} = 2\mathcal{D}_{y_+,y_-}. \tag{7.2.6}$$

Using Eq. (7.2.3), Eq. (7.2.4) and Eq. (7.2.5) we see that we obtain Eq. (4.2.8) and that the differential operators match the mapping:

$$\frac{\mathcal{D}_{r,\eta}}{2} = \frac{r^2}{2}\partial_r^2 + \nu(\eta\partial_\eta - r\partial_r) + \frac{1}{2}(\eta\partial_\eta - r\partial_r) - \frac{1}{2}(1-\eta^2)\partial_\eta^2 + 2r^2\left(\frac{(1-2\eta^2+r^2)r\partial_r + 2\eta(1-\eta^2)\partial_\eta}{1+r^4-2r^2(2\eta^2-1)} - \frac{\nu r\partial_r}{1-r^2}\right). \tag{7.2.7}$$

The way the terms match is not straightforward. Specifically the $\mathcal{D}_{y_0}$ matches with parts of $\mathcal{D}_{y_+}$ and $\mathcal{D}_{y_-}$ giving the mixed term of Eq. (4.2.8):

$$2r\partial_r - \frac{2r}{1+r^2}\partial_r + \eta\partial_\eta - \frac{1}{\eta}\partial_\eta + \frac{-4r^3\eta^3(1-r^2)\partial_r + (1+r^2)^3(\eta^2-1)\partial_\eta}{\eta(1+r^2)(1+r^4-2r^2(2\eta^2-1))} = 2r^2\frac{(1-2\eta^2+r^2)r\partial_r + 2\eta(1-\eta^2)\partial_\eta}{1+r^4-2r^2(2\eta^2-1)}. \tag{7.2.8}$$

When considering the large D limit of [34] we set the mixed term operator Eq. (7.2.5) to have a much smaller contribution than the other two so that we can neglect it for large D. This would not be equivalent to neglecting the mixed term of [28] for large D. This opens up a discussion about several large D limits of the Casimir equation.

7.3 Large Dimensional Limit Types of the Casimir Equation

In this section, we will emphasize that there does not exist one single large D limit for the Casimir equation. In [34] the large D limit was taken by including a leading and a next to leading order in D for the differential operators. The large D limit for the leading and next to leading order in the radial/angular decomposition [28] turns out to be different than [34]. We will denote the differential operators by $\mathcal{D}^{(k)}$ where k is the dimensional scaling, so that $k = 2$ is of leading order i.e. $\sim D^2$ and $k = 1$ is of next to leading order i.e. $\sim D^1$.

We have already established in section 5.1 that $\partial_{y_\pm}$ adds a D to the counting of dimensional order. The Casimir operator of [34] consists of a cross term $\mathcal{D}_{y_0}$, that contains a D dependence. The non-cross terms $\mathcal{D}_{y_+}$ and $\mathcal{D}_{y_-}$ are of leading order i.e. $\sim D^2$, but actually only a part of these operators splits into a leading order $\mathcal{D}^{(2)}_{y_\pm}$ and a next to leading order $\mathcal{D}^{(1)}_{y_\pm}$:

$$\mathcal{D}^{(2)}_{y_\pm} = 2y_\pm^2(1-y_\pm)\partial^2_{y_\pm} - y_\pm D\partial_{y_\pm}, \qquad \mathcal{D}^{(1)}_{y_\pm} = -y_\pm(y_\pm - 2)\partial_{y_\pm}. \tag{7.3.1}$$

In [34] the non-cross terms should seperate and solve the Casimir equation nicely. The operators for the non-cross terms translate for the $\{r, \eta\}$ coordinates into:

$$\mathcal{D}^{(2)}_{y_+} = \frac{r^2}{2}\partial_r^2 + \frac{(8r^2 - 3r^4 - 1)}{2(1-r^4)} r\partial_r, \qquad \mathcal{D}^{(1)}_{y_+} = \frac{1+r^4}{1-r^4} r\partial_r, \tag{7.3.2}$$

$$\mathcal{D}^{(2)}_{y_-} = -\frac{1-\eta^2}{2}\partial_\eta^2 - \frac{3(1-\eta^2)}{2\eta}\partial_\eta, \qquad \mathcal{D}^{(1)}_{y_-} = \frac{1}{2}\left(\frac{1}{\eta} - 2\eta\right)\partial_\eta. \tag{7.3.3}$$

Based on this we do not see any direct mapping from neither $\mathcal{D}^{(2)}$ or $\mathcal{D}^{(1)}$ between the $\{y_+, y_-\}$ and $\{r, \eta\}$ Casimir operators. We rather have a mix of leading order and next to leading order of operators when transforming between $\{y_+, y_-\}$ and $\{r, \eta\}$.

Assuming now that both the ∂_r and ∂_η add to the dimensional counting, the homogeneuos differential operator $\mathcal{D}_0$ of [28] is given in Eq. (4.2.8) which would imply the following leading order and subleading order in D:

$$\mathcal{D}^{(2)}_0 = r^2\partial_r^2 - Dr\partial_r - (1-\eta^2)\partial_\eta^2 + D\eta\partial_\eta, \qquad \mathcal{D}^{(1)}_0 = r\partial_r - \eta\partial_\eta, \tag{7.3.4}$$

while the homogeneity increasing part will have the leading D order:

$$\tilde{\mathcal{D}}^{(2)} = -\frac{2Dr^3}{1-r^2}\partial_r. \tag{7.3.5}$$

The approximation holds as long as the denominator does not become smaller than $1/D$. Like it broke down when $y_+ - y_- \ll 1/D$ for [34], i.e. $1 + r^4 - 2r^2(2\eta^2 - 1) \ll 1/D$ the approximation will break down.

The homogeneity preserving part does not contain any next to leading order terms, up to a relation between ν and D. We, therefore, investigate the corresponding block in section 8.1 with the expression of a full $\mathcal{D}_0$, because it simplifies the recursion relation and a leading order of $\tilde{\mathcal{D}}$.

Instead of the assumption that the derivatives ∂_r and ∂_η count a D one could argue that only the ∂_r derivative contributes to the leading order in D, whereas the angular ∂_η does not change the dimensional order, because the scaling of the conformal block in [28] is given by $G_{\Delta,l} \sim r^\Delta$. This is an interesting part of future work but not a path we will pursue in this thesis.

We can conclude that meaningful large D limits of the Casimir operators can be structured in several ways. A leading order for $\{y_+, y_-\}$ or $\{r, \eta\}$, and a leading plus next to leading order in $\{y_+, y_-\}$ or $\{r, \eta\}$. This gives 4 combinations since the Casimir operators can be transformed into the other coordinates. On top of that one can question how the dimensional counting plays out for the $\{r, \eta\}$ coordinates. The reason that the $\{y_+, y_-\}$ approximation for large D blocks worked so well is presumably because it both included a leading and next to leading order in D and that the mixed term operator was of order D^0 which was well approximated to vanish for large D.

Chapter 8

Different Large Dimensional Conformal Blocks and Bounds

In chapter 7 we found a coordinate relation between the large D scalar block suggested variables $\{y_+, y_-\}$ and the radial/angular composed variables $\{r, \eta\}$. This correspondence motivated a discussion on different large D limits of the Casimir. In this chapter we consider some of these specific large D limits going beyond the scope of [28, 34], and derive the conformal blocks corresponding to each limit. This is derived by building a recursion relation on similar footings as in chapter 4. One may be tempted to compare the conformal blocks of the radial/angular decomposition and the large D limit directly using our coordinate relation from Eq. (7.1.2) since we have an expression for both from chapter 4 and 5. But, as we show in appendix F, this leads to coefficients in the linear combination of Gegenbauer polynomials which depend on the coordinates themselves. Therefore, we restrict ourselves to solving the Casimir equation recursion to obtain the conformal blocks in this chapter.

8.1 Action of Leading Order Homogeneity Increasing Part of the Casimir Operator in Large Dimensions

We consider the specific large D limit where we impose that the differential Casimir operator consists of the homogeneity preserving part $\mathcal{D}_0$ which has the full structure of Eq. (4.2.9) and the homogeneity increasing part of leading order in D Eq. (7.3.5):

$$\mathcal{D} = \mathcal{D}_0 + \tilde{\mathcal{D}}^{(2)}. \tag{8.1.1}$$

We will build a recursion so that we can find the conformal blocks in this specific large D limit. We know how the $\mathcal{D}_0$ acts on the conformal block, since it satisfies the Casimir equation:

$$\mathcal{D}_0 G_{\Delta,l}(r,\eta) = \sum_{n=0}^{\infty} \sum_j C_{\Delta+n,j} B_{n,j} \mathcal{P}_{\Delta+n,j}(r,\eta). \tag{8.1.2}$$

Let us then act with $\tilde{\mathcal{D}}^{(2)}$ on the $\mathcal{P}_{E,j}$ function:

$$\tilde{\mathcal{D}}^{(2)} \mathcal{P}_{E,j}(r,\eta) = -2ED \frac{j!}{(2\nu)_j} C_j^{\nu}(\eta) \sum_{k=0}^{\infty} r^{E+2(1+k)} = -2ED \sum_{k=0}^{\infty} \mathcal{P}_{E+2(k+1),j}(r,\eta). \tag{8.1.3}$$

These actions yield the combined differential operator action on the conformal block, where the energies are given by the primary and descendants $E = \Delta + n$:

$$\mathcal{D}G_{\Delta,l}(r,\eta) = \sum_{n=0}^{\infty}\sum_{j} C_{\Delta+n,j}B_{n,j}\mathcal{P}_{\Delta+n,j}(r,\eta) - \sum_{n=0}^{\infty}\sum_{j} 2(\Delta+n)DB_{n,j}\sum_{k=0}\mathcal{P}_{\Delta+n+2(k+1),j}(r,\eta). \quad (8.1.4)$$

The whole differential operator simultanously satisfies the Casimir equation:

$$\mathcal{D}G_{\Delta,l}(r,\eta) = C_{\Delta,l}G_{\Delta,l}(r,\eta). \quad (8.1.5)$$

Combining Eq. (8.1.4) with the Casimir equation we obtain a recursion relation, where the sum over n and j may be neglected. We also change the sum over k into n' as we did for the usual radial/angular D dependent block. This allows us to omit the $\mathcal{P}_{\Delta+n,j}$ functions since they agree on both sides of the recursion:

$$(C_{\Delta+n,j} - C_{\Delta,l})B_{n,j} = 2(\Delta+n)D\sum_{n'=0,2,\ldots,n-2} B_{n',j}. \quad (8.1.6)$$

For $n = 0$ we get the normalization condition $B_{0,j} = \delta_{jl}$. The spin dependence becomes the same throughout the recursion $j = l$, and we get the first levels:

$$B_{2,l} = \frac{2D(\Delta+2)}{C_{\Delta+2,l} - C_{\Delta,l}}, \qquad B_{4,l} = \frac{2D(\Delta+4)}{C_{\Delta+4,l} - C_{\Delta,l}}(1 + B_{2,l}), \qquad B_{6,l} = \frac{2D(\Delta+6)}{C_{\Delta+6,l} - C_{\Delta,l}}(1 + B_{2,l} + B_{4,l}). \quad (8.1.7)$$

Defining the factor $f_n \equiv \frac{2D(\Delta+n)}{C_{\Delta+n,l} - C_{\Delta,l}}$, lets us write the levels as:

$$B_{2,l} = f_2, \qquad B_{4,l} = f_4(1+f_2), \qquad B_{6,l} = f_6(1+f_4)(1+f_2), \qquad B_{8,l} = f_8(1+f_6)(1+f_4)(1+f_2), \quad (8.1.8)$$

while generalizing to the $2m'th$ level we have a product over all integers of k:

$$B_{2m,l} = f_{2m}\prod_{k=1}^{m-1}(1+f_{2k}). \quad (8.1.9)$$

For a general k we have the expression within the product:

$$1 + f_{2k} = \frac{(2k+D)(k+\Delta)}{k(2k+2\Delta-D)}. \quad (8.1.10)$$

This enables us to write the coefficient for a general level:

$$B_{2m,l} = \frac{(\Delta+2m)\left(\frac{D}{2}\right)_m(\Delta)_m}{m!\Delta\left(\Delta-\frac{D}{2}+1\right)_m}, \quad (8.1.11)$$

which yields the conformal scalar block:

$$G_{\Delta,0}(r,\eta) = \sum_{m=0}^{\infty}\frac{(\Delta+2m)\left(\frac{D}{2}\right)_m(\Delta)_m}{m!\Delta\left(\Delta-\frac{D}{2}+1\right)_m}r^{\Delta+2m} = r\partial_r\left(\frac{r^{\Delta}}{\Delta}{}_2F_1\left(\Delta,\frac{D}{2},\Delta-\frac{D}{2}+1,r^2\right)\right). \quad (8.1.12)$$

The scalar block i.e. $l = 0$ seems to be more justifiable in this approximation of leading orders since we have completely neglected the spin dependency for the differential operator. The behavior of this block does not resemble that of the large D block behavior if one was to plot them. Therefore the leading order behavior is presumably not a good approximation. Furthermore, this derivation served a purpose as a warm-up for section 8.3 where we will look at a different differential operator, which comes closer to the large D block structure.

8.2 Action of $\{y_+, y_-\}$ Leading Order and Next to Leading Order Operators in $\{r, \eta\}$ Coordinates

We consider the specific large D limit that corresponds to the large D limit of [34] i.e. the $\mathcal{D}_{y+}$ and $\mathcal{D}_{y_-}$ operators written in $\{r, \eta\}$ coordinates with a vanishing $\mathcal{D}_{y_0}$ operator. This differential operator in $\{y_+, y_-\}$ translates into the following in $\{r, \eta\}$:

$$\mathcal{D} = \mathcal{D}_0 + \tilde{\mathcal{D}}_r + \tilde{\mathcal{D}}_\eta, \qquad \tilde{\mathcal{D}}_r = 4r^3 \left(\frac{1}{1+r^2} - \frac{\nu}{1-r^2} \right) \partial_r, \qquad \tilde{\mathcal{D}}_\eta = 2 \left(\eta - \frac{1}{\eta} \right) \partial_\eta. \tag{8.2.1}$$

The $\mathcal{D}_0$ operator acting on the conformal block gives a Casimir eigenvalue of Eq. (8.1.2). The action of $\tilde{\mathcal{D}}_r$ operator, while using the geometric series expansion, yields:

$$\tilde{\mathcal{D}}_r \mathcal{P}_{E,j}(r,\eta) = 4r^3 \left(\frac{4}{1-r^4} - \frac{D}{1-r^2} \right) \partial_r \mathcal{P}_{E,j}(r,\eta) = 2E \sum_{k=0}^{\infty} 4\mathcal{P}_{E+4k+2,j}(r,\eta) - D\mathcal{P}_{E+2k+2,j}(r,\eta). \tag{8.2.2}$$

Regarding the $\tilde{\mathcal{D}}_\eta$ action on $\mathcal{P}_{E,j}(r,\eta)$, we can re-write it as:

$$\tilde{\mathcal{D}}_\eta \mathcal{P}_{E,j}(r,\eta) = 2 \left(\eta - \frac{1}{\eta} \right) \partial_\eta \mathcal{P}_{E,j}(r,\eta) = -\frac{2}{\eta}(1-\eta^2) \partial_\eta \mathcal{P}_{E,j}(r,\eta). \tag{8.2.3}$$

No Gegenbauer identity, to our knowledge, includes an expression for the $1/\eta$ operator action on a Gegenbauer polynomial. The problem does not seem to simplify when going to a specific dimension. E.g. for $D = 3$ we would obtain Legendre polynomials, which neither have identities for this operator. Therefore we are unable to pursue this path, but we can restrict ourselves to the scalar block instead.

8.3 Action of the Radial Dependent Operator with a Vanishing Angular Operator

In section 8.2 we were not able to find the action of $\tilde{\mathcal{D}}_\eta$ on the conformal block, so we will now assume it to be vanishing. Then our differential operator reads:

$$\mathcal{D} = \mathcal{D}_0 + \tilde{\mathcal{D}}_r, \tag{8.3.1}$$

for this section. We will therefore focus on the action of the radial operator $\tilde{\mathcal{D}}_r$ which will enable us to fix the scalar block. The action is:

$$\tilde{\mathcal{D}}_r G_{\Delta,l} = \sum_{n=0}^{\infty} \sum_j 2(\Delta+n) B_{n,j} \sum_{k=0} [4\mathcal{P}_{\Delta+n+4k+2,j}(r,\eta) - D\mathcal{P}_{\Delta+n+2k+2,j}]. \tag{8.3.2}$$

Together with Eq. (8.1.2) a recursion relation is implied:

$$(C_{\Delta+n,j} - C_{\Delta,l}) B_{n,j} = 2(\Delta+n) \left[\sum_{n'=0,2,4,6,\ldots,n-2} D B_{n',j} - \sum_{n'=0,4,8,12,\ldots,n-2} 4 B_{n',j} \right]. \tag{8.3.3}$$

The sum over k has been changed to n' and for the first term we have $n' = 2k+2$ while for the second $n' = 4k+2$. Therefore the second sum shifts for every 4th index while the end of the sum is shifted by 2. Then all $P_{\Delta+n+n',j}$ functions agree and we can neglect them when looking at the recursion. We normalize

through the condition $B_{0,j} = \delta_{l,j}$ as previously, giving the levels:

$$\begin{aligned}
B_{2,l} =& \frac{2(\Delta+2)}{C_{\Delta+2,l} - C_{\Delta,l}}(D-4), \\
B_{4,l} =& \frac{2(\Delta+4)}{C_{\Delta+4,l} - C_{\Delta,l}}((D-4) + DB_{2,l}), \\
B_{6,l} =& \frac{2(\Delta+6)}{C_{\Delta+6,l} - C_{\Delta,l}}((D-4)(1+B_{4,l}) + DB_{2,l}), \\
B_{8,l} =& \frac{2(\Delta+8)}{C_{\Delta+8,l} - C_{\Delta,l}}((D-4)(1+B_{4,l}) + D(B_{2,l}+B_{6,l})), \\
B_{10,l} =& \frac{2(\Delta+10)}{C_{\Delta+10,l} - C_{\Delta,l}}((D-4)(1+B_{4,l}+B_{8,l}) + D(B_{2,l}+B_{6,l})).
\end{aligned} \tag{8.3.4}$$

Using the definintion $g_n \equiv \frac{2(\Delta+n)}{C_{\Delta+n,l} - C_{\Delta,l}}$ we can write the levels as:

$$\begin{aligned}
B_{2,l} =& g_2(D-4), \\
B_{4,l} =& g_4(D-4)(1+Dg_2), \\
B_{6,l} =& g_6(D-4)(1+Dg_2)(1+(D-4)g_4), \\
B_{8,l} =& g_8(D-4)(1+Dg_2)(1+(D-4)g_4)(1+Dg_6), \\
B_{10,l} =& g_{10}(D-4)(1+Dg_2)(1+(D-4)g_4)(1+Dg_6)(1+(D-4)g_8).
\end{aligned} \tag{8.3.5}$$

We are then able to write up a closed expression for the general level, by a product over even and odd integers:

$$B_{2m,l} = (D-4)g_{2m} \prod_{k=1,3,5,\ldots}^{m-1} (1+Dg_{2k}) \prod_{i=2,4,6,\ldots}^{m-1} (1+(D-4)g_{2i}). \tag{8.3.6}$$

We evaluate the expressions within the products:

$$\begin{aligned}
1 + Dg_{2k} &= \frac{(2k+D)(k+\Delta)}{k(2k+2\Delta-D)}, \\
1 + (D-4)g_{2i} &= \frac{(2i+D-4)(i+\Delta)-4i}{i(2i+2\Delta-D)}.
\end{aligned} \tag{8.3.7}$$

Setting $l = 0$ we obtain a closed expression for the scalar block:

$$\begin{aligned}
G_{\Delta,0} = &\sum_{m=0}^{\infty} \frac{(D-4)(\Delta+2m)}{2^m m!(\Delta-\frac{D}{2}+1)_m} r^{\Delta+2m} \\
&\times \prod_{k=1,3,5,..}^{m-1} (2k+D)(k+\Delta) \prod_{i=2,4,6,\ldots}^{m-1} \left((2i+D-4)(i+\Delta)-4i\right).
\end{aligned} \tag{8.3.8}$$

By this composition, it seems as $D = 4$ is a special case since it vanishes in this representation. In Figure 8.1 we compare the structure with that of the large D conformal block for $l = 0$ and for $D = 5$ and $D = 19$, where we have evaluated the sum of Eq. (8.3.8) up to $m_{max} = 25$. The approximation would be better when turning up m_{max} so that the function would converge.

We have shown in this chapter that the Casimir equation recursion method is a way to write up the scalar and radial part of the conformal block from the large D limit in the $\{r, \eta\}$ coordinates. We have also shown that the conformal block contains some of the same features as the large D block, which would assumably become better when the sum over m from Eq. (8.3.8) converges.

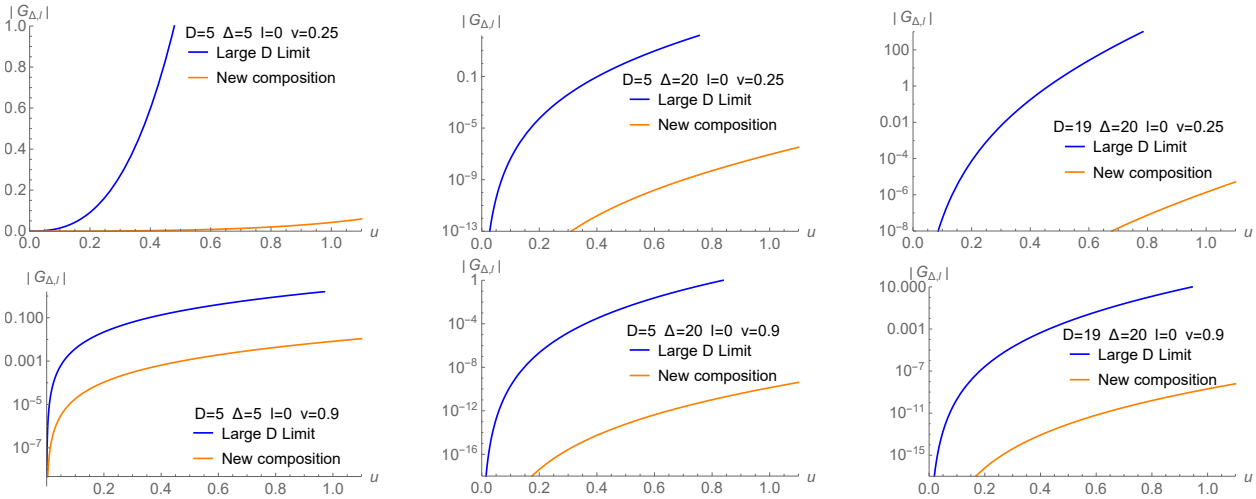

Figure 8.1: *The absolute value of the newly composed large D conformal block* $|G_{\Delta,l}(u,v)|$ *(orange) plotted with the large D conformal block (blue), both evaluated for scalars* $l = 0$ *and as functions of the cross-ratio* u*. Both blocks are evaluated at different fixed values of scaling dimension* Δ*, dimension* D *and cross-ratio* v*.*

Chapter 9

Conclusion and Outlook

Throughout the thesis, we have been developing the languages of CFTs and AdS spaces and we have elaborated on the gauge/gravity duality and holography between the two theories. In chapter 3 we looked at a scaling for the OPE coefficient of the 3-point correlation function with one stress tensor. The scaling was $\lambda_{\mathcal{O}\mathcal{O}T} \sim D^D$, a similar scaling as for the power of radiation of a D-dimensional BH. It could be interesting to see whether this scaling would enable us to put bounds on these specific correlation functions. Then we turned our attention to the conformal theories where we reviewed 3 papers of general dimensional and large D CFTs.

Using the radial quantization and the ρ-picture of operator locations we were in chapter 4 able to decompose the conformal blocks into Gegenbauer polynomials and by recursion determining the levels. We commented how the unit box bounds were realized in these new $\{r, \eta\}$ coordinates, and how the rest of the unit circle in the ρ-picture could be accessed by crossing relations. The power series in which the conformal block is represented by converges for $|\rho| < 1$. It could be interesting to see the implications for the conformal block given that the unit box only covers a slice of the ρ unit circle.

Starting with the expression from a scalar block in $\{u, v\}$ coordinates some suggestive large D variables $\{y_+, y_-\}$ were proposed in chapter 5. These simplified the Casimir equation greatly in the large D limit, and they even matched the features of conformal block for low dimensions such as $D = 4$. We further plotted the conformal block of the radial/angular decomposition to test whether it resembled the same structure as those for large D and exact D evaluated at the specific dimension $D = 4$. We found that it did for the first two levels $n = 0, 2$. By including a larger amount of terms we would expect the expression to improve the block structure so that it converges to the exact $D = 4$ block structure. This specific numerical test would assumably be enlightening to incorporate so that we are sure about the validity of the conformal block decomposition. Doing this analysis for higher levels might give some information about which spins, and whether the smallest or largest spin dominates at large D so that one could simplify the structure of the radial/angular conformal block. In the case of the maximal twist, we had such a simplification in the sense that the descendants decoupled which simplified the block structure greatly because all other levels than $A_{n,l+n}$ vanished.

In chapter 6, we studied the properties of large D CFTs whose conformal scaling dimension and spin scaled linearly with D i.e. $\Delta = \delta D$ and $l = \omega D$ for fixed values of δ and ω. The block was studied by applying a saddle-point approximation so that the conformal block could be written without a hypergeometric function representation. The scaling of Δ was justified through the unitarity bound, but the scaling of l seemed to lack a physical justification. The questioning of the linear scaling and saddle-point approximation was motivated by the conformal block plots which did not seem to resemble the same structure as for large D blocks for neither $D = 4$ or $D = 101$. If it resembled the same large D limit, the conformal block should supposedly have matched when $D = 101$. Evaluating the conformal blocks in even larger dimensions say $D = 10^6$ made the numerical code lose its precision because it could not represent these small numbers and thus the plot

could not be trusted. Therefore we did not evaluate at a higher dimension than $D = 101$.

Furthermore, the spin scaling could have been picked to be $1 - l = \omega D$ so that the symmetry of the conformal block parts $A_\Delta(y_+)$ and $A_{1-l}(y_-)$ would be preserved. For future work, it would be interesting to explore the light transform from [36] since it resembled a comparable symmetry to the spin conformal block part.

Nevertheless, we used the linearly scaled Δ and l conformal block and applied some new coordinates $\{\sigma, \tau\}$ with constants $\{a, b\}$. This enabled us to put restrictions on the CFT data using crossing symmetry. Specifically, it gave us a bound for the external scaling dimension which was $\Delta_\phi / D > 1$ to have a consistent unitary CFT in large D. The crossing relation of the radial/angular decomposed conformal block could be interesting to explore similarly.

In chapter 7 we found a new relation between the large D scalar block suggested variables $\{y_+, y_-\}$ and the radial/angular coordinates of the ρ-picture $\{r, \eta\}$, that seperated the radial $y_+(r)$ and angular $y_-(\eta)$ coordinates:

$$y_+ = \frac{4r^2}{(1+r^2)^2}, \qquad y_- = \frac{1}{\eta^2}. \tag{9.0.1}$$

We were able to locate how the different terms in the differential Casimir operator have connected in the two coordinate systems and this lead to a discussion of different large D limits. The operators could then be divided into a leading, a subleading, and a next to subleading order in D. The leading order of the large D scalar block did not map to the leading order in the radial/angular block, and neither did such a mapping occur for the subleading order. If one was to resemble the same large D limit in $\{r, \eta\}$ then one should consider how they map. This mapping could further be investigated, to see which large D limit for the radial/angular block would best compare to the $\{y_+, y_-\}$ conformal block in large D.

In chapter 8 we considered a few suggestive large D limits and derived the conformal blocks in $\{r, \eta\}$ coordinates specified by the discussion from section 7.3. We did find an expression for the scalar conformal block in $\{r, \eta\}$ coordinates which were comparable to the large D conformal block evaluated at $D = 5$ and $D = 19$. The expression indicated that $D = 4$ was a special case since it vanished for $D = 4$. This might turn out differently if we had been able to derive the full conformal block with spin. One specific problem we had when transforming the large D limit of [34] to $\{r, \eta\}$ coordinates was how to interpret the action of $\eta^{-1} C_j^\nu(\eta)$. It could be interesting to see how this angular part would be represented in the recursion.

Acknowledgments

I would like to express my gratitude to my supervisors David McGady and Niels Obers. David McGady for being able to give me extensive supervision with meetings twice a week throughout the whole thesis. We have had a great number of fruitful discussions and explanations about conformal field theories and topics both closely and peripherally related. The focus has mainly been on learning a large portion of physics which we both have found fascinating, and I have enjoyed this approach to the thesis. Niels Obers for discussions about derivations and physical arguments neither David nor I could answer satisfactorily in our research. It has been a true pleasure to collaborate with both David McGady and Niels Obers. Furthermore, I would like to thank Benjamin Søgaard, Mads Larsen, and Mikkel Lauritzen for a great working environment at the office and educational discussions on the gauge/gravity duality and other aspects of high energy theory.

Appendices

Appendix A

AdS Space

A.1 Derivation of the Friedmann Equations in a D-Dimensional Spacetime

In this appendix, we will derive the Friedmann equation in a D-dimensional spacetime from the Friedmann-Lemaître-Robertson-Walker (FLRW) metric. When imposing an ansatz that assumes a homogeneity and isotropic universe, one will end up with a metric in D dimensions [37]:

$$ds^2 = -dt^2 + e^{2\beta(r)}dr^2 + r^2 d\theta^2 + r^2 \sin^2\theta d\phi^2 + ..., \tag{A.1.1}$$

where the extra terms should be thought of as angular variables adding up to the $d\Omega_{D-2}^2$ factor. For the universe to be maximally symmetric there is imposed a constraint on the Ricci tensor:

$$R_{ij} = \frac{(D-2)k}{a(t)^2} g_{ij}, \tag{A.1.2}$$

with $\{i, j\} = 1, 2, 3, ..., D-1$. $k = \{-1, 0, 1\}$ determines the geometry of the universe, $k = 1$ gives a spherical universe (dS space) $k = 0$ gives a flat universe, and $k = -1$ gives the hyperbolic universe (AdS space). $a(t)$ is interpreted as the scale factor of the universe. When using this ansatz one can use the Ricci tensors from the Schwarzschild metric in D dimensions [31] by setting $\alpha(r) = 0$. This gives the two interesting parts of the Ricci tensor:

$$R_{rr} = \frac{D-2}{r}\partial_r\beta(r), \qquad R_{\theta\theta} = re^{-2\beta(r)} + (D-3)(1 - e^{-2\beta(r)}), \tag{A.1.3}$$

where $R_{tt} = 0$ and the other angular parts are copies of $R_{\theta\theta}$ with additional factors. Setting these equal to the given constraints, putting the equations together and solving for $e^{-2\beta(r)}$ gives:

$$e^{-2\beta(r)} = 1 - \frac{kr^2}{a^2}. \tag{A.1.4}$$

One can then do a transformation $\frac{r}{a} \to r$ by absorbing the r-dependency into the scale factor. One can then write up the D-dimensional FLRW metric:

$$ds^2 = -dt^2 + a^2(t)\left(\frac{dr^2}{1 - kr^2} + r^2 d\Omega_{D-2}^2\right), \tag{A.1.5}$$

which seems as a trivial generalization of the metric to D-dimensional space time, since the only thing that have changed from $D = 4$ is that the angular dependency is generalized $d\Omega_2 \to d\Omega_{D-2}$. Next we consider

the non zero Christoffel symbols:

$$\begin{gathered}\Gamma^t_{ii} = \frac{\dot{a}}{a} g_{ii}, \quad \Gamma^i_{ti} = \frac{\dot{a}}{a}, \quad \Gamma^r_{rr} = \frac{kr}{1-kr^2}, \quad \Gamma^r_{\theta_x\theta_x} = -r(1-kr^2)\prod_{i=1}^{x-1}\sin^2\theta_k, \\ \Gamma^{\theta_x}_{\theta_x r} = \frac{1}{r}, \quad \Gamma^{\theta_x}_{\theta_y\theta_y} = -\sin\theta_x\cos\theta_x\prod_{i=x+1}^{y-1}\sin^2\theta_i, \quad \Gamma^{\theta_y}_{\theta_x\theta_y} = \cot\theta_x,\end{gathered} \tag{A.1.6}$$

where $\{x, y\} = 1, 2, 3...D-2$ with $x < y$ and $\{\theta_1, \theta_2, , ...\} = \{\theta, \phi, ...\}$. For the Ricci tensor, the R_{tt} component is given by:

$$R_{tt} = R^{\rho}_{t\rho t} = R^t_{ttt} + R^i_{tit}, \tag{A.1.7}$$

where i is implicitly summed over. Due to the antisymmetry of the Riemann tensor one finds that $R^t_{ttt} = 0$. Then the Riemann tensor becomes:

$$R_{tt} = \partial_i\Gamma^i_{tt} - \partial_t\Gamma^i_{it} + \Gamma^i_{i\lambda}\Gamma^{\lambda}_{tt} - \Gamma^r_{t\lambda}\Gamma^{\lambda}_{rt}. \tag{A.1.8}$$

The Christoffel symbols with double t's vanish. The only Christoffel symbol left contributes $D-1$ times:

$$R_{tt} = (D-1)\left(-\partial_t\frac{\dot{a}}{a} - \frac{\dot{a}}{a}\right) = -(D-1)\frac{\ddot{a}}{a}. \tag{A.1.9}$$

Then lets look at the R_{ij} components. We can split them into:

$$R_{ij} = R^t_{itj} + R^r_{irj} + \sum_x R^{\theta_x}_{i\theta_x j}. \tag{A.1.10}$$

The specific cases for $\{ij\} = \{rr, \theta\theta, \phi\phi, ...\}$:

$$\begin{aligned}R_{rr} =& R^t_{rtr} + R^{\theta}_{r\theta r} + R^{\phi}_{r\phi r} + ... = \left(\partial_t\Gamma^t_{rr} - \Gamma^t_{rr}\Gamma^r_{tr}\right) + \left(-\partial_r\Gamma^{\theta}_{\theta r} + \Gamma^{\theta}_{\theta t}\Gamma^t_{rr} + \Gamma^{\theta}_{\theta r}\Gamma^r_{rr} - (\Gamma^{\phi}_{r\phi})^2\right) \\ &+ \left(-\partial_r\Gamma^{\phi}_{\phi r} + \Gamma^{\phi}_{\phi t}\Gamma^t_{rr} + \Gamma^{\phi}_{\phi r}\Gamma^r_{rr} - (\Gamma^{\phi}_{r\phi})^2\right) + ... = \left(\frac{\ddot{a}}{a} + (D-2)\frac{\dot{a}^2+k}{a^2}\right) g_{rr}, \\ R_{\theta\theta} =& R^t_{\theta t\theta} + R^r_{\theta r\theta} + R^{\phi}_{\theta\phi\theta} = \left(\partial_t\Gamma^t_{\theta\theta} - \Gamma^t_{\theta\theta}\Gamma^{\theta}_{t\theta}\right) + \left(\partial_r\Gamma^r_{\theta\theta} + \Gamma^r_{rt}\Gamma^t_{\theta\theta} + \Gamma^r_{rr}\Gamma^r_{\theta\theta} - \Gamma^r_{\theta\theta}\Gamma^{\theta}_{r\theta}\right) \\ &+ \left(-\partial_\theta\Gamma^{\phi}_{\theta\phi} + \Gamma^{\phi}_{\phi t}\Gamma^t_{\theta\theta} + \Gamma^{\phi}_{\phi r}\Gamma^r_{\theta\theta} - (\Gamma^{\phi}_{\theta\phi})^2\right) + ... = \left(\frac{\ddot{a}}{a} + (D-2)\frac{\dot{a}^2+k}{a^2}\right) g_{\theta\theta}, \\ R_{\phi\phi} =& R^t_{\phi t\phi} + R^r_{\phi r\phi} + R^{\theta}_{\phi\theta\phi} + ... = \left(\frac{\ddot{a}}{a} + (D-2)\frac{\dot{a}^2+k}{a^2}\right) g_{\phi\phi},\end{aligned} \tag{A.1.11}$$

where $(...)$ denotes that we have higher terms similarly to the two last parenthesis just with a new angle giving us the $(D-2)$ dependency due to the repeated terms. In general this is:

$$R_{ij} = \left(\frac{\ddot{a}}{a} + (D-2)\frac{\dot{a}^2+k}{a^2}\right) g_{ij}. \tag{A.1.12}$$

Computing the Ricci tensor:

$$R = (D-1)\left(\frac{2\ddot{a}}{a} + (D-2)\frac{\dot{a}^2+k}{a^2}\right). \tag{A.1.13}$$

We will re-instate the D-dimensional Newtonian constant $G_N^{(D)}$ so the Einstein field equations read:

$$R_{tt} - \frac{1}{2}g_{tt}R = 8\pi G_N^{(D)}T_{tt}, \qquad R_{ij} - \frac{1}{2}g_{ij}R = 8\pi G_N^{(D)}T_{ij}, \tag{A.1.14}$$

where we assume the EM tensor is given by a perfect fluid i.e. $T_{tt} = \rho$ and $T_{ij} = pg_{ij}$. The Friedmann equations in D dimensions turns out to be [38, 39]:

$$\frac{\dot{a}^2}{a^2} = \frac{16\pi G_N^{(D)}}{(D-1)(D-2)}\rho - \frac{k}{a^2}, \tag{A.1.15}$$

$$\frac{\ddot{a}}{a} = -\frac{8\pi G_N^D}{D-2}\left(p + \frac{D-3}{D-1}\rho\right). \tag{A.1.16}$$

To analyze the evolution of the universe, we need to consider the trace and conservation of the EM tensor:

$$\begin{aligned} T =& g^{\mu\nu}T_{\mu\nu} = g^{tt}T_{tt} + g^{ij}T_{ij} = -\rho + (D-1)p, \\ 0 =& \nabla_\mu T^\mu_t = \partial_\mu T^\mu_t + \Gamma^\mu_{\mu t}T^t_t - \Gamma^\rho_{\mu t}T^\mu_\rho = -\dot{\rho} - (D-1)\frac{\dot{a}}{a}(\rho + p), \end{aligned} \tag{A.1.17}$$

Using the equation of state $p = \omega\rho$ with Eq. (A.1.17) we find the differential equation [40]:

$$\frac{\dot{\rho}}{\rho} = -(D-1)(1+\omega)\frac{\dot{a}}{a}, \tag{A.1.18}$$

the density that solves this is:

$$\rho \propto a^{-(D-1)(1+\omega)}. \tag{A.1.19}$$

The parameter ω describes what kind of stuff is in the universe. When pressure vanishes $p = 0$ we have matter, hence $\omega = 0$. When the trace of the EM tensor vanishes $T^\mu_\mu = 0$ we have a CFT intepreted as radiation, this happens at $-\rho + (D-1)\omega\rho = 0$ hence $\omega = \frac{1}{D-1}$. Dark energy is given by a negative pressure $p = -\rho$. The density solution now reads:

$$\begin{aligned} &\rho_\gamma \propto a^{-D} \qquad \text{Radiation } \left(\omega = \frac{1}{D-1}\right), \\ &\rho_m \propto a^{-(D-1)} \qquad \text{Matter } (\omega = 0), \\ &\rho_\Lambda \propto a^0 \qquad \text{Dark energy } (\omega = -1). \end{aligned} \tag{A.1.20}$$

One can further use these densities to analyze the evolution of the universe in various dimensions, but that is beyond the scope of this thesis.

A.2 The Periodicity Trick

The periodicity trick method assigns a temperature to the BH radiation by insisting on a smooth spacetime manifold. Originally the temperature was given by Gibbons and Hawking considered the BH radiation by a path integral approach. The periodicity trick method is an equivalent argument to derive the same temperature.

An observer in Minkowski space or AdS space with a constant distance to a BH will be in an accelerated frame of reference, where the observer will experience thermal radiation from the BH. We therefore want to compare the AdS space of Eq. (2.0.11) and that of a flat circular space called Rindler space:

$$ds^2 = -f(r)dt^2 + \frac{dr^2}{f(r)}, \qquad f(r) = 1 + \frac{r^2}{a^2}, \qquad ds^2 = d\rho^2 + \rho^2 d\phi^2, \tag{A.2.1}$$

where ρ is the radial variable and ϕ is an angular. We want to make a Wick rotation that sends $t \to it_E$, where t_E is the Euclidean time.

When applying the periodicity trick we transform our coordinates from $r \to \rho$ and $t_E \to \phi$. The periodicity of ϕ is is $\phi \in [0, 2\pi]$ while if we multiplied a factor we would have the periodicity of $\phi' \in [0, 2\pi a]$.

If this was the case then imagine a cone, made out of a piece of paper that is folded. If one projected the cone to a plane we would not get a periodicity of 2π, only when the cone becomes flat. If the cone is flat there is no sharp point on this embedding space where the cone lives. In other words, we insist on the smoothness of the two manifolds so that we can take the Euclidean time to be periodic in β, which makes the metric smooth and complete. Another way to argue that the Euclidean time must be periodic in β is given when considering a thermal Greens function [41]:

$$G_\beta(t_E, x) = -Tr\left(\tilde{\rho} T_E[\mathcal{O}(t_E, x)\mathcal{O}(0,0)]\right) = -\frac{1}{Z} Tr\left(e^{-\beta H} T_E[\mathcal{O}(t_E, x)\mathcal{O}(0,0)]\right), \tag{A.2.2}$$

with T_E being the Euclidean time ordering and $\tilde{\rho}$ is the density matrix, which can be expressed as a Hamiltonian H, an inverse temperature β, and a partition function Z. The time ordering does not chance the fields $\mathcal{O}$, so that it can be neglected:

$$G_\beta(t_E, x) = -\frac{1}{Z}\left(Tre^{-\beta H}\mathcal{O}(t_E, x)\mathcal{O}(0,0)\right). \tag{A.2.3}$$

Due to the trace being cyclic we can write:

$$G_\beta(t_E, x) = -\frac{1}{Z} Tr\left(\mathcal{O}(0,0)e^{-\beta H}\mathcal{O}(t_E, x)\right), \tag{A.2.4}$$

commuting the operator with the $e^{-\beta H}$ we obtain a β inside the operator-function:

$$G_\beta(t_E, x) = -\frac{1}{Z} Tr\left(e^{-\beta H}\mathcal{O}(\beta, 0)\mathcal{O}(t_E, x)\right), \tag{A.2.5}$$

and we can identify this as the new Greens function:

$$G_\beta(t_E, x) = G_\beta(t_E - \beta, x), \tag{A.2.6}$$

we have the same expression for the Greens function, so it must be periodic in β.

When comparing the metrics we need the two radial distances to agree:

$$\frac{dr^2}{f(r)} = d\rho^2, \tag{A.2.7}$$

the function can be expanded to first order around the horizon $f(r) = f(r_0) + f'(r_0)(r - r_0)$. The horizon is defined to be at $f(r_0) = 0$. The radial component of the flat metric must therefore by linked by:

$$\rho = \int \frac{dr}{\sqrt{f'(r_0)(r - r_0)}} = 2\sqrt{\frac{r - r_0}{f'(r_0)}} \to f'(r_0)(r - r_0) = \rho^2 \frac{f'(r_0)^2}{4}. \tag{A.2.8}$$

Applying a Wick rotation we have the re-written AdS metric is:

$$ds^2 = f'(r_0)(r - r_0)dt_E^2 + \frac{dr^2}{f'(r_0)(r - r_0)}, \tag{A.2.9}$$

which can be transformed into the mixed coordinate metric:

$$ds^2 = \frac{f'(r_0)}{4}\rho^2 dt_E^2 + d\rho^2. \tag{A.2.10}$$

In order to have the smooth metric the transformation between the Euclidean time and the angular variable must be:

$$\phi = \frac{f'(r_0)}{2} t_E. \tag{A.2.11}$$

The periodicities of ϕ implies a periodicity of t:

$$\phi \to \phi + 2\pi, \qquad t \to t + i\beta, \tag{A.2.12}$$

and so we have the inverse temperature β:

$$\beta = \frac{4\pi}{f'(r_0)}. \tag{A.2.13}$$

This result is applied for the Schwarzschild metric and AdS Schwarzschild metric in section 2.1.

Appendix B

The Conformal Algebra and Conformal Field Theories

B.1 Raising and Lowering Operators of the Conformal Algebra

In this appendix, we will show how the translation operator P_μ can be viewed as a raising operator, and the operator of SCTs K_μ can be viewed as a lowering operator in the radial quantization. Using the commutators:

$$[D, P_\mu] = iP_\mu, \qquad [D, K_\mu] = -iK_\mu. \tag{B.1.1}$$

We have that the dilatiation operator gives the conformal scaling dimension as the eigenvalue, when acted upon a state $|\Delta\rangle$:

$$D\,|\Delta\rangle = i\Delta\,|\Delta\rangle\,. \tag{B.1.2}$$

We then apply the commutator:

$$[D, P_\mu]\,|\Delta\rangle = (DP_\mu - P_\mu D)\,|\Delta\rangle\,. \tag{B.1.3}$$

By acting with the dilatation operator on the state and using the result of the commutator we find the expression:

$$(DP_\mu - i\Delta P_\mu)\,|\Delta\rangle = iP_\mu, |\Delta\rangle\,, \tag{B.1.4}$$

that is equivalent to:

$$DP_\mu\,|\Delta\rangle = i(\Delta+1)P_\mu\,|\Delta\rangle\,, \tag{B.1.5}$$

one can then view $P_\mu\,|\Delta\rangle$ as the state with an eigenvalue $i(\Delta+1)$ of operator D, hence P_μ have raised the level of scaling dimension. Similar for K_μ by following similar steps we get:

$$[D, K_\mu]\,|\Delta\rangle = (DK_\mu - K_\mu D)\,|\Delta\rangle\,, \tag{B.1.6}$$

$$(DK_\mu - i\Delta K_\mu)\,|\Delta\rangle = -iK_\mu\,|\Delta\rangle\,, \tag{B.1.7}$$

$$DK_\mu\,|\Delta\rangle = i(\Delta-1)K_\mu\,|\Delta\rangle\,, \tag{B.1.8}$$

concluding that K_μ works as a lowering operator. In this way we can construct all levels:

$$(P_\mu)^n\,|\Delta\rangle = |\Delta+n\rangle\,, \qquad (K_\mu)^n\,|\Delta\rangle = |\Delta-n\rangle\,, \qquad K_\mu\,|0\rangle = 0, \tag{B.1.9}$$

where $|0\rangle$ is the ground state, which gets annihilated.

B.2 Connection to String Theory

The idea in ST is that we modify the notion of a moving particle to a moving string. The particle follows a worldline and we can parameterize this path by the parameter τ. This is mapped from the one-dimensional parameter to the target space that is of dimension D by:

$$\tau \to X^\mu(\tau). \tag{B.2.1}$$

In ST we shift this from a worldline of one varaible to a worldsheet of two variables (τ, σ) onto a new target space:

$$(\tau, \sigma) \to X^\mu(\tau, \sigma). \tag{B.2.2}$$

We therefore have a two dimensional space embedded within a higher dimensional space. The action in this space is the Polyakov action and it contains some symmetries. Two of them being that it is invariant under Weyl transformations and diffeomorphisms. This yields that the (τ, σ) space is a 2 dimensional CFT. We will now compare the algebras. If we write up the CFT generators Eq. (3.1.7) for $\mu = 1, 2$ being (x, y) coordinates, we get:

$$\begin{aligned}
&P_1 = -i\partial_x, \qquad P_2 = -i\partial_y, \qquad D = -ix\partial_x - iy\partial_y, \\
&M_{11} = M_{22} = 0, \qquad M_{12} = -M_{21} = i(x\partial_y - y\partial_x), \\
&K_1 = -2ix(x\partial_x + y\partial_y) + i(x^2 + y^2)\partial_x, \qquad K_2 = -2iy(x\partial_x + y\partial_y) + i(x^2 + y^2)\partial_y.
\end{aligned} \tag{B.2.3}$$

Let us then introduce the complex variables $z = x + iy$ with $\bar{z} = x - iy$, with derivatives:

$$\partial_z = \frac{1}{2}(\partial_x - i\partial_y), \qquad \partial_{\bar{z}} = \frac{1}{2}(\partial_x + i\partial_y), \tag{B.2.4}$$

while using the Witt algebra:

$$\mathcal{L}_n = -iz^{n+1}\partial_z, \tag{B.2.5}$$

for $n = \{-1, 0, 1\}$ we have:

$$\mathcal{L}_{-1} = -i\partial_z, \qquad \mathcal{L}_0 = -iz\partial_z, \qquad \mathcal{L}_1 = -iz^2\partial_z, \tag{B.2.6}$$

and similar there exist a $\bar{\mathcal{L}}_n$ for the complex conjugated variables. This allows for the generators to be re-written in terms of the Witt generators:

$$\begin{aligned}
&P_1 = \mathcal{L}_{-1} + \bar{\mathcal{L}}_{-1}, \qquad P_2 = i(\mathcal{L}_{-1} - \bar{\mathcal{L}}_{-1}), \qquad D = \mathcal{L}_0 - \bar{\mathcal{L}}_0, \\
&M_{11} = M_{22} = 0, \qquad M_{12} = -M_{21} = i(\mathcal{L}_0 - \bar{\mathcal{L}}_0), \\
&K_1 = \mathcal{L}_1 + \bar{\mathcal{L}}_1, \qquad K_2 = -i(\mathcal{L}_1 - \bar{\mathcal{L}}_1).
\end{aligned} \tag{B.2.7}$$

The commutator of the Witt algebra is:

$$[\mathcal{L}_m, \mathcal{L}_n] = (m - n)\mathcal{L}_{m+n}, \tag{B.2.8}$$

which is the same as the Virasoro algebra, without a central extension added i.e. $\left(\frac{c}{12}m^3 + km\right)\delta_{n+m,0}$. The commutator of any two CFT generator will be a linear combination of the Virasoro algebra. The CFT algebra is therefore contained in the Virasoro algebra when we work in 2 spacetime dimensions.

B.3 Fixing Operator Product Expansion Coefficient

In this appendix, we will consider that a 3-point function can be written as a power series of operators that act on a 2-point function. We will show how one can fix the constants of the power series. In general terms the relation between the 3-point function and 2-point function with a power series is given by:

$$\langle \phi_1(x_1)\phi_2(0)\Phi(z)\rangle = \lambda_\Phi C_\Phi(x, \partial_y) \langle \Phi(0)\Phi(z)\rangle, \quad C_\Phi(x, \partial_y) = \frac{1}{|x|^{2\delta-\Delta}} \left(1 + \gamma x^\mu \partial_\mu + \alpha x^\mu x^\nu \partial_\mu \partial_\nu + \beta x^2 \partial^2 + ...\right), \tag{B.3.1}$$

where the 2-point function is:

$$\langle \Phi(0)\Phi(z)\rangle = \frac{1}{|z|^{2\Delta}}, \tag{B.3.2}$$

and the 3-point function in general is:

$$\langle \phi_1(x_1)\phi_2(x_2)\phi_3(x_3)\rangle = \frac{\lambda_{123}}{|x_{12}|^{2\alpha_{123}}|x_{13}|^{2\alpha_{132}}|x_{23}|^{2\alpha_{231}}}, \tag{B.3.3}$$

with $x_{ij} = x_i - x_j$ and $2\alpha_{ijk} = \Delta_i + \Delta_j - \Delta_k$. For our case we have that $\Delta_1 = \Delta_2 = \delta$, $\Delta_3 = \Delta_\Phi = \Delta$, and we have fixed the location for $x_2 = y = 0$ while we write $x_1 = x$ and $x_3 = z$ so the 3-point function becomes:

$$\langle \phi_1(x_1)\phi_2(0)\Phi(z)\rangle = \frac{\lambda_\Phi}{|x|^{2\delta-\Delta}|x-z|^{\Delta}|z|^{\Delta}}. \tag{B.3.4}$$

Eq. (B.3.1) may then be written as:

$$\frac{\lambda_\Phi}{|x|^{2\delta-\Delta}|x-z|^{\Delta}|z|^{\Delta}} = \frac{\lambda_\Phi}{|x|^{2\delta-\Delta}}\left(1 + \gamma x^\mu\partial_\mu + \alpha x^\mu x^\nu\partial_\mu\partial_\nu + \beta x^2\partial^2 + ...\right)\frac{1}{|z|^{2\Delta}}. \tag{B.3.5}$$

We may then evaluate this power series operator. The individual terms acting with derivatives on the 2-point function becomes:

$$x^\mu\partial_\mu\frac{1}{|z|^{2\Delta}} = \frac{-2\Delta x\cdot z}{|z|^{2\Delta+2}}, \tag{B.3.6}$$

$$x^\mu x^\nu\partial_\mu\partial_\nu\frac{1}{|z|^{2\Delta}} = 2\Delta(2\Delta+2)\frac{(z\cdot x)^2}{|z|^{2\Delta+4}} - \frac{2\Delta x^2}{|z|^{2\Delta+2}}, \tag{B.3.7}$$

$$x^2\partial^2\frac{1}{|z|^{2\Delta}} = 2\Delta(2\Delta+2)\frac{z^2x^2}{|z|^{2\Delta+4}} - \frac{2\Delta D x^2}{|z|^{2\Delta+2}}, \tag{B.3.8}$$

where we get $\partial_\mu z^\mu = D$ due to the Euclidean signature. Then we look at the expansion around $x = 0$ for the RHS to 2nd order which can be thought of as a multipole expansion:

$$\frac{1}{|x-z|^{\Delta}} \simeq \frac{1}{|x-z|^{\Delta}}|_{x=0} - x^\mu\partial_\mu\frac{1}{|x-z|^{\Delta}}|_{x=0} + \frac{1}{2}x^\mu x^\nu\partial_\mu\partial_\nu\frac{1}{|x-z|^{\Delta}}|_{x=0} - .... \tag{B.3.9}$$

So each that term becomes:

$$\frac{1}{|x-z|^{\Delta}}|_{x=0} = \frac{1}{|z|^{\Delta}}, \tag{B.3.10}$$

$$x^\mu\partial_\mu\frac{1}{|x-z|^{\Delta}}|_{x=0} = \frac{\Delta x\cdot z}{|z|^{\Delta+2}}, \tag{B.3.11}$$

$$x^\mu x^\nu\partial_\mu\partial_\nu\frac{1}{|x-z|^{\Delta}}|_{x=0} = \Delta(\Delta+2)\frac{(z\cdot x)^2}{|z|^{\Delta+4}} - \frac{\Delta x^2}{|z|^{\Delta+2}}. \tag{B.3.12}$$

Since we only want to fix the first few constants in the series we neglect higher order than 2 in x^μ. Then combined expansion of the LHS of Eq. (B.3.1) becomes:

$$\frac{1}{|x-z|^{\Delta}|z|^{\Delta}} \simeq \frac{1}{|z|^{2\Delta}} - \frac{\Delta x\cdot z}{|z|^{2\Delta+2}} + \frac{\Delta}{2}(\Delta+2)\frac{(z\cdot x)^2}{|z|^{2\Delta+4}} - \frac{\Delta x^2}{2|z|^{2\Delta+2}} + ... \tag{B.3.13}$$

Comparing to what we have on the RHS of Eq. (B.3.1):

$$\frac{1}{|z|^{2\Delta}} + \gamma\frac{-2\Delta x\cdot z}{|z|^{2\Delta+2}} + \alpha\left(2\Delta(2\Delta+2)\frac{(z\cdot x)^2}{|z|^{2\Delta+4}} - \frac{2\Delta x^2}{|z|^{2\Delta+2}}\right) + \beta\left(2\Delta(2\Delta+2)\frac{z^2x^2}{|z|^{2\Delta+4}} - \frac{2\Delta D x^2}{|z|^{2\Delta+2}}\right) + ... \tag{B.3.14}$$

Eq. (B.3.13) and Eq. (B.3.14) become equal when:

$$\begin{aligned} -\Delta &= -2\Delta\gamma, \\ \frac{\Delta}{2}(\Delta+2) &= \alpha 2\Delta(2\Delta+2), \\ -\frac{\Delta}{2} &= -2\Delta\alpha + \beta(2\Delta(2\Delta+2) - 2\Delta D), \end{aligned} \tag{B.3.15}$$

which happens at the specific fixed constants:

$$\gamma = \frac{1}{2}, \qquad \alpha = \frac{\Delta+2}{8(\Delta+1)}, \qquad \beta = \frac{-\Delta}{16(\Delta+1)(\Delta-\frac{D}{2}+1)}. \tag{B.3.16}$$

Giving the following expression for the power series:

$$C_\phi(x,\partial_y) = \frac{1}{|x|^{2\delta-\Delta}}\left(1 + \frac{1}{2}x^\mu\partial_\mu + \frac{\Delta+2}{8(\Delta+1)}x^\mu x^\nu\partial_\mu\partial_\nu + \frac{-\Delta}{16(\Delta-D/2+1)(\Delta+1)}x^2\partial^2 + ...\right). \tag{B.3.17}$$

B.4 Conformal Casimir Coordinate Change $\{z,\bar{z}\} \to \{u,v\}$

In this section we would like to change the variables of the Casimir differential operator between the Dolan-Osborn coordinates and the conformal cross-ratios $\mathcal{D}(z,\bar{z}) \to \mathcal{D}(u,v)$. We start with the expression of the differential operator from [26]:

$$\mathcal{D} = 2z^2(1-z)\partial_z^2 - 2z^2\partial_z + (z \rightleftarrows \bar{z}) + 2(D-2)\frac{z\bar{z}}{z-\bar{z}}((1-z)\partial_z - (z \rightleftarrows \bar{z})). \tag{B.4.1}$$

The coordinates are connected by:

$$u = z\bar{z}, \qquad v = (1-z)(1-\bar{z}), \tag{B.4.2}$$

with the inverse:

$$z = \frac{u-v+1+\sqrt{(u-v+1)^2-4u}}{2}, \qquad \bar{z} = \frac{u-v+1-\sqrt{(u-v+1)^2-4u}}{2}. \tag{B.4.3}$$

For simplicity we keep a mix of coordinates in the derivatives, by using the chain rule:

$$\partial_z = \bar{z}\partial_u - (1-\bar{z})\partial_v, \qquad \partial_{\bar{z}} = z\partial_u - (1-z)\partial_v, \tag{B.4.4}$$

$$\partial_z^2 = \bar{z}^2\partial_u^2 + (1-\bar{z})^2\partial_v^2 - 2\bar{z}(1-\bar{z})\partial_u\partial_v, \qquad \partial_{\bar{z}}^2 = z^2\partial_u^2 + (1-z)^2\partial_v^2 - 2z(1-z)\partial_u\partial_v. \tag{B.4.5}$$

One can identify the expressions:

$$\frac{z\bar{z}}{z-\bar{z}}((1-z)\partial_z - (z \rightleftarrows \bar{z})) = -u\partial_u, \tag{B.4.6}$$

$$-z^2\partial_z + (z \rightleftarrows \bar{z}) = -(u-v+1)u\partial_u + ((1-v)^2 - u(1+v))\partial_v, \tag{B.4.7}$$

$$z^2(1-z)\partial_z^2 + (z \rightleftarrows \bar{z}) = (1-u+v)u^2\partial_u^2 + ((1-v)^2 - u(1+v))v\partial_v^2 - 2(1+u-v)uv\partial_u\partial_v. \tag{B.4.8}$$

Leaving us with the Casimir differential operator in $\{u,v\}$ coordinates:

$$\begin{aligned} \frac{\mathcal{D}}{2} &= [(1-v)^2 - u(1+v)]v\partial_v^2 + (1-u+v)u^2\partial_u^2 - (1+u-v)u\partial_u \\ &\quad + [(1-v)^2 - u(1+v)]\partial_v - 2(1+u-v)uv\partial_u\partial_v - (D-2)u\partial_u. \end{aligned} \tag{B.4.9}$$

Appendix C

Radial/Angular Decomposition of Conformal Blocks

C.1 Gegenbauer Polynomial in Various Dimensions

In this appendix, we consider which spherical functions the Gegenbauer polynomials represent in specific dimensions $D = 2, 3, 4$, and the strict limit of $D \to \infty$.

C.1.1 $D = 2$

This case corresponds to $\nu = 0$ we would therefore like to prove that:

$$\lim_{\nu\to 0} \frac{1}{\nu} C_j^\nu(\cos\theta) = \frac{2}{j}\cos(j\theta). \tag{C.1.1}$$

We write the Gegenbauer in the hypergeometric function representation so the LHS of Eq. (C.1.1) is:

$$\lim_{\nu\to 0} \frac{(2\nu)_j}{\nu j!} {}_2F_1\left(-j, 2\nu+j, \nu+1/2, \frac{1-\cos\theta}{2}\right). \tag{C.1.2}$$

The pre-factor, contains a Pochhammer that can be written as a the rising product:

$$\lim_{\nu\to 0} \frac{(2\nu)_j}{\nu j!} = \lim_{\nu\to 0} \frac{2\nu(2\nu+1)(2\nu+2)\times ...\times (2\nu+j-1)}{\nu j!} = \frac{2}{j!}\cdot 1\cdot 2\times ...\times (j-1) = \frac{2\Gamma(j)}{j!} = \frac{2}{j}, \tag{C.1.3}$$

where ν cancelled and simplified the expression when $\nu \to 0$. For the hypergeometric function we may simplify it:

$$\lim_{\nu\to 0} {}_2F_1\left(-j, 2\nu+j, \nu+1/2, \frac{1-\cos\theta}{2}\right) = {}_2F_1\left(-j, j, 1/2, \frac{1-\cos\theta}{2}\right) = \cos\left(2j\sin^{-1}\left[\sqrt{\frac{1-\cos\theta}{2}}\right]\right). \tag{C.1.4}$$

To see why the last equality holds consider the series expansion, which defnes the hypergeometric function. It is straightforward to compute the hypergeometric function for the first specific terms using its definition as a sum over Pochhammer functions:

$${}_2F_1\left(-j, j, 1/2, x^2\right) = 1 - 2j^2x^2 + \frac{2j^2}{3}(j^2-1)x^4 + \mathcal{O}(x^6), \tag{C.1.5}$$

while we have defined $x \equiv (1-\cos\theta)/2$. Then consider the function:

$$f(x) = \cos(2j\sin^{-1}(x)). \tag{C.1.6}$$

Notice that $\sin^{-1}(0) = 0$ and $\frac{d}{dx}\sin^{-1}(x) = (1-x^2)^{-1/2}$. Then we get:

$$f(0) = 1, \qquad f'(x) = -2j\sin(2j\sin^{-1}(x))(1-x^2)^{-1/2}, \qquad f'(0) = 0, \tag{C.1.7}$$

$$f''(x) = -4j^2\cos(2j\sin^{-1}(x))(1-x^2)^{-1} - 2jx\sin(2j\sin^{-1}(x))(1-x^2)^{-3/2}, \qquad f''(0) = -4j^2, \tag{C.1.8}$$

giving us the expansion:

$$\cos(2j\sin^{-1}(x)) = 1 - 2j^2x^2 + \frac{2j^2}{3}(j^2-1)x^4 + \mathcal{O}(x^6). \tag{C.1.9}$$

The expressions Eq. (C.1.5) and Eq. (C.1.9) agrees term by term. Applying the trigonometric identity of the half angle formula:

$$\sin^2\left(\frac{\theta}{2}\right) = \frac{1-\cos\theta}{2}, \tag{C.1.10}$$

to obtain the relation:

$$2F_1\left(-j, j, 1/2, \frac{1-\cos\theta}{2}\right) = \cos(j\theta), \tag{C.1.11}$$

and so we find the given limit of Eq. (C.1.1).

C.1.2 $D = 3$

In this case we have $\nu = 1/2$. We can use that Gegenbauer polynomials can be represented as Jacobi polynomials $P_n^{\alpha,\beta}$ [42]:

$$C_j^{\nu}(\eta) = \frac{(2\nu)_j}{(\nu+1/2)_j}P_j^{\nu-1/2,\nu-1/2}(\eta). \tag{C.1.12}$$

The Jacobi Polynomial reduces to a Legendre Polynomial for $\alpha, \beta = 0$.

$$C_j^{1/2}(\cos\theta) = \frac{(1)_j}{(1)_j}P_j^{0,0}(\cos\theta) = P_j(\cos\theta). \tag{C.1.13}$$

C.1.3 $D = 4$

In this case we have $\nu = 1$. Then we would like to prove that we get the simplification:

$$C_j^1(\cos\theta) = \frac{\sin((j+1)\theta)}{\sin\theta}. \tag{C.1.14}$$

Applying the hypergeometric function representation of the Gegenbauer polynomial, and further expressing the function explicitly as a sum over Pochhammer functions:

$$C_j^1(\cos\theta) = \frac{(2)_j}{j!}\sum_{n=0}^{\infty}\frac{(-j)_n(j+2)_n}{(3/2)_n n!}\left(\frac{1-\cos\theta}{2}\right)^n. \tag{C.1.15}$$

The prefactor reduces to:

$$\frac{(2)_j}{j!} = \frac{\Gamma(j+2)}{\Gamma(2)\Gamma(j+1)} = j+1. \tag{C.1.16}$$

Defining $x \equiv (1-\cos\theta)/2$ again, we can write out the first few terms of the sum:

$$C_j^1(\cos\theta) = (j+1) - \frac{2}{3}j(j+1)(j+2)x^2 + \frac{2}{15}(j-1)j(j+1)(j+2)(j+3)x^4 + \mathcal{O}(x^6). \tag{C.1.17}$$

We define the RHS of Eq. (C.1.14) as a function $f(x)$:

$$f(x) \equiv \frac{\sin((j+1)\theta)}{\sin\theta} = \frac{\sin(2(j+1)\sin^{-1}(x))}{\sin(2\sin^{-1}(x))}. \tag{C.1.18}$$

Applying a series expansion around $x = 0$ and the L'Hopital rule in the limit of $x \to 0$, we can evaluate the function to the same series as Eq. (C.1.17). Then the two expressions matches term by term, and thus we have proven Eq. (C.1.14) holds.
In the $D = 4$ case of the Gegenbauer polynomial expression is a character χ of a SU(2) representation. To see this we write the sin functions as exponential functions, and define $y \equiv e^{i\theta}$, $n = j+1$:

$$\frac{\sin((j+1)\theta)}{\sin\theta} = \frac{e^{i(j+1)\theta} - e^{-i(j+1)\theta}}{e^{i\theta} - e^{-i\theta}} = \frac{y^n - y^{-n}}{y - y^{-1}} = y^{1-n}\frac{y^{2n}-1}{y^2-1}. \tag{C.1.19}$$

Define the series:

$$s \equiv 1 + y^2 + y^4 + ... + y^{2n-4} + y^{2n-2}, \tag{C.1.20}$$

multiply it by y^2:

$$y^2 s = y^2 + y^4 + ... + y^{2n-2} + y^{2n}, \tag{C.1.21}$$

subtracting Eq. (C.1.21) from Eq. (C.1.20)

$$s - y^2 s = 1 - y^{2n}, \tag{C.1.22}$$

solving for s we have a new expression for the series:

$$s = \frac{y^{2n}-1}{y^2-1}. \tag{C.1.23}$$

We can therfore write Eq. (C.1.19) as:

$$y^{1-n}(1 + y^2 + y^4 + ... + y^{2n-4} + y^{2n-2}) = y^{1-n} + y^{3-n} + y^{5-n} + ... + y^{n-3} + y^{n-1}, \tag{C.1.24}$$

reinstating $j+1$ and $e^{i\theta}$ and swapping the order, we may collect the terms to a sum:

$$e^{ij\theta} + e^{i(j-2)\theta} + ... + e^{-i(j-2)\theta} + e^{-ij\theta} = \sum_{n=0}^{j} e^{i(j-2n)\theta}, \tag{C.1.25}$$

one can identify this as the character, χ of a SU(2) representation, Π with weights $j, j-2, ..., -(j-2), -j$, given by $\chi = Tr[\Pi]$ as:

$$\chi_j(\theta) = \sum_{|j|\le l} \langle lj|e^{iL_3\theta}|lj\rangle, \tag{C.1.26}$$

with the quantized angular momentum $L_3 |lj\rangle = j |lj\rangle$. Evaluating this sum by applying the operator, is equivalent to Eq. (C.1.25). It can also be written directly as a SU(2) matrix, which we take the trace of:

$$\chi_j(\theta) = \chi\begin{pmatrix} e^{i\theta} & 0 \\ 0 & e^{-i\theta}\end{pmatrix} = Tr\begin{pmatrix} e^{ij\theta} & 0 & 0 & \dots & 0 \\ 0 & e^{i(j-2)\theta} & 0 & \dots & 0 \\ 0 & 0 & \ddots & 0 & 0 \\ \vdots & \vdots & 0 & e^{-i(j-2)\theta} & 0 \\ 0 & 0 & 0 & 0 & e^{-ij\theta}\end{pmatrix} = \frac{\sin((j+1)\theta)}{\sin\theta}. \tag{C.1.27}$$

C.1.4 $D \to \infty$ Limit

This is equivalent to the strict $\nu \to \infty$ limit. The Gegenbauer polynomial simplifies [43]:

$$\lim_{\nu\to\infty} \frac{1}{(2\nu)_j} C_j^\nu(\eta) = \frac{\eta^j}{j!}. \tag{C.1.28}$$

We will now prove this relation. We apply the Rodrigues representation of the Gegenbauer polynomial:

$$C_j^\nu(\eta) = \frac{(-1)^j}{2^j j!} \frac{\Gamma(\nu+\frac{1}{2})\Gamma(j+2\nu)}{\Gamma(2\nu)\Gamma(\nu+j+\frac{1}{2})} (1-\eta^2)^{-\nu+1/2} \frac{d^j}{d\eta^j}((1-\eta^2)^{j+\nu-1/2}). \tag{C.1.29}$$

Define $y(\eta) \equiv (1-\eta^2)$ and $\sigma \equiv j+\nu-\frac{1}{2}$. The third derivative of $y(\eta)$ with respect to j is vanishing. The j'th derivative to leading order in D and thereby leading order in σ for $y(\eta)$ is:

$$\frac{d^j}{d\eta^j} y^\sigma = \sigma(\sigma-1) \times ... \times (\sigma-(j-1)) y^{\sigma-j} (y')^j + ... \tag{C.1.30}$$

In the strict $D \to \infty$ limit the subleading terms will vanish. The following terms have fewer derivatives. This gives less factors of σ and essentially D. For the whole expression of the Gegenbauer one will end up with a factors of $1/D$ which taking to $D \to \infty$ vanishes. Using falling factorials one can re-write:

$$\sigma \times ... \times (\sigma-(j-1)) = \frac{\Gamma(\sigma+1)}{\Gamma(\sigma-j+1)}. \tag{C.1.31}$$

The Gegenbauer polynomial now reads:

$$C_j^\nu(\eta) = \frac{(-1)^j}{2^j j!} \frac{\Gamma(j+2\nu)}{\Gamma(2\nu)} (-2\eta)^j (1-\eta^2)^{\nu-1/2} (1-\eta^2)^{-\nu+1/2} + ... \tag{C.1.32}$$

Moving the Γ-functions that can be identified as $(2\nu)_j$ to the opposite side:

$$\frac{1}{(2\nu)_j} C_j^\nu(\eta) = \frac{\eta^j}{j!} + \mathcal{O}\left(\frac{1}{D}\right) \tag{C.1.33}$$

Taking the limit $\nu \to \infty$ will have vanishing subleading terms as mentioned and thus we have proven:

$$\lim_{\nu\to\infty} \frac{1}{(2\nu)_j} C_j^\nu(\eta) = \frac{\eta^j}{j!}. \tag{C.1.34}$$

C.2 Conformal Casimir Coordinate Change $\{z, \bar{z}\} \to \{s, \xi\}$

In this appendix, we will show how the Casimir differential operator transforms from the Dolan-Osborn coordinates to the radial/angular coordinates of the z-picture i.e. $\mathcal{D}(z,\bar{z}) \to \mathcal{D}(s,\xi)$. Starting with the Conformal Casimir differential operator in Dolan-Osborn coordinates:

$$\mathcal{D} = 2z^2(1-z)\partial_z^2 - 2z^2\partial_z + (z \rightleftarrows \bar{z}) + 2(D-2)\frac{z\bar{z}}{z-\bar{z}}((1-z)\partial_z - (z \rightleftarrows \bar{z})), \tag{C.2.1}$$

we can apply the chain rule, and get the derivatives while we keep a mix of coordinates for simplicity:

$$\partial_z = \frac{1}{2s}\left(\bar{z}\partial_s + \left(1-\frac{\xi\bar{z}}{s}\right)\partial_\xi\right), \qquad \partial_{\bar{z}} = \frac{1}{2s}\left(z\partial_s + \left(1-\frac{\xi z}{s}\right)\partial_\xi\right), \tag{C.2.2}$$

$$\partial_z^2 = \frac{\bar{z}^2}{4s^2}\partial_s^2 + \frac{1}{4s^2}\left(1+\frac{\xi^2\bar{z}^2}{s^2} - \frac{2\xi\bar{z}}{s}\right)\partial_\xi^2 + \frac{\bar{z}}{2s^2}\left(1-\frac{\xi\bar{z}}{s}\right)\partial_s\partial_\xi - \frac{\bar{z}^2}{4s^3}\partial_s + \left(\frac{3\xi\bar{z}^2}{4s^4} - \frac{\bar{z}}{2s^3}\right)\partial_\xi, \tag{C.2.3}$$

where the $\partial_{\bar{z}}^2$ is completely similar to ∂_z^2 when interchanging $\bar{z} \rightleftarrows z$ due to the symmetry of the coordinates, like it has been shown for the differential operator of first order. Using some algebra a few nice relations are:

$$z - \bar{z} = 2s\sqrt{\xi^2 - 1}, \qquad z + \bar{z} = 2\xi s, \qquad z^2 + \bar{z}^2 = 2s^2(2\xi^2 - 1), \qquad z^3 + \bar{z}^3 = 2s^3(4\xi^3 - 3\xi). \tag{C.2.4}$$

The specific sections of the Casimir differential operator are:

$$-z^2\partial_z - \bar{z}^2\partial_{\bar{z}} = -\xi s^2\partial_s + s\partial_\xi - s\xi^2\partial_\xi, \tag{C.2.5}$$

$$(1-z)\partial_z - (1-\bar{z})\partial_{\bar{z}} = \sqrt{\xi^2-1}\left(\frac{\xi}{s}\partial_\xi - \partial_\xi - \partial_s\right), \tag{C.2.6}$$

$$2\nu\frac{z\bar{z}}{z-\bar{z}} = \frac{\nu s}{\sqrt{\xi^2-1}}, \tag{C.2.7}$$

$$\begin{aligned} &z^2(1-z)\partial_z^2 + \bar{z}^2(1-\bar{z})\partial_{\bar{z}}^2 \\ &= \frac{s^2}{2}(1-\xi s)\partial_s^2 + \frac{1}{2}(-1+\xi^2+3s\xi^3-3\xi s)\partial_\xi^2 + (1-\xi^2)s^2\partial_s\partial_\xi - \frac{s}{2}(1-\xi s)\partial_s + \frac{1}{2}(\xi+\xi^2 s-2s)\partial_\xi. \end{aligned} \tag{C.2.8}$$

Multiplying by two to match the Casimir equation conventions, one obtains:

$$\mathcal{D} = 2\nu(\xi\partial_\xi - s\partial_\xi - s\partial_s) - \xi s^2\partial_s - s\partial_s + 2(1-\xi^2)s^2\partial_s\partial_\xi + s^2(1-\xi s)\partial_s^2 + (-1+\xi^2+s\xi-s\xi^3)\partial_\xi^2 + (\xi-\xi^2 s)\partial_\xi. \tag{C.2.9}$$

Re-arranging these operators so that we have a homogeneity preserving and increasing part of the operator:

$$\begin{aligned} \mathcal{D} &= \mathcal{D}_0 + \mathcal{D}_1, \\ \mathcal{D}_0 &= s^2\partial_s^2 + (2\nu+1)(\xi\partial_\xi - s\partial_s) - (1-\xi^2)\partial_\xi^2, \\ \mathcal{D}_1 &= s(-\xi s^2\partial_s^2 + 2(1-\xi^2)s\partial_s\partial_\xi - \xi s\partial_s - (2\nu+\xi^2)\partial_\xi + \xi(1-\xi^2)\partial_\xi^2). \end{aligned} \tag{C.2.10}$$

C.3 Conformal Transformation from ρ- to z-Picture

In this section we will find the right conformal transformation which brings us from the ρ to the z-configuration of conformal operators. The coordinate system in the z-picture written in the complex plane $\{x_1, x_2, x_3, x_4\} = \{0, z, 1, \infty\}$ can be formulated as vectors in the $\mathbb{R}^2$ plane:

$$x_1 = \begin{pmatrix}0\\0\end{pmatrix}, \qquad x_2 = \begin{pmatrix}x\\y\end{pmatrix}, \qquad x_3 = \begin{pmatrix}1\\0\end{pmatrix}, \qquad x_4 \to \infty, \tag{C.3.1}$$

likewise for the ρ-picture in the complex plane $\{x_1, x_2, x_3, x_4\} = \{-\rho, \rho, 1, -1\}$ can be represented with the vectors:

$$x_1 = \begin{pmatrix}-\tilde{x}\\-\tilde{y}\end{pmatrix}, \qquad x_2 = \begin{pmatrix}\tilde{x}\\\tilde{y}\end{pmatrix}, \qquad x_3 = \begin{pmatrix}1\\0\end{pmatrix}, \qquad x_4 = \begin{pmatrix}-1\\0\end{pmatrix}, \tag{C.3.2}$$

Using a series of conformal transformations, i.e. translations, rotations, dilations or SCTs on all operator locations, one is able to go from one picture to the other. The SCT K_μ consists of an inversion R then a translation P_μ and then an inversion again. x_4 must be send to infinity in the z-picture, which comes from an inversion of the null vector in general:

$$\begin{pmatrix}a\\b\end{pmatrix} \xrightarrow{R} \frac{1}{a^2+b^2}\begin{pmatrix}a\\b\end{pmatrix} \xrightarrow{P_\mu} \begin{pmatrix}0\\0\end{pmatrix} \xrightarrow{R} \infty. \tag{C.3.3}$$

Applying this for x_4:

$$x_4 = \begin{pmatrix}-1\\0\end{pmatrix} \xrightarrow{R} \begin{pmatrix}-1\\0\end{pmatrix} \xrightarrow{P_\mu} \begin{pmatrix}0\\0\end{pmatrix} \xrightarrow{R} \infty, \tag{C.3.4}$$

the translation required is $P_\mu : x^\mu \to (x')^\mu = x^\mu + c^\mu$ with $c^\mu = (1, 0)$. Now we apply the same SCT on the other coordinates:

$$x_1 = \begin{pmatrix} -\tilde{x} \\ -\tilde{y} \end{pmatrix} \xrightarrow{R} \frac{-1}{\tilde{x}^2+\tilde{y}^2} \begin{pmatrix} \tilde{x} \\ \tilde{y} \end{pmatrix} \xrightarrow{P_\mu} \frac{-1}{\tilde{x}^2+\tilde{y}^2} \begin{pmatrix} \tilde{x}-\tilde{x}^2-\tilde{y}^2 \\ y \end{pmatrix} \xrightarrow{R} \frac{-1}{(1-\tilde{x})^2+\tilde{y}^2} \begin{pmatrix} \tilde{x}-\tilde{x}^2-\tilde{y}^2 \\ \tilde{y} \end{pmatrix}, \tag{C.3.5}$$

$$x_2 = \begin{pmatrix} \tilde{x} \\ \tilde{y} \end{pmatrix} \xrightarrow{R} \frac{1}{\tilde{x}^2+\tilde{y}^2} \begin{pmatrix} \tilde{x} \\ \tilde{y} \end{pmatrix} \xrightarrow{P_\mu} \frac{1}{\tilde{x}^2+\tilde{y}^2} \begin{pmatrix} \tilde{x}+\tilde{x}^2+\tilde{y}^2 \\ \tilde{y} \end{pmatrix} \xrightarrow{R} \frac{1}{(1+\tilde{x})^2+\tilde{y}^2} \begin{pmatrix} \tilde{x}+\tilde{x}^2+\tilde{y}^2 \\ \tilde{y} \end{pmatrix}, \tag{C.3.6}$$

$$x_3 = \begin{pmatrix} 1 \\ 0 \end{pmatrix} \xrightarrow{R} \begin{pmatrix} 1 \\ 0 \end{pmatrix} \xrightarrow{P_\mu} \begin{pmatrix} 2 \\ 0 \end{pmatrix} \xrightarrow{R} \begin{pmatrix} 1/2 \\ 0 \end{pmatrix}. \tag{C.3.7}$$

Next we rotate x_1 down to the x-axis with x_3 as the center of rotation. In order to do a rotation around x_3 it has to be in the origin, this can be fullfilled by the translation $c^\mu = (-1/2, 0)$:

$$\begin{aligned} x_1 &= \frac{1}{(1-\tilde{x})^2+\tilde{y}^2} \begin{pmatrix} 1/2(\tilde{x}^2+\tilde{y}^2-1) \\ -\tilde{y} \end{pmatrix}, & x_2 &= \frac{1}{(1+\tilde{x})^2+\tilde{y}^2} \begin{pmatrix} 1/2(\tilde{x}^2+\tilde{y}^2-1) \\ \tilde{y} \end{pmatrix}, \\ x_3 &= \begin{pmatrix} 0 \\ 0 \end{pmatrix}, & x_4 &= \infty. \end{aligned} \tag{C.3.8}$$

The rotation $R(\theta)$ matrix is:

$$M_{\mu\nu} : R(\theta) = \begin{pmatrix} \cos\theta & -\sin\theta \\ \sin\theta & \cos\theta \end{pmatrix}. \tag{C.3.9}$$

The angle of rotation is restricted by when the $\tilde{y}$ component of the new coordinate for position $x_1' = R(\theta)x_1$ vanishes:

$$\theta = \tan^{-1}\left(\frac{2\tilde{y}}{\tilde{x}^2+\tilde{y}^2-1}\right). \tag{C.3.10}$$

The operators locations of x_3 and x_4 is invariant under this transformation. The rotation matrix can be written as:

$$R(x, y) = \frac{1}{\sqrt{\tilde{x}^2+\tilde{y}^2-1}\sqrt{\tilde{x}^2+\tilde{y}^2-1+2\tilde{y}}} \begin{pmatrix} \tilde{x}^2+\tilde{y}^2-1 & -2\tilde{y} \\ 2\tilde{y} & \tilde{x}^2+\tilde{y}^2-1. \end{pmatrix} \tag{C.3.11}$$

The rotation leaves us with the following vectors:

$$\begin{aligned} x_1 &= \frac{\frac{1}{2}(\tilde{x}^2+\tilde{y}^2-1)^2+2\tilde{y}^2}{(-\tilde{x}^2+\tilde{y}^2+1)\sqrt{\tilde{x}^2+\tilde{y}^2-1}\sqrt{\tilde{x}^2+\tilde{y}^2-1+2\tilde{y}}} \begin{pmatrix} 1 \\ 0 \end{pmatrix}, & x_3 &= \begin{pmatrix} 0 \\ 0 \end{pmatrix}, & x_4 &= \infty, \\ x_2 &= \frac{1}{(1+\tilde{x}^2+\tilde{y}^2)\sqrt{\tilde{x}^2+\tilde{y}^2-1+2\tilde{y}}\sqrt{\tilde{x}^2+\tilde{y}^2-1}} \begin{pmatrix} \frac{1}{2}(\tilde{x}^2+\tilde{y}^2-1)^2+2\tilde{y}^2 \\ 2\tilde{y}(\tilde{x}^2+\tilde{y}^2-1). \end{pmatrix} \end{aligned} \tag{C.3.12}$$

Next we do a translation so that x_1 is at the origin:

$$x_1 - x_1 = \begin{pmatrix} 0 \\ 0 \end{pmatrix}, \qquad x_2 - x_1, \qquad x_3 - x_1, \qquad x_4 - x_1 = x_4, \tag{C.3.13}$$

and scale the coordinate system by a dilatation. We fix the amount of scaling λ so that $(x_3 - x_1)\lambda = (1, 0)$. This λ is:

$$\lambda = -\frac{(1-\tilde{x}^2+\tilde{y}^2)\sqrt{\tilde{x}^2+\tilde{y}^2-1}\sqrt{\tilde{x}^2+\tilde{y}^2+2\tilde{y}-1}}{\frac{1}{2}(\tilde{x}^2+\tilde{y}^2-1)^2+2\tilde{y}^2}, \tag{C.3.14}$$

our coordinates then reads:

$$x_1 = \begin{pmatrix} 0 \\ 0 \end{pmatrix}, \qquad x_2 = \begin{pmatrix} \frac{\tilde{x}^2-\tilde{y}^2-1}{\tilde{x}^2+\tilde{y}^2+1} \\ \frac{4\tilde{y}((\tilde{x}^2-1)^2-\tilde{y}^4)}{(1+\tilde{x}^2+\tilde{y}^2)(-1+\tilde{x}^2+5\tilde{y}^2)} \end{pmatrix}, \qquad x_3 = \begin{pmatrix} 1 \\ 0 \end{pmatrix}, \qquad x_4 = \infty, \tag{C.3.15}$$

we then have the freedom to relabel the coordinates of x_2 as x, y so that it matches the z-picture. When finding the relationship between the z and ρ coordinates it is more instructive to do so by a mapping over the conformal cross-ratios.

C.4 $\rho(z)$ Derivation

In this appendix, we derive the relationship between the z and ρ coordinates, by relating each configuration to the conformal cross-ratios $\{u, v\}$. Starting with the vector representation in the z-picture and ρ-picture configurations of operator positions Eq. (C.3.1) and Eq. (C.3.2). The conformal cross-ratios consists of squares of the distances between operators. These can be directly related to z and ρ:

$$z = x + iy, \qquad \bar{z} = x - iy, \qquad \rho = \tilde{x} + i\tilde{y}, \qquad \bar{\rho} = \tilde{x} - i\tilde{y}. \tag{C.4.1}$$

This implies for z coordinates:

$$\begin{aligned} &x_{12}^2 = x^2 + y^2 = z\bar{z}, \qquad x_{34}^2 = x_4^2, \qquad x_{24}^2 = x_4^2, \qquad x_{13}^2 = 1, \\ &x_{23}^2 = (x-1)^2 + y^2 = (1-z)(1-\bar{z}), \qquad x_{14}^2 = x_4^2, \end{aligned} \tag{C.4.2}$$

and ρ coordinates:

$$\begin{aligned} &x_{12}^2 = 4(\tilde{x}^2 + \tilde{y}^2) = 4\rho\bar{\rho}, \qquad x_{34}^2 = 4, \qquad x_{24}^2 = (\tilde{x}+1)^2 + \tilde{y}^2 = (1+\rho)(1+\bar{\rho}), \\ &x_{13}^2 = (\tilde{x}+1)^2 + \tilde{y}^2 = (1+\rho)(1+\bar{\rho}), \qquad x_{23}^2 = (\tilde{x}-1)^2 + \tilde{y}^2 = (1-\rho)(1-\bar{\rho}), \\ &x_{14}^2 = (\tilde{x}-1)^2 + \tilde{y}^2 = (1-\rho)(1-\bar{\rho}). \end{aligned} \tag{C.4.3}$$

The two configurations yields the conformal cross-ratios:

$$u = z\bar{z}, \qquad v = (1-z)(1-\bar{z}), \qquad u = \frac{16\rho\bar{\rho}}{(1+\rho)^2(1+\bar{\rho})^2}, \qquad v = \frac{(1-\rho)^2(1-\bar{\rho})^2}{(1+\rho)^2(1+\bar{\rho})^2}. \tag{C.4.4}$$

The conformal cross-ratios must be the same so the transformation between ρ and z becomes:

$$z = \frac{4\rho}{(1+\rho)^2}, \qquad \bar{z} = \frac{4\bar{\rho}}{(1+\bar{\rho})^2}, \tag{C.4.5}$$

which may be inverted:

$$\rho = \frac{z}{(1+\sqrt{1-z})^2}, \qquad \bar{\rho} = \frac{\bar{z}}{(1+\sqrt{1-\bar{z}})^2}. \tag{C.4.6}$$

C.5 Degeneracy of the Conformal Field Partition Functions

In this appendix, we will make a review of appendix A in [44]. We will here consider the degeneracy of the partition function of scalars, fermions, and gauge vector fields, and generalize to D dimensions. Considering the partition function for degenerate states d_i and energies E_i:

$$Z = \sum_i d_i e^{-\beta E_i}. \tag{C.5.1}$$

Using a shorthand notation $q \equiv e^{-\beta/R}$, where β is the radius of S^1 and R is the radius of S^3 in the manifold $M_4 = S_1 \times S_3$. The energies are being replaced by the scaling dimension in a CFT and summed over these:

$$z_{\mathcal{O}}(q) = \sum_\Delta d_\Delta q^\Delta, \tag{C.5.2}$$

which is the partition function associated with the primary operator. It is a sum over the descendant operators, so we use the scaling dimension for the descendants $\Delta_{\mathcal{O}} + n$ to write it on the form:

$$z_{\mathcal{O}}(q) = q^{\Delta_{\mathcal{O}}} \sum_{n=0}^{\infty} d_n q^n, \tag{C.5.3}$$

with n being the new index. If we then consider any EOM on the form $\mathcal{D}\mathcal{O} = 0$, the descendants should vanish:

$$\mathcal{O}_n^{EOM} = \partial_{\alpha_1}\partial_{\alpha_2}...\partial_{\alpha_n}(\mathcal{D}\mathcal{O}) = 0. \tag{C.5.4}$$

The scaling dimension of such an object must be the same as the descendants scaling dimension while adding the dimension of the differential operator $\Delta(\mathcal{O}_n^{EOM}) = [\mathcal{D} + \Delta_\mathcal{O} + n]$. E.g. the Laplacian has the scaling dimension: $[\mathcal{D} = \nabla^2] = 2$. Since they vanish these EOM descendants shouldn't be counted in the partition function:

$$Z_\mathcal{O}(q) = z_\mathcal{O}(q) - z_\mathcal{O}^{EOM}(q) = q^{\Delta_\mathcal{O}}(1 - q^{[\mathcal{D}]})\sum_{n=0}^{\infty} d_n q^n. \tag{C.5.5}$$

In this process each degenerate state of the EOM matches another original degenerate state, so that each term in the sum is equivalent, making the descendant states decouple from the chain.
To find the degeneracy d_n we have to consider the amount of combinations of $\partial_{\alpha_1}\partial_{\alpha_2}...\partial_{\alpha_n}\mathcal{O}$ which has n operators with each operator having D different kinds. For instance $D = 2$ can have $\partial_1\partial_2\partial_2\partial_1...\partial_1$ with n of these derivatives. The tensor $\mathcal{O}_{(n)}$ is completely symmetric since all derivatives commutes. So in general we have the structure:

$$\partial_1...\partial_1\partial_2...\partial_2\partial_3...\partial_3...\partial_D...\partial_D. \tag{C.5.6}$$

In this way one can view $n = 1$ as a vector ∂_{α_1} of D objects, so it must have D combinations. For $n = 2$ one can view $\partial_{\alpha_1}\partial_{\alpha_2}$ as a $D \times D$ dimensional symmetric matrix and so it must have $D(D+1)/2$ DOF's. For $n = 3$ it is likewise a symmetric 3-rank tensor, and for a general symmetric tensors with D objects and n indices we have the combination:

$$\binom{n + D - 1}{n} = \frac{(n + D - 1)!}{n!(D - 1)!}. \tag{C.5.7}$$

We also have to count the number of internal DOF noted $\mathcal{N}_\mathcal{O}$. So we have the degeneracy:

$$d_n = \mathcal{N}_\mathcal{O}\frac{(n + D - 1)!}{n!(D - 1)!}. \tag{C.5.8}$$

The sum can now be computed using the binomial series for negative powers:

$$\sum_{n=0}^{\infty}\binom{n + D - 1}{n}q^n = \frac{1}{(1 - q)^D}. \tag{C.5.9}$$

Applying this to the partition function [44]:

$$Z_\mathcal{O}(q) = \mathcal{N}_\mathcal{O}\frac{q^{\Delta_\mathcal{O}}(1 - q^{[\mathcal{D}]})}{(1 - q)^D}. \tag{C.5.10}$$

If we consider a scalar ϕ it has $\Delta_\phi = 1$ and $\mathcal{N}_\phi = 1$ where it satisfies the Laplacian as the EOM:

$$Z_\phi(q) = \frac{q^2(1 - q^2)}{(1 - q)^D} = \frac{q^2(1 + q)(1 - q)}{(1 - q)^D} = \frac{q + q^2}{(1 - q)^{D-1}}. \tag{C.5.11}$$

For fermions we have $\Delta_\psi = (D - 1)/2$ and $\mathcal{N}_\psi = 2^{D/2}$ while they satisfy the massless Dirac equation with scaling dimension $[i\gamma^\mu\partial_\mu] = 1$ we get:

$$Z_\psi(q) = 2^{D/2}\frac{q^{(D-1)/2}(1 - q)}{(1 - q)^D} = \frac{(2^D q^{D-1})^{1/2}}{(1 - q)^{D-1}}. \tag{C.5.12}$$

For a gauge field A_μ we have the same row of operators:

$$\partial_{\alpha_1}\partial_{\alpha_2}...\partial_{\alpha_n}A_\mu. \tag{C.5.13}$$

$\mathcal{N}_{A_\mu} = D$ for each component in the vector, so we have the degeneracy:

$$D\binom{n+D-1}{n}. \tag{C.5.14}$$

We then consider each level. For $n = 0$ we only have the object A_{α_1} which is not gauge invariant, since it changes by:

$$A_{\alpha_1} + \partial_{\alpha_1} f(x). \tag{C.5.15}$$

For the first level $n = 1$ we should have a linear combination which is gauge invariant. The only object which satisfies this is the field strength tensor $F_{\alpha_1\alpha_2}$. We should therefore subtract the symmetric combinations given by the radial gauge:

$$A_{\alpha_1} = 0, \quad \partial_{\alpha_1} A_{\alpha_2} + \partial_{\alpha_2} A_{\alpha_1} = 0, \quad \partial_{\alpha_1}\partial_{\alpha_2} A_{\alpha_3} + \partial_{\alpha_3}\partial_{\alpha_1} A_{\alpha_2} + \partial_{\alpha_2}\partial_{\alpha_3} A_{\alpha_1} = 0 \quad , ..., \sum_{\text{perm}} \partial_{\alpha_1}\partial_{\alpha_2}...\partial_{\alpha_n} A_{\alpha_{n+1}} = 0. \tag{C.5.16}$$

This row has dimension $n + 1$ so that we have the actual degeneracy:

$$d_n = D\binom{n+D-1}{n} - \binom{n+1+D-1}{n+1}. \tag{C.5.17}$$

Then the vector partition function becomes:

$$z_{A_\mu}(q) = \sum_{n=0}^{\infty} \left(D\binom{n+D-1}{n} - \binom{n+1+D-1}{n+1} \right) q^{n+1}, \tag{C.5.18}$$

but it still have to subtract the descendant states from the EOM, and so we call it the off-shell vector partition function. The scaling dimension of the vector field is $\Delta_n = n + 1$, with $\Delta_{A_\mu} = 1$. We can then use the same binomial series as for the scalar case, and in addition we changes the second sum from $n + 1 \to n$ while the $n = 0$ term is $\binom{n}{n} = 1$ giving the extra term:

$$z_{A_\mu}(q) = \frac{Dq}{(1-q)^D} - \left(\frac{1}{(1-q)^D} - 1 \right) = \frac{Dq-1}{(1-q)^D} + 1. \tag{C.5.19}$$

We then consider the EOM for the gauge field, which has the form: $\partial_\mu F^{\mu\nu} = 0$ without sources. This EOM already contains 2 derivatives and we can act with n derivtives giving a symmetric combination of $n - 2$ derivatives, sending $n \to n - 2$, while the internal DOF is $\mathcal{N}_{A_\mu} = D$:

$$D\binom{n-2+D-1}{n-2}. \tag{C.5.20}$$

But since $F_{\mu\nu}$ is antisymmetric a symmetric contraction with $\partial_\mu\partial_\nu$ will also vanish, only due to the anti-symmetric. Therefore we have to add these terms to avoid double counting. This combination has one less derivative so we take $n \to n - 3$ giving us:

$$d_n^{EOM} = D\binom{n-2+D-1}{n-2} - \binom{n-3+D-1}{n-3}, \tag{C.5.21}$$

which yields the sum:

$$z_{A_\mu}^{EOM}(q) = \sum_{n=0}^{\infty} \left(D\binom{n-2+D-1}{n-2} - \binom{n-3+D-1}{n-3} \right) q^{n+1}, \tag{C.5.22}$$

we can then manipulate the two sums:

$$\begin{aligned} \sum_{n=0}^{\infty} D\binom{n-2+D-1}{n-2} q^{n+1} &= Dq^3 \sum_{n=0}^{\infty} \binom{n-2+D-1}{n-2} q^{n-2} \\ = Dq^3 \sum_{n=-2}^{\infty} \binom{n+D-1}{n} q^n &= Dq^3 \sum_{n=0} \binom{n+D-1}{n} = \frac{Dq^3}{(1-q)^D}, \end{aligned} \tag{C.5.23}$$

since the 1st and 2nd terms includes factorials of negative integers in the denominator, that is divergent in the Γ-function representation, these terms vanish. Likewise for the second sum:

$$\sum_{n=0}^{\infty}\binom{n-3+D-1}{n-3}q^{n+1}=\frac{q^4}{(1-q)^D}. \tag{C.5.24}$$

So the partition function of a gauge field EOM is:

$$z_{A_\mu}^{EOM}=q^3\left(\frac{D-q}{(1-q)^D}+q(D+1)\left(\frac{D}{2}+1\right)-D(D+1)\right). \tag{C.5.25}$$

The single particle vector partition function then becomes [44]:

$$Z_{A_\mu}=z_{A_\mu}(q)-z_{A_\mu}^{EOM}(q)\frac{(1+q)(Dq-1-q^2)+(1-q)^{D-1}}{(1-q)^{D-1}}. \tag{C.5.26}$$

Evaluated at $D=4$ it gives us $Z_{A_\mu}|_{D=4}=2(3-q)q^2/(1-q)^3$, in agreement with [44].

Appendix D

Large Dimensional Scalar Block Suggested Variables

D.1 From Scalar Block to large D Variables by Saddle-Point Approximation

Consider the scalar block of Eq. (5.1.1) we can re-write it as:

$$G_{\Delta,0}(u,v)=\sum_{n,m=0}^{\infty}\frac{(\frac{\Delta}{2})_n^2(\frac{\Delta}{2})_n^2(\frac{\Delta}{2}+n)_m^2}{(\Delta+1-\frac{D}{2})_n(\Delta)_{2n}(\Delta+2n)_m}\frac{u^{\frac{\Delta}{2}+n}}{n!}\frac{(1-v)^m}{m!}, \tag{D.1.1}$$

when applying the identity $(x)_{m+n}=(x)_m(x+m)_n$. Using the hypergeometric representation we have:

$$G_{\Delta,0}(u,v)=\sum_{n=0}^{\infty}\frac{(\frac{\Delta}{2})_n^4}{(\Delta+1-\frac{D}{2})_n(\Delta)_{2n}}{}_2F_1\left(\frac{\Delta}{2}+n,\frac{\Delta}{2}+n,\Delta+2n;1-v\right)\frac{u^{\frac{\Delta}{2}+n}}{n!}. \tag{D.1.2}$$

The hypergeometric function can be represented by an integral:

$${}_2F_1(a,b,c;z)=\frac{\Gamma(c)}{\Gamma(b)\Gamma(c-b)}\int_0^1 dt t^{b-1}(1-t)^{c-b-1}(1-zt)^{-a}, \tag{D.1.3}$$

The integral of our intrest is on the form:

$${}_2F_1(a,a,2a;z)=\frac{\Gamma(2a)}{\Gamma(a)^2}\int_0^1\frac{dt}{t(1-t)}\exp\left(a\ln\left(\frac{t(1-t)}{1-tz}\right)\right). \tag{D.1.4}$$

We are working in the large D limit and since the scaling dimension Δ is proportional to D we have that a is also proportional to D, and so we consider the large a limit. To do this we apply the saddle-point approximation.
We consider appendix A of [34] and the asymptotic expansion of a single saddle-point from [45]. We have an integral of the form, where t in general is thought of as a vector:

$$\int dt f(t)e^{aS(t)}=e^{aS(t_0)}(f(t_0)+O(a^{-1}))\prod_{j=1}^{n}(-\mu_j)^{-\frac{1}{2}}\left(\frac{2\pi}{a}\right)^{\frac{n}{2}}, \tag{D.1.5}$$

where the saddle-point t_0 is given by $\nabla S(t_0)=0$. μ_j is the eigenvalue of the Hessian matrix, and n is the number of variables integrated over. In our case we integrate over one variable giving us a scalar, and we

only consider it to leading order in a. This simplifies the integral:

$$\int dt f(t) e^{aS(t)} = f(t_0) e^{aS(t_0)} \sqrt{\frac{2\pi}{-a\partial_t^2 S(t_0)}}. \tag{D.1.6}$$

The saddle-point is at:

$$t_0 = \frac{1 \pm \sqrt{1-z}}{z}. \tag{D.1.7}$$

Then using some algebra we can evaluate the integral so that our hypergeometric function is on the form:

$${}_2F_1\left(\frac{\Delta}{2}+n, \frac{\Delta}{2}+n, \Delta+2n; 1-v\right) \approx \frac{\Gamma(\Delta+2n)}{\Gamma(\frac{\Delta}{2}+n)^2}\sqrt{\frac{\pi}{\frac{\Delta}{2}+n}}\frac{1}{v^{\frac{1}{4}}(1+\sqrt{v})^{\Delta+2n-1}}. \tag{D.1.8}$$

The scalar conformal block is now on the form:

$$G_{\Delta,0}(u,v) \approx \sqrt{\pi}\frac{1+\sqrt{v}}{v^{\frac{1}{4}}}\sum_{n=0}^{\infty}\frac{\Gamma(\Delta+2n)}{\Gamma(\frac{\Delta}{2}+n)^2}\frac{(\frac{\Delta}{2})_n^4}{(\Delta+1-\frac{D}{2})_n(\Delta)_{2n}}\frac{1}{\sqrt{n+\frac{\Delta}{2}}}\frac{\left(\frac{u}{(1+\sqrt{v})^2}\right)^{\frac{\Delta}{2}+n}}{n!}. \tag{D.1.9}$$

Applying the identity $(x)_n = \frac{\Gamma(x+n)}{\Gamma(x)}$ we can write:

$$G_{\Delta,0}(u,v) \approx \sqrt{\pi}\frac{1+\sqrt{v}}{v^{\frac{1}{4}}}\frac{\Gamma(\Delta)}{\Gamma(\frac{\Delta}{2})^2}\sum_{n=0}^{\infty}\frac{(\frac{\Delta}{2})_n^2}{(\Delta+1-\frac{D}{2})_n}\frac{1}{\sqrt{n+\frac{\Delta}{2}}}\frac{\left(\frac{u}{(1+\sqrt{v})^2}\right)^{\frac{\Delta}{2}+n}}{n!}. \tag{D.1.10}$$

Using Stirlings approximation $\Gamma(z) \approx \sqrt{2\pi}e^{-z}z^{z-1/2}$ we have the relations:

$$\frac{\Gamma(n+\frac{\Delta}{2}-\frac{1}{2})}{\Gamma(n+\frac{\Delta}{2})} \approx \frac{1}{\sqrt{n+\frac{\Delta}{2}}}, \qquad \frac{\Gamma(\frac{\Delta}{2})}{\Gamma(\frac{\Delta+1}{2})} \approx \frac{1}{\sqrt{\frac{\Delta}{2}}} \qquad \frac{\Gamma(\frac{\Delta-1}{2})}{\Gamma(\frac{\Delta}{2})} \approx \frac{1}{\sqrt{\frac{\Delta}{2}}}. \tag{D.1.11}$$

Using these with the Legendre duplication formula $\Gamma(z)\Gamma(z+\frac{1}{2}) = 2^{1-2z}\sqrt{\pi}\Gamma(2z)$ a new hypergeometric function appears enabeling us to write the scalar conformal block as:

$$G_{\Delta,0}(u,v) \approx 2^{\Delta-1}\frac{1+\sqrt{v}}{v^{\frac{1}{4}}}\left(\frac{u}{(1+\sqrt{v})^2}\right)^{\frac{\Delta}{2}}{}_2F_1\left(\frac{\Delta-1}{2}, \frac{\Delta}{2}, \Delta-\frac{D}{2}+1, \frac{u}{(1+\sqrt{v})^2}\right). \tag{D.1.12}$$

D.2 Solving the Conformal Casimir Differential Equation in Large Dimensional Suggested Coordinates

When we solve the Casimir differential equation, we have seen from the scalar conformal block that we have a mixed denominator of $\{y_+, y_-\}$ coordinates. This suggests a seperation of the form:

$$G_{\Delta,l} = \frac{1}{\sqrt{y_- - y_+}}H_{\Delta,l}. \tag{D.2.1}$$

The derivatives act the following way on the prefactor:

$$\begin{aligned}
\partial_{y_+}\frac{1}{\sqrt{y_- - y_+}} &= \frac{1}{2(y_- - y_+)^{3/2}}, \quad \partial_{y_-}\frac{1}{\sqrt{y_- - y_+}} = \frac{-1}{2(y_- - y_+)^{3/2}}, \\
\partial_{y_+}^2\frac{1}{\sqrt{y_- - y_+}} &= \frac{3}{4(y_- - y_+)^{5/2}}, \quad \partial_{y_-}^2\frac{1}{\sqrt{y_- - y_+}} = \frac{3}{4(y_- - y_+)^{5/2}},
\end{aligned} \tag{D.2.2}$$

while the operators acts as:

$$\begin{aligned}
\mathcal{D}_{y_+}\frac{1}{\sqrt{y_- - y_+}}H_{\Delta,l} &= \left(\frac{3y_+^2(1-y_+)}{2(y_- - y_+)^{5/2}} - \frac{y_+(y_+ + D - 2)}{2(y_- - y_+)^{3/2}} + \frac{\mathcal{D}_{y_+}}{(y_- - y_+)^{1/2}}\right)H_{\Delta,l},\\
\mathcal{D}_{y_-}\frac{1}{\sqrt{y_- - y_+}}H_{\Delta,l} &= \left(\frac{3y_-^2(1-y_-)}{2(y_- - y_+)^{5/2}} + \frac{y_-(y_- + D - 2)}{2(y_- - y_+)^{3/2}} + \frac{\mathcal{D}_{y_-}}{(y_- - y_+)^{1/2}}\right)H_{\Delta,l},\\
\mathcal{D}_{y_0}\frac{1}{\sqrt{y_- - y_+}}H_{\Delta,l} &= \left(\frac{y_+^2(1-y_+) + y_-^2(1-y_-)}{(y_+ - y_-)(y_- - y_+)^{3/2}} + \frac{\mathcal{D}_{\hat{y}}}{(y_- - y_+)^{1/2}}\right)H_{\Delta,l}.
\end{aligned} \tag{D.2.3}$$

Putting these into the conformal Casimir equation, and using some algebra yields:

$$\left(\mathcal{D}_{y_+} + \mathcal{D}_{y_-} + \mathcal{D}_{y_0} - \frac{y_+ y_-}{2(y_+ - y_-)^2}(y_+ + y_- - 2)\right)H_{\Delta,l} = \frac{1}{2}(C_{\Delta,l} - D + 1)H_{\Delta,l}. \tag{D.2.4}$$

The mixed term operator is of order D^1 and the mixed coordinate term is of order D^0. The behavior at leading order in D is given by $\mathcal{D}_{y_\pm}$ operators of order D^2:

$$\left(\mathcal{D}_{y_+} + \mathcal{D}_{y_-}\right)H_{\Delta,l} = \frac{1}{2}(C_{\Delta,l} - D + 1)H_{\Delta,l}. \tag{D.2.5}$$

This allows for a seperable solution:

$$H_{\Delta,l} = A_\Delta(y_+)A_{1-l}(y_-). \tag{D.2.6}$$

Acting with the differential operators on the LHS of Eq. (D.2.5) and inserting the eigenvalue on the RHS of Eq. (3.1.3) we get:

$$A_\Delta(y_+)\mathcal{D}_{y_-}A_{1-l}(y_-) + A_{1-l}(y_-)\mathcal{D}_{y_+}A_\Delta(y_+) = \frac{1}{2}(\Delta(\Delta - D) + l(l + D - 2) - D + 1)A_\Delta(y_+)A_{1-l}(y_-). \tag{D.2.7}$$

We can identify this as two eigenvalue equations:

$$\begin{aligned}
\mathcal{D}_{y_-}A_{1-l}(y_-) &= \frac{1}{2}(l-1)(l+D-1)A_{1-l}(y_-),\\
\mathcal{D}_{y_+}A_\Delta(y_+) &= \frac{1}{2}\Delta(\Delta - D)A_\Delta(y_+).
\end{aligned} \tag{D.2.8}$$

The solutions to these eigenvalue equations are:

$$\begin{aligned}
A_\Delta(y_+) &= y_+^{\Delta/2}{}_2F_1\left(\frac{\Delta-1}{2}, \frac{\Delta}{2}, \Delta - \frac{D}{2} + 1, y_+\right),\\
A_{1-l}(y_-) &= y_-^{(1-l)/2}{}_2F_1\left(-\frac{l}{2}, \frac{1-l}{2}, -l - \frac{D}{2} + 2, y_-\right).
\end{aligned} \tag{D.2.9}$$

We will check whether we can claim this to be a solution. We will check this for $A_\Delta(y_+)$ where the argument will follow the same lines by changing $y_+ \to y_-$ and $\Delta \to 1 - l$. The derivatives acts with:

$$\begin{aligned}
\partial_{y_+}A_\Delta(y_+) &= \frac{\Delta}{2}y_+^{\frac{\Delta}{2}-1}{}_2F_1 + y_+^{\Delta/2}{}_2F_1',\\
\partial_{y_+}^2A_\Delta(y_+) &= \frac{\Delta}{2}(\frac{\Delta}{2} - 1)y_+^{\frac{\Delta}{2}-2}{}_2F_1 + \Delta y_+^{\frac{\Delta}{2}-1}{}_2F_1' + y_+^{\Delta/2}{}_2F_1'',
\end{aligned} \tag{D.2.10}$$

where we have omittted the functional parenthesis of ${}_2F_1\left(\frac{\Delta-1}{2}, \frac{\Delta}{2}, \Delta - \frac{D}{2} + 1, y_+\right)$ for now. We then apply the full operator:

$$\begin{aligned}
\mathcal{D}_{y_+}A_\Delta(y_+) =& \frac{1}{2}\Delta(\Delta - D)y_+^{\Delta/2}{}_2F_1 + \frac{1}{2}\Delta(1-\Delta)y_+^{\frac{\Delta}{2}+1}{}_2F_1\\
&+(2\Delta + 2 - D)y_+^{\frac{\Delta}{2}+1}{}_2F_1' + (-2\Delta - 1)y_+^{\frac{\Delta}{2}+2}{}_2F_1' + 2y^{\frac{\Delta}{2}+2}{}_2F_1'' - 2y_+^{\frac{\Delta}{2}+3}{}_2F_1''.
\end{aligned} \tag{D.2.11}$$

The first term contains the eigenvalue. In other words we have to prove that the other terms combined vanishes. We check whether:

$$y_+^{\frac{\Delta}{2}+1}\left(\frac{1}{2}\Delta(1-\Delta)_2F_1+(2\Delta+2-D-2\Delta y_+-y_+)_2F_1'+(2y_+-2y_+^2)_2F_1''\right)\stackrel{?}{=}0. \tag{D.2.12}$$

The derivative of a hypergeometric function can be taking by applying it to the y_+^n dependency. Applying this and writing all as a combined sum:

$$\sum_{n=0}^{\infty}\frac{\left(\frac{\Delta-1}{2}\right)_n\left(\frac{\Delta}{2}\right)_n}{\left(\Delta-\frac{D}{2}+1\right)_n}\frac{y_+^n}{n!}\left(\frac{1}{2}\Delta(1-\Delta)+(2\Delta+2-D)\frac{n}{y_+}-(2\Delta+1)n+2(n-1)\frac{n}{y_+}-2n(n-1)\right)\stackrel{?}{=}0. \tag{D.2.13}$$

Multiply with y_+ and split into two sums directed by their dependency on y_+:

$$\sum_{n=0}^{\infty}\frac{\left(\frac{\Delta-1}{2}\right)_n\left(\frac{\Delta}{2}\right)_n}{\left(\Delta-\frac{D}{2}+1\right)_n}\frac{y_+^n}{n!}\left(2n^2+n(2\Delta-D)\right)+\sum_{n=0}^{\infty}\frac{\left(\frac{\Delta-1}{2}\right)_n\left(\frac{\Delta}{2}\right)_n}{\left(\Delta-\frac{D}{2}+1\right)_n}\frac{y_+^{n+1}}{n!}\left(-2n^2+n(1-2\Delta)+\frac{1}{2}\Delta(1-\Delta)\right)\stackrel{?}{=}0. \tag{D.2.14}$$

We then change the sum of the second term to $n\to n-1$, then the sum starts at $n=1$ but this can just be changed to $n=0$ since the first term is 0 for $n=0$. Then we combine the two sums:

$$\sum_{n=0}^{\infty}\frac{y_+^n}{(n-1)!}\left(\frac{\left(\frac{\Delta-1}{2}\right)_n\left(\frac{\Delta}{2}\right)_n}{\left(\Delta-\frac{D}{2}+1\right)_n}(2n+(2\Delta-D))+\frac{\left(\frac{\Delta-1}{2}\right)_{n-1}\left(\frac{\Delta}{2}\right)_{n-1}}{\left(\Delta-\frac{D}{2}+1\right)_{n-1}}(-2(n-1)^2+(n-1)(1-2\Delta)+\frac{1}{2}\Delta(1-\Delta))\right)\stackrel{?}{=}0, \tag{D.2.15}$$

where we have used that $n!=(n-1)!n$ so that we could cancel n's from the first term. Then we use the relation:

$$m_n=\frac{(m+n-1)!}{(m-1)!}=\frac{(m+n-2)!}{(m-1)!}(m+n-1)=m_{n-1}(m+n-1), \tag{D.2.16}$$

on the Pochhammer function of the first term, so that we can pull this out:

$$\begin{aligned}&\sum_{n=0}^{\infty}\frac{y_+^n}{(n-1)!}\frac{\left(\frac{\Delta-1}{2}\right)_{n-1}\left(\frac{\Delta}{2}\right)_{n-1}}{\left(\Delta-\frac{D}{2}+1\right)_{n-1}}\\&\times\left(\frac{(\frac{\Delta}{2}+n-1)(\frac{\Delta-1}{2}+n-1)}{\Delta-\frac{D}{2}+1+n-1}2\left(n+\Delta-\frac{D}{2}\right)+(-2(n-1)^2+(n-1)(1-2\Delta)+\frac{1}{2}\Delta(1-\Delta))\right)\stackrel{?}{=}0.\end{aligned} \tag{D.2.17}$$

The expression indside the parenthesis is satisfied for all n's:

$$\to\frac{1}{2}\Delta(\Delta-1)+(2\Delta-1)(n-1)+2(n-1)^2-2(n-1)^2+(n-1)(1-2\Delta)+\frac{1}{2}\Delta(1-\Delta)=0, \tag{D.2.18}$$

and thus we have proven that $A_\Delta(y_+)$ is a solution to the eigenvalue equation from Eq. (D.2.8).

Appendix E

Approximation of the Large D Scalar Block with Linear Scalings

Consider the scalar block Eq. (5.1.1). We use the linear scaling $\Delta = \delta D$, $n = \alpha D$ and $m = \beta D$. For large values of D the discrete sums of n, m may be turned into integrals over α, β:

$$G^D_{\Delta,0}(u,v) = \int d\alpha d\beta \frac{\Gamma^2(\delta D/2+\alpha D)\Gamma^2(\delta D/2+\alpha D+\beta D)\Gamma(\delta D+1-D/2)\Gamma(\delta D)u^{\delta D/2+\alpha D}(1-v)^{\beta D}}{\Gamma^4(\delta D/2)\Gamma(\delta D+1-D/2+\alpha D)\Gamma(\delta D+2\alpha D+\beta D)\Gamma(\alpha D)\Gamma(\beta D)\alpha\beta D^2}, \tag{E.0.1}$$

by rewriting the Pochhammers as Γ-functions and that $x! = \Gamma(x+1) = x\Gamma(x)$. We have also used the coordinates of $\{u, v\} = \{a^2 e^{\sigma/D}, b^2 e^{\tau/D}\}$. Using the Stirling expansion in $1/D$ for all Γ-functions while pulling out the D-dependence we get:

$$\begin{aligned} G^D_{\Delta,0}(u,v) = \int \frac{d\alpha d\beta D}{8\pi} \sqrt{\frac{\delta^3(\delta-1/2)(\delta+2\alpha+\beta)}{\alpha\beta(\delta/2+\alpha)^2(\delta/2+\alpha+\beta)^2(\delta-1/2+\alpha)}} \exp\left(\sigma(\delta/2+\alpha)+\tau\beta\right) \\ \times \exp\left(D\ln\left(\frac{a^{\delta+2\alpha}(1-b^2)^\beta 4^\delta(\delta/2+\alpha)^{\delta+2\alpha}(\delta/2+\alpha+\beta)^{\delta+2\alpha+2\beta}}{\alpha^\alpha\beta^\beta\delta^\delta(\delta-1/2)^{1/2-\delta}(\delta-1/2+\alpha)^{1/2-\delta-\alpha}(\delta+2\alpha+\beta)^{-\delta-\beta-2\alpha}}\right)\right), \end{aligned} \tag{E.0.2}$$

here the integration meausure also contributes with D^2 factor. Note that evaluating Γ-functions by first using $\Gamma(x+1) = x\Gamma(x)$ then the expansion, or evaulating the expansion first, can leave a discrepancy of e^{-1} for each Γ-function. Now we would like to use the saddle-point approximation of two variables. We define:

$$S(\alpha,\beta) \equiv \ln\left(\frac{a^{\delta+2\alpha}(1-b^2)^\beta 4^\delta(\delta/2+\alpha)^{\delta+2\alpha}(\delta/2+\alpha+\beta)^{\delta+2\alpha+2\beta}}{\alpha^\alpha\beta^\beta\delta^\delta(\delta-1/2)^{1/2-\delta}(\delta-1/2+\alpha)^{1/2-\delta-\alpha}(\delta+2\alpha+\beta)^{-\delta-\beta-2\alpha}}\right). \tag{E.0.3}$$

The saddle-point is where both $\partial_\alpha S(\alpha^*,\beta^*) = 0$ and $\partial_\beta S(\alpha^*,\beta^*) = 0$ is satisfied. The derivatives are:

$$\partial_\alpha S(\alpha,\beta) = \ln\left(\frac{a^2(\alpha+\delta/2)^2(\alpha+\beta+\delta/2)^2}{\alpha(\alpha+\delta-1/2)(2\alpha+\beta+\delta)^2}\right), \tag{E.0.4}$$

$$\partial_\beta S(\alpha,\beta) = \ln\left(\frac{(1-b^2)(\delta/2+\alpha+\beta)^2}{\beta(\delta+2\alpha+\beta)}\right), \tag{E.0.5}$$

which yields two coupled equations:

$$a^2(\alpha+\delta/2)^2(\alpha+\beta+\delta/2)^2 = \alpha(\alpha+\delta-1/2)(2\alpha+\beta+\delta)^2, \tag{E.0.6}$$

$$(1-b^2)(\delta/2+\alpha+\beta)^2 = \beta(\delta+2\alpha+\beta). \tag{E.0.7}$$

The solutions are:

$$\alpha^* = \left(1+\frac{1}{b}\right)k_+ - \frac{\delta}{2}, \qquad \beta^* = -\left(1-\frac{1}{b^2}\right)k_+, \tag{E.0.8}$$

where:

$$k_+ \equiv \frac{b(1+b)}{4((1+b)^2-a^2)}\left(1+\sqrt{1+4\delta(\delta-1)\left(1-\frac{a^2}{(1+b)^2}\right)}\right), \tag{E.0.9}$$

k_+ dominates the sum or integral over the scalar block since this contains the D dependency $\Delta = D\delta$. We would like to substitute α^* and β^* back into the conformal block and obtain the $\{\sigma,\tau\}$ dependency, so we look at the $\{u,v\}$ behavior of the conformal scalar block:

$$u^{\Delta/2+n} = (a^2 e^{\sigma/D})^{\delta D/2+\alpha^* D} = \exp\left(k_+\left(1+\frac{1}{b}\right)\sigma\right), \tag{E.0.10}$$

$$(1-v)^m = (1-b^2e^{\tau/D})^{\beta^\star D} = (1-b^2e^{\tau/D})^{-k_+ D(1-1/b^2)}. \tag{E.0.11}$$

If we expand the following expression to first order in D we get:

$$\frac{1}{(1-b^2e^{\tau/D})^2} = \frac{1}{(1-b^2)^2}\left(1+\frac{b^2}{1-b^2}\frac{2\tau}{D}+\mathcal{O}(1/D^2)\right). \tag{E.0.12}$$

We then write this expansion in the desired expression:

$$\left(\frac{1}{(1-b^2)^2}\left(1+\frac{b^2}{1-b^2}\frac{2\tau}{D}\right)\right)^{k_+ D(1-1/b^2)/2}. \tag{E.0.13}$$

We then use that one can write Eulers number as:

$$e = \lim_{n\to\infty}\left(1+\frac{1}{n}\right)^n. \tag{E.0.14}$$

D is our expansion parameter so we take this to ∞, or rather $n = \frac{(1-b^2)D}{2b^2\tau}$, and if $D\to\infty$ so does n. We notice we got this expression in the exponent if we mulitply with τ/τ therefore we get:

$$\lim_{n\to\infty}\left(\frac{1}{(1-b^2)^2}\left(1+\frac{1}{n}\right)\right)^{-k_+\tau n} \sim e^{-k_+\tau}, \tag{E.0.15}$$

we only count what is in the exponential, so we suppress the factor in front, and thereby have shown the dependency:

$$G^D_{\Delta,0}(\sigma,\tau) \sim \exp\left(k_+\left(1+\frac{1}{b}\right)\sigma - k_+\tau\right). \tag{E.0.16}$$

Appendix F

Decomposing the Large D Conformal Block in Gegenbauer Polynomials

In this appendix we will compare the conformal block in large D scalar suggested variables and radial/angular variables, so that we can circumvent the Casimir equation method by comparing the conformal blocks directly. We already have the two conformal blocks thanks to [28, 34]. This demands a decomposition of the conformal block. We will focus on the decomposition of the large D block in Gegenbauer polynomials in this section. Therefore we consider how one in general can expand a function $f(\eta)$ in Gegenbauer polynomials $C_n^\alpha(\eta)$, with coefficients χ_n:

$$f(\eta) = \sum_{n=0}^{\infty} \chi_n C_n^\alpha(\eta). \tag{F.0.1}$$

Using Dirac notation we can project a state $|f\rangle$ on the η-basis so that $f(\eta) = \langle \eta | f \rangle$. We can also write a complete set as $\sum_n |n\rangle \langle n|$ so we have:

$$\langle \eta | f \rangle = \sum_n \langle \eta | n \rangle \langle n | f \rangle , \tag{F.0.2}$$

with $\langle \eta | n \rangle = C_n^\alpha(\eta)$ equivalent to:

$$f(\eta) = \sum_n \langle n | f \rangle C_n^\alpha(\eta). \tag{F.0.3}$$

Comparing Eq. (F.0.3) to Eq. (F.0.1) we have that the coefficients must be $\chi_n = \langle n | f \rangle$. We would then like to identify these coefficients. We will use a complete set which in the Gegenbauer polynomial basis is given with a weigth function:

$$\int_{-1}^{1} d\eta (1-\eta^2)^{\alpha - 1/2} |\eta\rangle \langle \eta| , \tag{F.0.4}$$

the coefficients then reads:

$$\chi_n = \int_{-1}^{1} d\eta (1-\eta^2)^{\alpha-1/2} \langle n | \eta \rangle \langle \eta | f \rangle = N_n \int_{-1}^{1} d\eta (1-\eta^2)^{\alpha-1/2} C_n^\alpha(\eta) f(\eta), \tag{F.0.5}$$

with N_n being a normalization of the integral. In order to determine this normalization we consider the projection of the basis:

$$\langle n | m \rangle = N_n N_m \int_{-1}^{1} d\eta C_n^\alpha(\eta) C_m^\alpha(\eta) (1-\eta^2)^{\alpha-1/2} = \delta_{n,m} N_n^2 \frac{\pi 2^{1-2\alpha} \Gamma(n+2\alpha)}{n!(n+\alpha)\Gamma^2(\alpha)}. \tag{F.0.6}$$

In order for this to be an orthonormal basis when $n \neq m$ the integral must be vanishing. When we have $n = m$ we obtain:

$$1 = \langle n|n\rangle = N_n^2 \int_{-1}^{1} d\eta C_n^\alpha(\eta) C_n^\alpha(\eta)(1-\eta^2)^{\alpha-1/2} = N_n^2 \frac{\pi 2^{1-2\alpha}\Gamma(n+2\alpha)}{n!(n+\alpha)\Gamma^2(\alpha)}, \tag{F.0.7}$$

solving this for the normalization yields:

$$N_n = \sqrt{\frac{n!(n+\alpha)\Gamma^2(\alpha)}{\pi 2^{1-2\alpha}\Gamma(n+2\alpha)}}. \tag{F.0.8}$$

If you have a function $f(\eta)$ that you want to expand in Gegenbauer polynomials you have to solve the following integral to find the coefficients:

$$\chi_n = \sqrt{\frac{n!(n+\alpha)\Gamma^2(\alpha)}{\pi 2^{1-2\alpha}\Gamma(n+2\alpha)}} \int_{-1}^{1} d\eta (1-\eta^2)^{\alpha-1/2} C_n^\alpha(\eta) f(\eta). \tag{F.0.9}$$

We will now speciale to a specific conformal block Eq. (5.1.10) and therefore a specific $f(\eta)$. We will for simplicity set the spin $l = 0$ implying that the hypergeometric function in $A_{1-l}(y_-)$ only contributes with the first term, i.e. 1 and leave its prefactor, yielding the scalar block:

$$G_{\Delta,0} = \frac{2^\Delta \sqrt{y_-}}{\sqrt{y_- - y_+}} A_\Delta(y_+), \tag{F.0.10}$$

which can be re-written using the relation $y_- = \eta^{-2}$:

$$G_{\Delta,0} = (1-\eta^2 y_+)^{-1/2} 2^\Delta A_\Delta(y_+). \tag{F.0.11}$$

The angular coordinate η part of the block can be decomposed into a sum of Gegenbauer polynomials:

$$G_{\Delta,0} = 2^\Delta A_\Delta(y_+) \sum_{l=0}^{\infty} \chi_l C_l^\nu(\eta). \tag{F.0.12}$$

Defining the function we want to expand $f(\eta) \equiv (1-\eta^2 y_+)^{-1/2}$ gives the relation:

$$(1-\eta^2 y_+)^{-1/2} = \sum_{n=0}^{\infty} \chi_n C_n^\alpha(\eta). \tag{F.0.13}$$

We know in general terms how to determine the coefficients χ_n of such a function:

$$\chi_n = N_n I, \qquad I \equiv \int_{-1}^{1} d\eta (1-\eta^2)^{\alpha-1/2} C_n^\alpha(\eta)(1-\eta^2 y_+)^{-1/2}. \tag{F.0.14}$$

Applying the hypergeometric representation of the Gegenbauer polynomial:

$$I = \frac{(2\alpha)_n}{n!} \sum_{m=0}^{\infty} \frac{(-n)_m (2\alpha+n)_m}{2^m m!(\alpha+1/2)_m} \int_{-1}^{1} (1-\eta)^m (1-\eta^2 y_+)^{-1/2} (1-\eta^2)^{\alpha-1/2}. \tag{F.0.15}$$

The integral can be solved if one changes $(1-\eta)^m \to \eta^m$ and after it is evaluated use a binomial expansion:

$$\int_{-1}^{1} d\eta \eta^m (1-\eta^2 y_+)^{-1/2}(1-\eta^2)^{\alpha-1/2} = \frac{(1+(-1)^m)}{2} \frac{\Gamma(\frac{1+m}{2})\Gamma(\frac{1}{2}+\alpha)}{\Gamma(1+\frac{m}{2}+\alpha)} {}_2F_1\left(\frac{1}{2}, \frac{1+m}{2}, 1+\frac{m}{2}+\alpha, y_+\right), \tag{F.0.16}$$

we can then use the binomial expansion: $(1-\eta)^m = \sum_{k=0}^{m}(-1)^k\binom{m}{k}\eta^k$, then we find:

$$I = \frac{(2\alpha)_n}{n!}\sum_{m=0}^{\infty}\frac{(-n)_m(2\alpha+n)_m}{2^m m!(\alpha+\frac{1}{2})_m}\sum_{k=0}^{m}\binom{m}{k}\frac{(1+(-1)^k)}{2}\frac{\Gamma(\frac{1+k}{2})\Gamma(\frac{1}{2}+\alpha)}{\Gamma(1+\frac{k}{2}+\alpha)}{}_2F_1\left(\frac{1}{2},\frac{1+k}{2},1+\frac{k}{2}+\alpha,y_+\right). \tag{F.0.17}$$

Including the normalization factor and doing some algebra we have the coefficients:

$$\begin{aligned}\chi_n =& \frac{\Gamma^2(\alpha+\frac{1}{2})\Gamma(\alpha)}{\sqrt{\Gamma(2\alpha+n)}\Gamma(2\alpha)}\sqrt{\frac{n+\alpha}{\pi 2^{3-2\alpha}n!}}\sum_{m=0}^{\infty}\frac{(-n)_m\Gamma(2\alpha+n+m)}{2^m m!\Gamma(\alpha+\frac{1}{2}+m)}\\ &\times\sum_{k=0}^{m}\binom{m}{k}\frac{(1+(-1)^k)\Gamma(\frac{1+k}{2})}{\Gamma(1+\frac{k}{2}+\alpha)}{}_2F_1\left(\frac{1}{2},\frac{1+k}{2},1+\frac{k}{2}+\alpha,y_+\right).\end{aligned} \tag{F.0.18}$$

For another method of integral solution, let us apply the Rodrigues formula to the integral of Eq. (F.0.14):

$$I = \frac{(-1)^n\Gamma(\alpha+\frac{1}{2})\Gamma(n+2\alpha)}{2^n n!\Gamma(2\alpha)\Gamma(\alpha+n+\frac{1}{2})}\int_{-1}^{1}d\eta(1-\eta^2y_+)^{-1/2}\partial_\eta^n((1-\eta^2)^{n+\alpha-1/2}). \tag{F.0.19}$$

The integral is solved by considering a solution for each coefficient $n = 0, 1, 2, 3, ...$ All odd n's gives a vanishing integral. For the even n's we recognize the pattern to write up a closed expression:

$$\chi_n = \frac{2^\alpha\Gamma(\alpha+\frac{1}{2})}{\Gamma(\frac{n}{2}+1)}\sqrt{\frac{(-1)^n(n+\alpha)\Gamma(n+1)}{\Gamma(2\alpha+n)}}\sum_{k=0}^{n}(-1)^k\binom{n/2}{k}\frac{\Gamma(\alpha+\frac{n}{2}+k)}{\Gamma(\alpha+k+1)}{}_2F_1\left(\frac{1}{2},\frac{1}{2}+k,\alpha+k+1,y_+\right). \tag{F.0.20}$$

We have now expressed χ_n by solving the integral of Eq. (F.0.14) in two ways i.e. Eq. (F.0.18) and Eq. (F.0.20). The problem in both solutions of the integral representations is that $\chi_n(y_+)$ is not only a coefficient but dependent on a coordinate. In this way, it was not possible to factorize the y_+ dependency so that we could express the conformal block in a y_+ dependent part and a y_- dependent part. On top of that, it is a rather complicated expression we obtained, which will only become more complex when including the spin l.

Bibliography

[1] Kazunori Akiyama et al. First M87 Event Horizon Telescope Results. I. The Shadow of the Supermassive Black Hole. *Astrophys. J. Lett.*, 875:L1, 2019. doi: 10.3847/2041-8213/ab0ec7.

[2] S.W. Hawking. Black hole explosions. *Nature*, 248:30–31, 1974. doi: 10.1038/248030a0.

[3] Jacob D. Bekenstein. Black holes and entropy. *Phys. Rev. D*, 7:2333–2346, 1973. doi: 10.1103/PhysRevD.7.2333.

[4] Gerard 't Hooft. The Holographic principle: Opening lecture. *Subnucl. Ser.*, 37:72–100, 2001. doi: 10.1142/9789812811585_0005.

[5] Daniel Harlow. Jerusalem Lectures on Black Holes and Quantum Information. *Rev. Mod. Phys.*, 88: 015002, 2016. doi: 10.1103/RevModPhys.88.015002.

[6] S.W. Hawking and Don N. Page. Thermodynamics of Black Holes in anti-De Sitter Space. *Commun. Math. Phys.*, 87:577, 1983. doi: 10.1007/BF01208266.

[7] Tatsumi Aoyama, Masashi Hayakawa, Toichiro Kinoshita, and Makiko Nio. Tenth-Order QED Contribution to the Electron g-2 and an Improved Value of the Fine Structure Constant. *Phys. Rev. Lett.*, 109:111807, 2012. doi: 10.1103/PhysRevLett.109.111807.

[8] Troels Harmark. *Introduction to string theory - Lecture notes.* 2020.

[9] Juan Martin Maldacena. The Large N limit of superconformal field theories and supergravity. *Int. J. Theor. Phys.*, 38:1113–1133, 1999. doi: 10.1023/A:1026654312961.

[10] S. S. Gubser, Igor R. Klebanov, and Alexander M. Polyakov. Gauge theory correlators from noncritical string theory. *Phys. Lett. B*, 428:105–114, 1998. doi: 10.1016/S0370-2693(98)00377-3.

[11] Edward Witten. Anti-de Sitter space and holography. *Adv. Theor. Math. Phys.*, 2:253–291, 1998. doi: 10.4310/ATMP.1998.v2.n2.a2.

[12] P. A. R. Ade et al. Planck 2015 results. XIII. Cosmological parameters. *Astron. Astrophys.*, 594:A13, 2016. doi: 10.1051/0004-6361/201525830.

[13] Hong Zhe Chen, Robert C. Myers, Dominik Neuenfeld, Ignacio A. Reyes, and Joshua Sandor. Quantum Extremal Islands Made Easy, Part I: Entanglement on the Brane. *JHEP*, 10:166, 2020. doi: 10.1007/JHEP10(2020)166.

[14] Hong Zhe Chen, Robert C. Myers, Dominik Neuenfeld, Ignacio A. Reyes, and Joshua Sandor. Quantum Extremal Islands Made Easy, Part II: Black Holes on the Brane. 9 2020.

[15] Steven Weinberg. The Cosmological Constant Problem. *Rev. Mod. Phys.*, 61:1–23, 1989. doi: 10.1103/RevModPhys.61.1.

[16] L. D. Faddeev. Mass in Quantum Yang-Mills Theory: Comment on a Clay Millenium problem. 11 2009.

[17] David Simmons-Duffin. The Conformal Bootstrap. In *Theoretical Advanced Study Institute in Elementary Particle Physics: New Frontiers in Fields and Strings*, pages 1–74, 2017. doi: 10.1142/9789813149441_0001.

[18] Subir Sachdev. Condensed Matter and AdS/CFT. *Lect. Notes Phys.*, 828:273–311, 2011. doi: 10.1007/978-3-642-04864-7_9.

[19] Shahar Hod. Bulk emission by higher-dimensional black holes: Almost perfect blackbody radiation. *Class. Quant. Grav.*, 28:105016, 2011. doi: 10.1088/0264-9381/28/10/105016.

[20] M. Socolovsky. Schwarzschild Black Hole in Anti-De Sitter Space. *Adv. Appl. Clifford Algebras*, 28(1): 18, 2018. doi: 10.1007/s00006-018-0822-6.

[21] Edward Witten. Anti-de Sitter space, thermal phase transition, and confinement in gauge theories. *Adv. Theor. Math. Phys.*, 2:505–532, 1998. doi: 10.4310/ATMP.1998.v2.n3.a3.

[22] Andrew Strominger. Microscopic Origin of the Bekenstein-Hawking Entropy. 1996.

[23] Niels Obers Stefano Baiguera and Gerben Oling. *Lecture notes for gauge gravity duality 2021.* 2021.

[24] Slava Rychkov. *EPFL Lectures on Conformal Field Theory in D>= 3 Dimensions.* SpringerBriefs in Physics. 1 2016. ISBN 978-3-319-43625-8, 978-3-319-43626-5. doi: 10.1007/978-3-319-43626-5.

[25] F. A. Dolan and H. Osborn. Conformal partial waves and the operator product expansion. *Nucl. Phys. B*, 678:491–507, 2004. doi: 10.1016/j.nuclphysb.2003.11.016.

[26] F.A. Dolan and H. Osborn. Conformal Partial Waves: Further Mathematical Results. 8 2011.

[27] Joao Penedones, Joao A. Silva, and Alexander Zhiboedov. Nonperturbative Mellin Amplitudes: Existence, Properties, Applications. *JHEP*, 08:031, 2020. doi: 10.1007/JHEP08(2020)031.

[28] Matthijs Hogervorst and Slava Rychkov. Radial Coordinates for Conformal Blocks. *Phys. Rev. D*, 87: 106004, 2013. doi: 10.1103/PhysRevD.87.106004.

[29] Goethe Universität C. Gros. Phase transitions, 2021. URL `https://itp.uni-frankfurt.de/~gros/Vorlesungen/TD/6_Phase_transitions.pdf`.

[30] Joao Penedones. TASI lectures on AdS/CFT. In *Theoretical Advanced Study Institute in Elementary Particle Physics: New Frontiers in Fields and Strings*, pages 75–136, 2017. doi: 10.1142/9789813149441_0002.

[31] Frederik Holdt-Sørensen, David A. McGady, and Nico Wintergerst. Black hole evaporation and semiclassicality at large D. *Phys. Rev. D*, 102(2):026016, 2020. doi: 10.1103/PhysRevD.102.026016.

[32] Duccio Pappadopulo, Slava Rychkov, Johnny Espin, and Riccardo Rattazzi. OPE Convergence in Conformal Field Theory. *Phys. Rev. D*, 86:105043, 2012. doi: 10.1103/PhysRevD.86.105043.

[33] Abhijit Gadde and Trakshu Sharma. Constraining Conformal Theories in Large Dimensions. 2 2020.

[34] A.Liam Fitzpatrick, Jared Kaplan, and David Poland. Conformal Blocks in the Large D Limit. *JHEP*, 08:107, 2013. doi: 10.1007/JHEP08(2013)107.

[35] A. Liam Fitzpatrick and Jared Kaplan. Unitarity and the Holographic S-Matrix. *JHEP*, 10:032, 2012. doi: 10.1007/JHEP10(2012)032.

[36] Petr Kravchuk and David Simmons-Duffin. Light-ray operators in conformal field theory. *JHEP*, 11: 102, 2018. doi: 10.1007/JHEP11(2018)102.

[37] Troels Harmark. *General Relativity and Cosmology- Lecture notes.* 2018.

[38] B. Ryden. *Introduction to cosmology.* Cambridge University Press, 1970. ISBN 978-1-107-15483-4, 978-1-316-88984-8, 978-1-316-65108-7. doi: 10.1017/9781316651087.

[39] Rodrigo F. L. Holanda. On the dynamics of the universe in D spatial dimensions. *Rev. Mex. Astron. Astrofis.*, 48:251, 2012.

[40] Shouxin Chen, Gary W. Gibbons, Yijun Li, and Yisong Yang. Friedmann's Equations in All Dimensions and Chebyshev's Theorem. *JCAP*, 12:035, 2014. doi: 10.1088/1475-7516/2014/12/035.

[41] Thomas Hartman. *Lectures on Quantum Gravity and Black Holes*. 2015.

[42] National Institute of Standards and Technology. Gegenbauer polynomials, 2010. URL `https://dlmf.nist.gov/search/search?q=Gegenbauer+polynomials&p=0&r=0`.

[43] N. M. Temme, I. V. Toranzo, and J. S. Dehesa. Entropic functionals of Laguerre and Gegenbauer polynomials with large parameters. *J. Phys. A*, 50:215206, 2017. doi: 10.1088/1751-8121/aa6dc1.

[44] Gokce Basar, Aleksey Cherman, and David A. McGady. Bose-Fermi Degeneracies in Large N Adjoint QCD. *JHEP*, 07:016, 2015. doi: 10.1007/JHEP07(2015)016.

[45] Encyclopedia of Mathematics. Saddle point method, 2021. URL `https://encyclopediaofmath.org/index.php?title=Saddle_point_method`.